EFFECTS OF SERIAL PASSAGING ON WEST NILE VIRUS (SARAFEND) IN A MOUSE MODEL

CHIANG CERN CHER, SAMUEL

NATIONAL UNIVERSITY OF SINGAPORE

2008

EFFECTS OF SERIAL PASSAGING ON WEST NILE VIRUS (SARAFEND) IN A MOUSE MODEL

CHIANG CERN CHER, SAMUEL

B. Sc. (Hons), NUS

A THESIS SUBMITTED

FOR THE DEGREE OF MASTER OF SCIENCE

DEPARTMENT OF MICROBIOLOGY

NATIONAL UNIVERSITY OF SINGAPORE

2008

PUBLICATIONS AND PRESENTATIONS GENERATED BY THIS AUTHOR

Publications:

CHU, J. J. H., CHIANG, C. C. S., and Ng, M. L., (2007). Immunization of Flavivirus West Nile Recombinant Envelope Domain III Protein Induced Specific Immune Response and Protection against West Nile Virus Infection. *J. Immunol. 178: 2699-2705.*

Conference Presentations:

CHIANG, C. C. S., and Ng, M. L., (2007). West Nile Virus Adaptation to an Immune – Competent Mouse. *NHG Annual Scientific Congress 2007, Singapore*.

CHIANG, C. C. S., and Ng, M. L., (2008). The Effects of Multiple Passaging Regimes on West Nile Virus Genome and Infectability. *13th ICID (International Society for Infectious Diseases). Kuala Lumpur, Malaysia*.

CHIANG, C. C. S., and Ng, M. L., (2008). The Stability of West Nile Virus Genome and its Pathology in Mice After Multiple Passaging. *14th International Congress of Virology IUMS (International Union of Microbiological Socieities). Istambul, Turkey.*

CHIANG, C. C. S., and Ng, M. L., (2008). Ultrastructure of a Neural Culture Persistently Infected with West Nile Virus. *9th Asia-Pacific Microscopy Conference. Jeju, Republic of Korea.*

ACKNOWLEDGEMENT

I would like to express my sincere gratitude to:

Professor Ng Mah Lee for accepting me into the laboratory during my undergraduate days and seeing me through these five years of invaluable experience and hard work. I am humbled by the honour.

The members of Flavivirus Laboratory, especially Ms. R. Bhuvanakantham, Mr. Terence Tan, Mr. Melvin Tan, Ms. Fiona Chin, and Dr. Chu Jang Hann for their friendship, expert technical advice on different techniques, and constructive criticism.

Professor Dr. Wong Kum Thong, of the Department of Pathology, University Malaya, Kuala Lumpur and his staff, Mr. Yaiw Koon Choo and Mr. Ong Kein Chai for guiding me through the basics of immunohistochemistry and pathology.

Ms. Evelyn Teoh for introducing me to mice primary neural cells, Ms. Lynette Lim and Dr. Sashi of the Department of Biochemistry for protocols on neuron and glial cell isolation, Mr. Yeo Kim Long for introducing me to qPCR, Mr. Desmond Chan for extra lessons on mice handling, and Dr. Li Jun for timely advice on virus sequencing. Mr. Terence Tan and Ms. Josephine Howe for expert help with the electron microscopy work.

Mr. Edwin Liu, Mr. Adrian Cheong, and the other Flavilab members; Mr. Chong Mun Keat, Mr. Anthony Chua, and Mr. Vincent Pang.

Mr. Pallan for watching over my beloved mice.

My godmum Ms. Bessie Low for her concern and home-cooked dinners.

Last but most importantly, my parents who have never ceased supporting me.

Thank you for allowing me to be part of your lives.

TABLE OF CONTENTS

PAGE NUMBER

SUMMARY

West Nile virus (WNV) represents a rapidly emerging infectious disease today and causes symptoms ranging from febrile illness to fatal encephalitis. The strain WNV (Sarafend) having been passaged through cell culture repeatedly, has lost its ability to infect and cause mortality in mice. This study seeks to revive the virus' murine infectability by repeatedly passaging it through mice brains and a mosquito cell line, mimicking normal infectious cycles. We found that passaged WNV became more persistent in adult BALB/c mice and caused more severe pathogenesis in various organs. Unpassaged viruses could only be detected on day 1 post inoculation in the serum at 10^1 PFU/ml whereas mice inoculated with passaged viruses had viremia of 10^4 PFU/g tissue in brains and spleens at day 3 post inoculation. Suckling mice inoculated with the passaged viruses had an overall lower mean survival time of up to 48 hours when compared to suckling mice inoculated with unpassaged viruses. Additionally, the passaged virus gave higher titres for longer periods when infected onto primary neural cultures. An additional passaging regime where WNV was passaged repeatedly only in mouse brains was performed and this strain when compared to the first passaging regime was found less adapted to infecting adult mice, killed suckling mice slower, and gave lower titres in primary cultures. Sequencing the genes C, E, NS2, and NS4 found mutations in two hot spots in the C protein at amino acid residue 24 and 26. The region encompassing the first six amino acids for the NS2a gene was also found variable in the passaged viruses. These mutations are speculated to be important for virulence and adaptation of the virus to murine hosts.

LIST OF TABLES

PAGE NUMBER

LIST OF FIGURES

PAGE NUMBER

ABBREVIATIONS

<	-	less than
:	-	ratio
-	-	negative
%	-	Percentage
˚C	-	degrees Celsius
µg	-	microgram
µl	-	microlitre
µm	-	micrometer
x	-	times magnitude
x *g*	-	centrifugal force
α	-	alpha
β	-	beta
BALB/c	-	Bagg Albino strain c
BHK	-	baby hamster kidney
BSA	-	bovine serum albumin
BSL	-	biosafety level
cDNA	-	complementary deoxyribonucleic acid
cm	-	centimetre
CNS	-	central nervous system
DNA	-	deoxyribonucleic acid
DV	-	dengue virus
E16	-	embryonic day 16 mice
FBS	-	foetal bovine serum
g	-	gram(s)
IGSS	-	immnogold silver staining
IHC	-	immunohistochemistry
Log	-	logarithmic scale
M	-	molar
MOI	-	multiplicity of infection
min	-	minute(s)
ml	-	millilitre(s)

mm	-	millimetre(s)
NGC	-	New Guinea C strain
nm	-	nanometre(s)
NS	-	non structural
p	-	probability
PBS	-	phosphate buffered saline
PCR	-	polymerase chain reaction
PFU	-	plaque forming unit
PI	-	post infection
RNA	-	ribonucleic acid
RTPCR	-	reverse transcription polymerase chain reaction
SPF	-	specific pathogen free
TBS	-	tris buffered saline
UV	-	ultraviolet
WNV	-	West Nile virus
WNVS	-	West Nile virus Sarafend strain

CHAPTER 1
LITERATURE REVIEW

1.0 INTRODUCTION

1.1 FLAVIVIRIDAE

The viruses in the *Flaviviridae* family are the most common causative agent of viral encephalitis in humans (Farrar and Newton, 2000). Flaviviruses are mainly transmitted via arthropods, mosquitoes, and ticks, to their vertebrate hosts. The three genera found under *Flaviviridae* are *Flavivirus*, *Pestivirus*, and *Hepacivirus*. The genus *Flaviviridae* contains approximately 57 antigenically – related viruses such as dengue, West Nile, Japanese encephalitis, and the genus type species yellow fever virus (Latin 'Flavus' = yellow). The other two genera contain far fewer members with *Pestivirus* having six species and *Hepacivirus* with two species (International Committee on Taxonomy of Viruses, 2000). *Figure 1* shows the *Flaviviridae* classification.

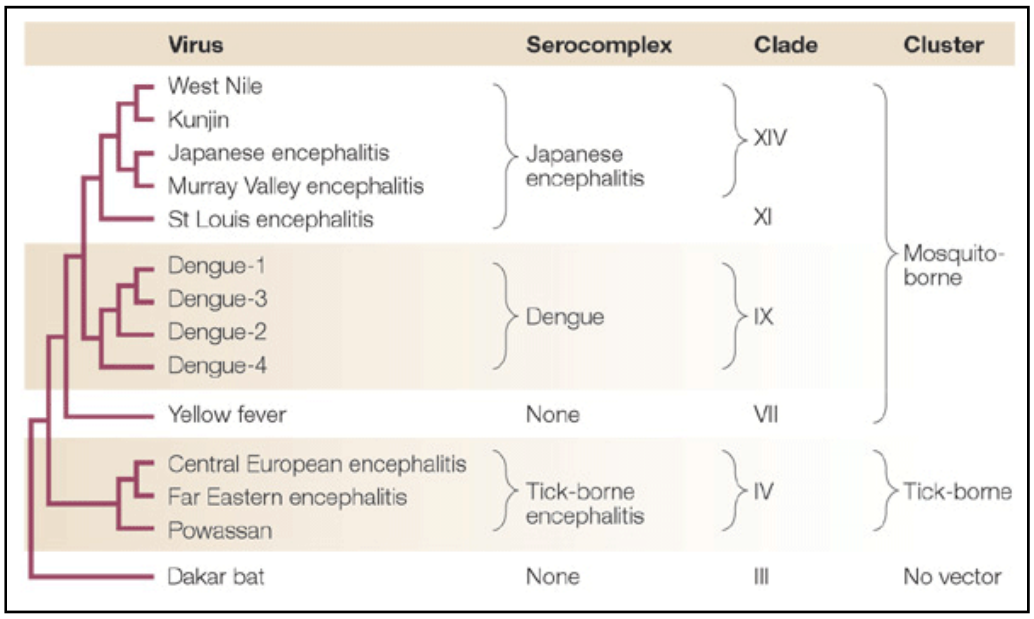

Figure 1: The Flaviviridae classification (Mukhopadhyay et al., 2005).

1.2 WEST NILE

West Nile virus (WNV) was first described in Uganda, 1937 when an adult female came down with a severe febrile disease (Smithburn *et al.*, 1940). It was later added to the Japanese encephalitis serocomplex which includes St. Louis encephalitis virus. This group was further expanded to include Murray Valley encephalitis, Kunjin, Usutu, Kokobera, Stratford, and Alfuy viruses after serological studies found antibodies against WNV could cross – detect antigens from many other viruses (Smithburn, 1942; De Madrid and Poterfield, 1974).

West Nile virus gained worldwide attention in 1999 when it was detected in New York, United States. The following year, it spread throughout the North American continent and later on to Latin America and the Caribbean (Hayes and Gubler, 2006). Before that, it has only been known to be the cause of sporadic outbreaks of febrile illness in Africa, Europe, and India (Russell and Dwyer, 2000).

1.3 WEST NILE VIRUS GENOME AND MORPHOLOGY

The WNV genome is a positive, single – strand RNA roughly 11029 bases long. The ends are flanked by noncoding untranslated regions (UTR) and contains a single open reading fame of 10301 bases that encodes for ten proteins. There are three structural proteins at the 5’ end: C, prM, and E; while the remaining portion encodes the non – structural proteins: the large highly conserved NS1, NS3, and NS5, and four small hydrophobic proteins; NS2a, NS2b, NS4a, and NS4b.

Figure 2 below shows the general genome layout for flaviviruses (International Committee on Taxonomy of Viruses, 2000).

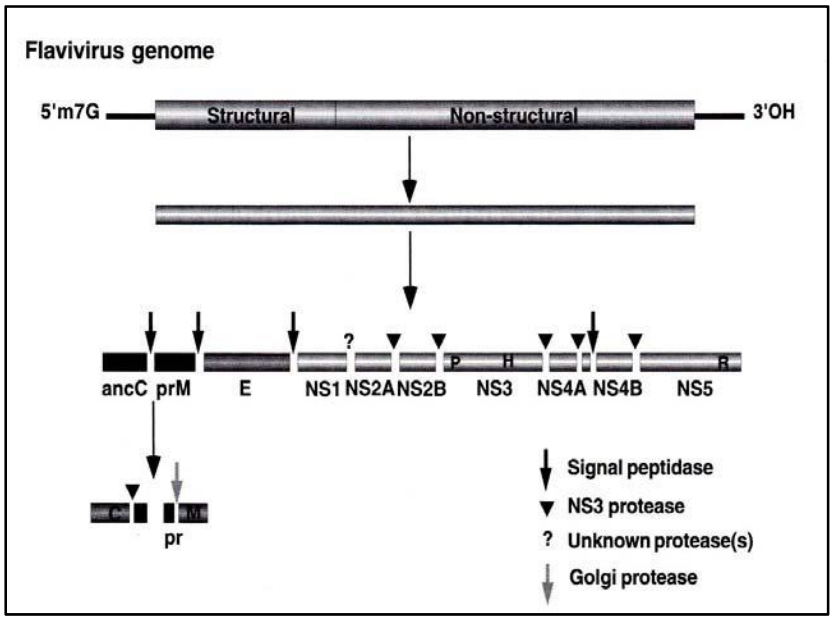

Figure 2: The flavivirus genome organisation.

The C protein is important for virus genome encapsidation and is highly conserved within the WNV strains as well as within the different dengue strains but significantly different when comparing the different members of flaviviruses (Ma *et al.*, 2004). The 25 – 30 nanometers diameter virus internal core containing RNA is encapsulated within C protein spherical or isometric neucleocapsid. Absence of this core gene results in infected cells releasing subviral particles lacking both neucleocapsid and virus RNA (Ferlenghi *et al.*, 2001). The core is surrounded by a lipid membrane. Interspersed throughout the membrane covering are the E and prM proteins (Mukhopadhyay *et al.*, 2003). The prM protein is processed to pr + M protein late in the virus maturation process by a convertase enzyme (furin). This results in mature 50 nanometers spherical virions (Mackenzie *et al.*, 2004). The virus then either buds from the infected cell for WNV Sarafend (WNVS) or

through exocytosis for other flaviviruses. The prM protein is an important chaperone for proper folding and transport of E protein during virus particle exocytosis (Lorenz *et al.*, 2002).

The E protein is the largest of structural proteins and is present on the virus surface. It possesses projections of 5 – 10 nanometers long with terminal knobs of two nanometers in diameter (Schlesinger, 1980). There are three domains within the E protein. Little is known of Domain I. Domain II is suggested to be important during virus entry process as exposure of this domain to low pH results in epitope destruction allowing virus fusion to the endocytic vesicle membrane (Mandl *et al.*, 1989). This is interesting because other flavivirus such as hepatitis C virus and bovine viral diarrhoea virus are acid resistant (Tscherne *et al.*, 2006). Domain III is strongly postulated to act as the receptor binding domain of the virus as it has an Ig – like fold commonly associated with glycoproteins with adhesion functions. This domain also extends perpendicularly up from the virus surface and is thus the most exposed region (Rey *et al.*, 1995). Moreover, mutations in domain III have been reported to cause changes in virus infectability in mice as well as cell cultures (Beasley *et al.*, 2002; Bordignon *et al.*, 2007; Ciota *et al.*, 2008).

Most of the non – structural (NS) proteins associate to form the replicase complex, which traditionally was thought to function only in RNA accumulation (Murray *et al.*, 2008). Recently, unique roles of various NS proteins are beginning to be known and have now emerged as integral components in the process of virion morphogenesis. The NS1 protein can be detected in both intracellular and extracellular fractions of infected cells at early

virus infection time points (Smith and Wright, 1985). It is thus postulated that NS1 protein has a role to play in early virus replication. It was also found to co – localise to double stranded viral RNA, NS4a protein, and intracellular membranes (Lindenbach and Rice, 1999). This shows that NS1 protein plays multiple roles during virus infection and replication.

The NS2a protein is an essential component of the virus replicase. Mutations in the NS2a gene results in uninfectious yellow fever virus production (Kummerer and Rice, 2002). The NS3 protein represents the main viral protease with its associated cofactors NS4a and NS2b protein (Murray *et al.*, 2008). It shows RNA helicase, serine protease, and nucleoside triphosphatase activities that are essential for viral RNA replication (Kramer *et al.*, 2007). The NS2b - NS3 protease mediates the cleavage of the virus polypeptide at various locations, in particular, the C protein from its membrane anchor C – prM precursor which is crucial for the proper maturation of C protein (Chambers *et al.*, 1990). NS4a and NS4b are cofactors which maintain proper NS3 structure by anchoring the enzyme to the membrane. The presence of NS4a also significantly increases the activity of NS3 (Agapov *et al.*, 2004).

NS5 is the largest and most conserved of the NS proteins. It is also known to be the viral RNA – dependant RNA polymerase (RdRp). It is important for RNA synthesis and genome capping. This region has very highly conserved zinc – binding motifs and is phosphorylated by a putative NS5a kinase. The polymerase activity of NS5 protein is of importance as replication – imcompetent genomes were not incorporated into WN Kunjin

virions (Khromykh *et al.*, 2001; Reed *et al.*, 1998; Yap *et al.*, 2007). NS5 protein also contains N-7 and 2'O-methyltransferase which is involved in the methylation of the 5' RNA cap structure (Kramer *et al.*, 2007).

1.4 WEST NILE LINEAGES

Nucleotide sequencing, serology, and phylogenetic analysis of WNV genomes based on the entire or partial viral gene sequences differentiated WNV into two lineages: lineage I and lineage II (Berthet *et al.*, 1997). Lineage I and II can only be separated by very specific molecular techniques because they are antigenically very similar (Linke *et al.*, 2007). Lineage I is divided into three clades. The first clade, Ia, is found worldwide (Africa, Europe, and North America), Ib is found in Australia as Kunjin virus (Lanciotti *et al*., 1999), while clade Ic were isolates from India (Umrigar and Pavri, 1977).

Lineage II on the other hand defines viruses from sub – Saharan Africa and Madagascar (Scherret *et al*., 2001). Lineage I has been traditionally linked to higher pathogenicity and outbreaks in human populations while lineage II is often associated with endemic zoonotic infections. Still, it has been shown that lineage II viruses could also cause outbreaks in South Africa and the Middle East (Burt *et al.*, 2002; Jia *et al.*, 1999). Recently, Rabensburg and Russian isolates were suggested to form lineage III and IV of WNV, respectively (Bakonyi *et al.*, 2005; Lvov *et al.*, 2004). Another group has recently proposed that WNV isolates from India form the fifth lineage of WNV (Bondre *et al.*, 2007).

1.5 CLINICAL SYMPTOMS OF WEST NILE VIRUS INFECTION

While the majority of WNV infections are asymptomatic, it can cause disease in humans and animals, with symptoms ranging from febrile illness to fatal encephalitis. About 20 percent of infected patients display a range of symptoms including fever, headache, malaise, back pain, myalgias, eye pain, pharyngitis, nausea, vomiting, diarrhoea, and abdominal pain. Incubation period is typically between two to fourteen days although in immunosuppressed patients it could last for much longer (Pealer *et al.*, 2003). Out of these 20 percent, maculopapular rash appears in approximately half the patients. The rash spreads to the chest, back, and arms, and generally lasts for less than one week. Other acute symptoms generally subside after two weeks but a subset of these patients would acquire more serious clinical manifestations, including neurological effects (Petersen and Roehrig, 2001; Watson *et al.*, 2004).

More serious manifestations of WNV are categorized as: encephalitis, meningitis, and flaccid paralysis, with the former two more common (Nash *et al.*, 2001). Muscle weakness and flaccid paralysis are particularly suggestive of WNV infection (Petersen and Marfin, 2002). Asymmetric acute flaccid paralysis syndrome could also occur independent of encephalitis and has been noted to be a sign of impending respiratory failure (Sejvar *et al.*, 2005). Neurological manifestations of WNV are quite similar to Japanese encephalitis and St. Louis encephalitis. Tissue damage is seen in the meninges contributing to meningitis, in the brain parenchyma contributing to encephalitis, and in the spinal cord contributing to myelitis. In the recent outbreak of WNV in North America, generalized muscle weakness, later described as poliovirus – like flaccid

paralysis was recognized in most of the infected patients (Sejvar *et al.*, 2003). Older (Chowers *et al.*, 2001) and immunocompromised individuals (George *et al.*, 1984) have an increased risk of developing fatal disease.

Long term studies on patients who recovered from WNV infections with meningitis or encephalitis have found that for patients below 65 years of age, only 37 percent achieved full recovery after 12 months (Marciniak *et al.*, 2004). Lasting abnormalities after 18 months for some patients included muscle weakness, loss of concentration, confusion, and light – headedness. For patients suffering from WNV poliomyelitis, there is incomplete recovery of limb strength resulting from profound residual deficits. In severe cases of quadriplegia and respiratory failure where there is a high level of mortality, recovery is slow and invariably incomplete (Betensley *et al.*, 2004). For nonneuroinvasive WNV infections, 92 patients with a mean age of 50 years were found to recover from fatigue, depression, and had full physical and mental function after one year (Loeb *et al.*, 2008). Evident latency of virus in humans has not been reported as yet.

1.6 TRANSMISSION

The WNV is transmitted by *Culex* mosquitoes primarily between birds, the amplifying hosts of the virus. Mosquitoes also function as bridge vectors for transmission to humans, and other mammals (Turell *et al.*, 2005). Although wild birds can develop high levels of viremia, most remain asymptomatic (Komar *et al.*, 2003). However, significant avian mortality has been reported in United States and Israel where both countries share similar WNV genetic strains (Swayne *et al.*, 2001). North American *Corvids*, including ravens,

jays, and crows, are susceptible to the virus. *Corvids* made up approximately sixty percent of collected dead birds tested positive for WNV (Tsai *et al.*, 1998).

Humans are considered dead – end hosts because they usually develop viremia at an insignificant level to facilitate further transmission of the virus. West Nile virus transmission has also been reported resulting from organ transplantation (DeSalvo *et al.*, 2004; Jain *et al.*, 2007; Murtagh *et al.*, 2005; Wadei *et al.*, 2004), blood transfusion (Macedo de Oliveira *et al.*, 2004; Montgomery *et al.*, 2006), pregnancy (Jamieson *et al.*, 2006; O'Leary *et al.*, 2006; Skupski *et al.*, 2006), and lactation (CDC, 2002a). Occupational WNV infections in laboratory workers have also been documented (Hamilton and Taylor, 1954).

1.7 EPIDEMIOLOGY

Following a 1998 European outbreak, WNV came into the spotlight in 1999 when it was identified for the first time in the Americas (Lanciotti *et al.*, 1999). The number of cases peaked in 2003 following the spread of WNV to the whole of Northern America, México, and Canada. *Table 1* summarises the case numbers in the United States from year 2000 to 2008 according to the Centers for Disease Control and Prevention (CDC) while *Figure 3* shows the global reach of various flaviviruses.

Table 1: Confirmed WNV case numbers from 2000 to 2008.

Year	Case numbers	Reference
2000	21	(CDC, 2002b)
2001	66	(CDC, 2002b)
2002	4,156	(O'Leary *et al.*, 2004)
2003	9,862	(CDC, 2003)
2005	2,744	(CDC, 2005)
2006	4,261	(CDC, 2007a)
2007	3,304	(CDC, 2007b)
2008 (Jan – Jul)	43	(CDC, 2008)

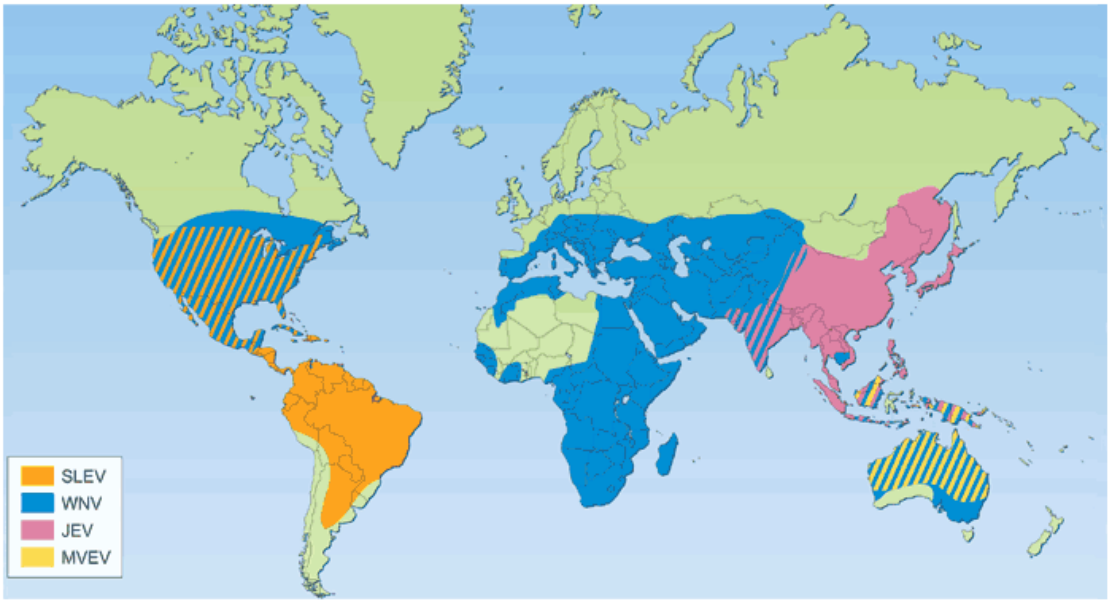

Figure 3: Spread of flaviviruses worldwide (Mackenzie et al., 2004).

Prior to this, WNV outbreaks had been sporadic and limited to febrile reactions until the 1990's when patients with more severe neurological disease started to appear in clusters of infection in Romania, Russia, and Israel (Chowers *et al.*, 2001; Platonov *et al.*, 2001; Tsai *et al.*, 1998). As the circulating strain in the United States is genetically identical (99.7 %) to a virus strain found in Israel, epidemiologists suggest that migrating birds imported the virus from the Mediterranean into United States (Ceccaldi *et al.*, 2004; Lanciotti *et al.*, 1999).

In 2001, a Cayman Islands resident was found to have developed WNV encephalitis (Bernard and Kramer, 2001). Later serological testing in birds and horses from surrounding regions showed WNV to be present in the Dominican Republic, Jamaica, Guadeloupe, El Salvador, Colombia, and Mexico (Cruz *et al.*, 2005; Estrada-Franco *et al.*, 2003; Mattar *et al.*, 2005; Quirin *et al.*, 2004). However, virus isolation from human or animal cases are infrequent, raising questions as the serological and morbidity reports

did not correlate. Another hypothesis could be that the virus had reverted from being neuroinvasive with severe morbidity to mild and lacking CNS infection potential.

WNV has not been isolated in Singapore but there is a significant probability that it could one day be endemic to this region as out of the 2500 species of mosquitoes found worldwide, Singapore has around 100 identified mosquito species including *Aedes albopictus* and 35 species from the *Culex* genra which are the main carriers of WNV in the United States (Walter Reed Biosystematics Unit, 2008). The small island is also known as an important site for migratory bird stopovers between north and central Asia to Australia. This is of significance as it was migratory birds coming from Israel into the United States that was suggested to be the propagator of WNV.

1.8 THE NEED FOR AN *IN VIVO* MODEL

Testing of drugs or vaccine candidates against WNV can only be successfully performed if there exists a good animal model that mimics the morbidity, symptoms of infection, and mortality rates seen in human patients. Consequences of infection and the virus pathogenicity needs to be understood in animal models before testing of promising therapies is possible. At the moment, only vaccines licensed for veterinary use are available.

1.8.1 Mouse Models to Study West Nile Virus

Mice are the most commonly used model for WNV investigation. There is a plethora of different strains to choose from, inbred and outbred, transgenic and knockout. Strains can also be divided into immunocompetent and immunoincompetent mice types; all having

different roles to play. The former predicts how a normal immune system would respond to an infection while displaying full viral pathogenesis; making it a good vaccine efficacy test model. Conversely, specific transgenic or knockout mice mimic immunocompromised subjects and are used to study particular immunological response pathways affected by either virus or host. *Table 2* summarizes some major strains of virus and mice used in past WNV studies. Note that models work as a pair; the virus and mouse strain must be specific.

Table 2: Summary of different mice and WNV strains tested.

Mouse strain	**WNV strain**	**Characteristics**	**Reference**
BALB/c	1952 human isolate	Neuroinvasive, 100 % mortality	(Ben-Nathan *et al.*, 2003)
Swiss	SA89, SEN90, USA99b	Neuroinvasive, 100 % mortality	(Beasley *et al.*, 2002)
	CYP68, AUS60, MAD78	Nonneuroinvasive, LD_{50} >10000	(Beasley *et al.*, 2002)
	NY99	Neuroinvasive, very virulent, LD_{50} = 17 PFU	(Borisevich *et al.*, 2006)
C57BL/6	NY2000	30 % mortality	(Sitati and Diamond, 2006)
	WNVS	At low dose: neuroinvasive but mortality approximately 30 %	(Wang *et al.*, 2003)
	Unnamed equine isolate	50 % mortality	(Garcia-Tapia *et al.*, 2006)
Wild field mice	Isr98	Resistant to infection	(Mashimo *et al.*, 2002)
$CD4^{-/-}$	NY2000	Persistent infection, low antibody response, 100 % death at 10^2 PFU	(Sitati and Diamond, 2006)
TLR3 $^{-/-}$	NY99	Reduced neuropathology and inflammation, 40 % less mortality	(Wang *et al.*, 2004a)
Fas Ligand $^{-/-}$	NY99	Eeffector of $CD4^+$ cells, 100 % mortality	(Sitati and Diamond, 2006)
	WNVS	Increased mortality if coupled with perforin knockout (29 % to 63 %)	(Wang, 2004b)
IFN β $^{-/-}$	NY99	High virulence, increased mortality from 90 % to 100 %	(Samuel and Diamond, 2005)

Mouse strain	WNV strain	Characteristics	Reference
IFN γ $^{-/-}$	WNVS, KUN	IFN γ does not play a significant role in WNV infection	(Wang *et al.*, 2006)
	NY99	Higher viremia, mortality increased from 30 to 90 %, neuroinvasive	(Shrestha *et al.*, 2006b)
$CD8^+$ T cell depleted	WNVS	Increased mortality from 27 % to 70 % at 10^2 PFU	(Wang *et al.*, 2003)
CCR5 $^{-/-}$	NY99	Increased mortality from 30 % to 100 %, reduced leukocyte trafficking	(Glass *et al.*, 2005)

Both the breed of mice and strain of virus play an important role in defining the pathogenicity and prognosis of the infection. This is clear from the different virus strains used to infect Swiss and BL6 mice as seen in *Table 2*. One interesting experiment found caught wild field mice totally resistant to WNV infection but nonsense point mutations in lab breed mice at the 2' - 5'oligoadenylate synthetase gene increased its susceptibility to WNV infection. Mashimo and colleagues (2002) mapped microsatellite markers from BALB/c, 129, C3H, C57BL/6, and eleven other lab mouse strains to arrive at this conclusion. The gene was later found to be regulated by IFNβ (Scherbik *et al.*, 2006). Similar markers if found in specific human populations would have grave implications.

Promising vaccines normally undergo preclinical tests for safety and efficacy on mice before clinical trials are conducted. A WNV / DV chimera DNA vaccine was tested on outbreed Swiss and SCID mice and the chimera showed greatly reduced neuroinvasiveness in mice (Pletnev *et al.*, 2006) while a WNV / Yellow fever chimera safety test successfully used ICR mice to ensure the virus showed no infectivity at high doses (Arroyo *et al.*, 2004). This mouse strain was also used to test a lentiviral delivery

system and the strong humoral response elicited was able to withstand a virus challenge later (Iglesias *et al.*, 2006). These vaccines are now in later phases of clinical trials.

Antibody treatment has been noted to be a potential WNV treatment strategy. Pregnant mice infected with WNV and treated with humanized anti – WNV immunoglobulins had a higher dam survival rate and could potentially be used to treat foetal WNV infection in humans (Julander *et al.*, 2005). This is important as WNV – infected pregnant BALB/c mice had an 88 percent higher chance of mortality as compared to uninfected pregnant mice (Cordoba *et al.*, 2007). Unfortunately, no parallel observation has been documented in humans.

To study the mechanism of neurovirulence and the body's immunological response, C57BL/6 mice were infected with WNV and sacrificed at different time points to determine the level of leukocyte infiltration into the central nervous system. It was found that the level of $CD45^+$ cells in the CNS was related to the severity of mice hind leg paralysis and three stages were recognized: non – infected, infected, and infected with paralysis. The three stages could also be differentiated by histopathology and virus antigen labelling by immunohistochemistry (Shrestha *et al.*, 2003). Antigens of WNV were found specifically in the cortex, hippocampus, and choroid plexus (Hunsperger and Roehrig, 2006). This confirms neurons as a target for WNV infection and improves our understanding on its specific brain tissue tropism. Macrophages are also an important factor for neuroinvasion and encephalitis as macrophage – depleted mice showed higher mortality levels compared to the wild type (Ben-Nathan *et al.*, 1996). IFNβ has been

found important for restricting the virus growth in both CNS and peripheral tissue. The high virus loads in IFNβ$^{-/-}$ mice resulted in neuronal apoptosis, encephalitis, and higher mortality (Samuel and Diamond, 2005).

Using knockdown animal models, the once unknown virus effectors and immune pathways involved can now be thoroughly studied. CD4^{+} T cell knockout mice was found unable to resolve primary WNV infection as without CD4^{+} cells, the virus retains very high titres in serum and organs, leading to mortality. CD4^{+} cells were able to prime antibody production, activate CD8^{+} cells, and kill virus – infected cells through the Fas – Fas ligand pathway (Sitati and Diamond, 2006). A screening of CD4^{+} levels in WNV patients could potentially serve as a means of prognosis.

CD8^{+} T cell on the other hand is important for both viral clearance and pathogenesis. At low viral loads, CD8^{+} cells blocked virus entry into the brain but at high viral load, CD8^{+} cells were overwhelmed and caused an inappropriate immune response that reduced survivability (Wang *et al.*, 2003). Further studies with perforin – knockout mice, a downstream effector of CD8^{+} cells, found that CD8^{+} cells alone were incapable of virus clearance without perforin (Shrestha *et al.*, 2006a).

Mice experiments are not without its conflicts. Different groups using similar IFNγ knockdown mice (another CD8^{+} effector), but different WNV strains and different route of infection published opposing results. One group found IFNγ$^{-/-}$ mice had slightly higher survival rate when injected intravenously with 10^{8} units of WNVS while another group

using 10^2 units of WNV NY99 injected through the mouse footpad had shorter mean survival times and higher viremia levels (Shrestha *et al.*, 2006b; Wang *et al.*, 2006). Clearly, although almost identical in nucleotide sequence, both virus strains utilise unique pathogenic pathways. Sarafend is a laboratory strain believed to be a human isolate from Israel from the 1950's (Scherret *et al.*, 2002) while WNV NY is a strain isolated from a dead crow during the 1999 outbreak (Komar *et al*., 2003).

Toll – like receptors (TLR) are key players in the innate immunity as it primes downstream immunological cascades. These receptors upregulate $CD4^+$ response and interferon levels. It was found that TLR3 knockout mice had higher levels of viremia in peripheral tissues but lower levels in the CNS and reduced signs of encephalitis, increasing survival rates (Wang *et al.*, 2004a). This suggests that TLR3 activation induces a cytokine storm causing the breach of the blood – brain barrier leading to encephalitis. CCR5 is a chemokine receptor that recruits NK, macrophages, $CD4^+$, and $CD8^+$ cells to the brain and can cause the blood – brain barrier to become porous and leaky, allowing viruses in. Intuitively, CCR5 should favour virus survival in the CNS but it was found that $CCR5^{-/-}$ mice showed lower virus burden but also had correspondingly lower levels of recruited immune cells, leading to increased mice mortality from 40 percent to 100 percent. Thus, the regulating of immune cells by CCR5 to the brain is vital for virus clearance (Glass *et al.*, 2005).

Mutations in the virus genome can also lead to the loss or acquisition of neurovirulence, specific organ tropism, or change in mortality levels. Point mutations in the NS4B region

of WNV were found to attenuate its neurovirulence (Wicker *et al.*, 2006) while mutations in NS2A or NS3 genes slowed down virus growth but led to persistent infection in Swiss mice (Rossi *et al.*, 2007). This is important as timely typing of circulating strains could predict the virus genetic drift, giving time to initiate health plans. Specific mutations in the domain III of the viral envelope protein can also give rise to viruses displaying different levels of neuroinvasiveness. (Chambers *et al.*, 1998).

1.8.2 Mouse Models to Study Dengue Virus

Dengue virus (DV) is a very close cousin of WNV from the same genus *Flaviviridae.* Over the years, two different animals were mainly used to model dengue infection; non – human primates and mice. Like for WNV, simian models are difficult to work with and may transmit the disease to man (Gubler and Kuno, 1997; Lei *et al.*, 2001). Even though monkeys are the closest model to mimic human infection, the lack of correlation with serious disease in humans makes it an unlikely choice. This is because monkeys can get infected with the virus but show little or no signs of infection (Eckels *et al.*, 1994). Since the study of dengue haemorrhagic fever (DHF) and dengue shock syndrome (DSS) relies greatly on histopathology and clinical signs, this model has been largely replaced by the mouse. There are a few mouse strains that were successfully infected with DV and showed high viremia (Charlier *et al.*, 2004).

The best known model is suckling mice inoculated intracerebrally with virus causing encephalitis (Despres *et al.*, 1998; Lucia and Kangwanpong, 1994). Encephalitis is something rare in human dengue infections (Lum *et al.*, 1996) making this an unrealistic

model for DHF since the clinical manifestation seen are not systemic and capillary leakage is rare in clinical cases. However, other immunocompetent mouse strains quickly clear the virus and have very short infection periods (Hotta *et al.*, 1981).

Severe combined immunodeficient (SCID) mice reconstituted with human hepatocarcinoma cells (Marianneau *et al.*, 1996) displays viremia in many organs after inoculation. However, there is difficulty in reconstituting graft cells and the low frequency of mice infection following virus inoculation makes it an unreliable model (An *et al.*, 1999; Wu *et al.*, 1995). Other models include the SCID mouse (An *et al.*, 2003), BL6 (Raut *et al.*, 1996), ICR (Boonpucknavig *et al.*, 1981), A/J (Shresta *et al.*, 2004a), C57BL (Chen *et al.*, 2004), and BALB/c (Huang *et al.*, 2000). Each model successfully duplicates one area of dengue infection but not the entire disease spectrum.

The C57Bl mouse is used to study T cell activation during virus infection, SCID is useful for CNS infection studies, ICR mouse model for studies focused on encephalitis while the BALB/c model displays thrombocytopenia. None however could replicate the whole spectrum of symptoms found in human infection (Huang *et al.*, 2000; Zhang *et al.*, 1988). However, *in vivo* models are still needed to understand viral pathogenesis (Kurane *et al.*, 1990; Marianneau *et al.*, 1999).

Interferons (IFN) are the first line of host defense against virus attacks as without it the virus infection increases in severity (Sen, 2001). This is of interest as immunocompetent mice have a low DV infection probability and viremia is almost impossible to establish

(Boonpucknavig *et al.*, 1981). Thus, the AG129 mouse with a double knockout of interferon α / β and γ receptors is more susceptible to DV infection (van den Broek *et al.*, 1995). Interferon alpha and beta share the same receptor while interferon gamma uses a unique one. IFNs also play important roles in complex antigen expression, inhibition of cell growth, hematopoiesis, and regulation of cellular and humoral immune response. However, Yang and colleagues (1995) reported on the importance of IFNs in initiating vascular leakage and shock. Also, soluble tumour necrosis factor receptor levels have been found to be correlated to disease severity in DHF patients (Bethell *et al.*, 1998). This suggests that AG129, lacking IFN receptors could be more susceptible to DV but unable to mount cytokine responses to such a magnitude as to cause haemorrhage or shock, making it a less useful dengue virus model.

Such fears were dispelled when DV was found able to replicate in and kill AG129 mice (Johnson and Roehrig, 1999; Shresta *et al.*, 2004b). These studies used mouse – adapted DV strains and found IFN receptor action to be more important in virus clearing compared to B or T cells. Mice were unable to survive for more than thirty days post inoculation with a 10^8 PFU virus load. However, no histopathological studies were performed.

1.9 TECHNIQUES USED TO STUDY PATHOLOGICAL CHANGES

To visualize the disease progression in a model, histopathological observation of tissue samples is essential. Differences between uninfected and infected samples will show virus activity and the tissue reactions. The standard haematoxylin and eosin method is

widely used and sections are processed from paraformaldehyde – fixed, paraffin – embedded tissue samples. Pathological evidences are usually consistent with disease progression (Peyrefitte *et al.*, 2003).

Immunolocalization of virus antigens is also of importance as the cells in which flaviviruses replicate in remain undeciphered (Rosen *et al.*, 1989). There are reports of flavivirus antigens and RNA being detected in many different cell types in the body. This includes the thymus, kidney, lung, skin, perivascular blood monocytes, liver, and spleen. Strong evidence also exists for monocytes, fibroblasts, epithelial cells, hepatocytes, and endothelial cells supporting DV replication (Jessie *et al.*, 2004; Killen and O'Sullivan, 1993). It is thus important to observe if the same cell types are involved in virus infection in mice and man.

Immunolabelling exploits the specific binding trait between antibodies with its corresponding antigen. This binding site is then identified by attaching a probe to the complex. Two types of probes are often used, i.e. fluorescent label or gold – silver complex. Immunogold staining was first used in electron microscopy (Faulk and Taylor, 1971) but soon extended to light microscopy (Holgate *et al.*, 1983). This technique has been evolving for more than two decades (Danscher and Norgaard, 1983) and is more specific than other enzyme markers like immunoperoxidase or immunofluorescence. Just two secondary antibodies with gold conjugates binding to the antibody – antigen complex are enough to initiate a silver deposit around the tissue area. This leads to the development of a silver signal that can be seen by light microscopy.

The coloured substrate, diaminobenzidine (DAB), which is a commonly used substrate, is known to give nonspecific staining and false positives (Danscher and Norgaard, 1983). Gold is not toxic compared to benzene, the parent compound of DAB, a potential carcinogen. The sensitivity level of gold – silver enhancement is far higher than that of avidin – biotin, another routinely used enhancer in immunoperoxidase methods. In addition, silver does not fade while chromogen stains do over time and double – labelling is easily performed with gold particles but not with immunoperoxidase. The amount of antibodies and reagents saved because of the heightened sensitivity of the gold labelling technique has been found to outweigh its costs (Holgate *et al.*, 1983).

The visualization of silver particles on tissue sections requires a technology known as reflection contrast microscopy (RCM) or epi – illumination, an established but not widely used method (Filler and Peuker, 2000). It is able to produce superior images and has been said to bridge the gap between light and electron microscopy (Prins *et al.*, 2006). The uniqueness of RCM is in its ability to suppress stray reflections which allows a wider useful range of magnification. Particles as small as five micrometers in diameter and sections as thin as 200 nanometers can be visualized using this method, allowing simultaneous processing destined for both light and electron microscopy. Because gold – silver granules strongly reflect light, it will appear as bright spots under RCM and can be easily identified (Gao *et al.*, 1995). The reflected light can also be complimented with transmitted light to display the regular morphology of the sections for better cell orientation (De Waele *et al.*, 1986). Biological markers will stand out much stronger with

RCM as compared to normal illumination, adding colour, quantitative ability, and sensitivity to detection methods (Neelissen *et al.*, 1999).

1.10 EFFECTS OF VIRUS PASSAGING

It is known that RNA viruses easily acquire genetic changes due to mutations or reassortment of its genome. These viruses utilize an error – prone RNA – dependent RNA polymerase replication system. Coupled with the large population sizes of viruses found in some hosts during infection, this would lead to high levels of genetic diversity (Moya *et al.*, 2004). A rate of approximately one mutation for every 10000 basepairs replicated was suggested for RNA viruses (Drake and Holland, 1999). Such rates of mutation could easily change the virus host specificity, possible modes and dose of transmission, shift in virulence, and antiviral drug reaction.

The SARS coronavirus can infect the respiratory tract of inbred mice but does not cause illness following infection. This virus was passaged through BALB/c mouse lungs for fifteen rounds and virus clones isolated from tissue homogenates were found to result in up to 100 percent mortality in adult BALB/c mice (Roberts *et al.*, 2007). A mutant tick – borne encephalitis virus carrying a deletion mutation that rendered it non – infectious in BHK cell culture could be rescued by natural mutation and selection after passaging the virus through BHK cells for five consecutive rounds (Elshuber and Mandl, 2005).

West Nile virus that was passaged for six rounds through HeLa cells was found attenuated 4000 – fold in adult mice when inoculated intraperitoneally or intranasally. The virus was also found antigenically different and temperature – sensitive. Another strain of WNV from Egypt was passaged through a similar six rounds and found to have lost its ability to infect Vero cells and no longer killed adult mice (Dunster *et al.*, 1990). The WNV passaged in hamsters for three rounds caused amino acid substitutions in the E, NS1, NS2B, and NS5 regions and produced an asymptomatic persistent infection in adult hamster kidneys. This was accompanied by a loss of virulence and a change in plaque morphology (Ding *et al.*, 2005).

In another study, strains of WNV from different passaging regimes were found to have different neuroinvasive properties and this was mapped to point mutations at the viral genomic position 68 corresponding to an E protein glycosylation site. Notably, a strain of highly mosquito cell – passaged WNV possessing this glycosylated site was found to be 325 – fold less neuroinvasive than its parental strain (Chambers *et al.*, 1998). However, another study using 19 distinct and differently passaged WNV strains found no strong correlation between presence or absence of potential glycosylation sites and mouse neuroinvasiveness (Beasley *et al.*, 2002) . The same study also showed that neuroinvasive virus strains had more variations in sequence as compared to noninvasive species. This tells us that viral neuroinvasiveness is controlled by multiple points in the genome and may be a result from an interplay between different regions of the virus genome or different subpopulations of viruses during a co – infection.

Homogeneous WNV from an infectious clone was passaged twenty times serially in either *Culex* mosquitoes or SPF chickens (Jerzak *et al.*, 2007). The mosquito – passaged virus showed greater genetic diversity and heterogeneity but killed fewer mice because certain acquired mutations resulted in noninvasiveness. The chicken – passaged virus however retained its level of virulence. A similar experiment using mosquito and avian cell cultures found WNV passaged through insect cell lines having increased relative fitness and replicative ability linked to more numerous amino acid changes in the viral genome. The opposite effect was found for virus grown in avian cell cultures (Ciota *et al.*, 2007c).

These experiments clearly exemplify the fact that viruses are ever evolving. As such, carefully planned experiments could in fact engineer the direction of viral evolution. Species infectivity and mortality levels are parameters that could be altered to adapt to new environments and hosts.

1.11 OBJECTIVES

West Nile virus and dengue virus infections are important emerging infectious diseases. Much effort has gone into the research of antivirals and other possible drugs to reduce or stop these viruses from spreading. Such a drive requires a good animal model to bolster experimental viability.

The objectives of this study can be summarised as:

a) To adapt the less pathogenic lineage II West Nile virus (Sarafend) from a mouse non – neuroinvasive to a neuroinvasive strain in an immunocompetent mouse lineage by serially passaging the virus in a manner mimicking its natural infectious cycle. This allows for studies on WNV pathogenesis to be performed at BSL 2 instead of BSL 3 which is required for WNV lineage I strains.
b) To document viral growth changes during this adaptive process.
c) To compare passaged and unpassaged virus characters in immunocompetent mice through:
    i. Detecting pathological differences in various organs of adult mice infected with passaged and unpassaged viruses.
    ii. Sequencing selected genes of passaged and unpassaged virus genomes to detect regions of mutations.
    iii. Testing of passaged and unpassaged virus morbidity and mortality levels in suckling and adult mice.
    iv. Infecting primary mouse neural cells with passaged and unpassaged viruses to observe for changes in virus growth kinetics.

Such a virus – mouse combination model would contribute greatly to the area of anti – viral and vaccine candidate testing.

CHAPTER 2
MATERIALS AND METHODS

2.0 MATERIALS AND METHODS

2.1 CELL CULTURE TECHNIQUES

All solutions and media for cell culture were made with deionised E - Pure™ water (Barnstead, New Hampshire, USA). All cell culture and media preparation works was performed under aseptic conditions in a Class II Type A2 BSC hood (Esco Pte. Ltd., Singapore).

Cells used in this study were grown in sterile 25 cm^2 or 75 cm^2 plastic tissue culture flasks (Iwaki Glass, Tokyo, Japan), and 24 – well or 96 – well tissue culture plates (Greiner Bio – One, St. Louis, USA). Cells were either cultured in a humidified incubator (Thermo Fisher Scientific, Massachusetts, USA) with carbon dioxide (5 %) or a dry incubator (Memmert GmbH, Schwabach, Germany). Only the mosquito cell line C6/36 was grown in the dry incubator.

2.1.1 Cell Lines

Cell lines that were used in this study are listed in *Table 3*. The media type, passage numbers used for experiments in this project, and origin of the cell lines are included. All lines used are adherent cell types.

2.1.2 Media and Solution for Cell Culture

Culture media supplemented with 10 % foetal bovine serum (PAA Laboratories GmbH, Austria) was used as the growth medium (*Appendix 1a to d*) for the respective cell lines. The media pH was adjusted to approximately 7.3 with 1 M sodium hydroxide and 1 M hydrochloric acid (*Appendices 1e and 1f*).

Table 3: Cell lines and related information.

Cell Line	Culture media	Cell Passage Levels	Origin
Vero, African Green Monkey Kidney cells	Media 199 (M199)	90 – 110	Kind gift from Emeritus Professor Edwin Westaway, Australia
C6/36, mosquito cell derived from *Aedes albopictus*	L15	70 – 100	Kind gift from Emeritus Professor Edwin Westaway, Australia
BHK 21 (clone 13), kidney fibroblast, baby hamster kidney	RPMI	95 – 150	American Type Culture Collection, USA
Primary neural mice cells, from foetal mice	Neurobasal or DME	1	Laboratory produced

2.1.3 Cultivation and Propagation of Cell Lines

Flasks of cells were sub – cultured from confluent 75cm^2 flask monolayers at a ratio of 1 : 5 (Vero and BHK 21 cells) or 1 : 4 (for C6/36 cells). The growth medium (*Appendix 1a to d*) was first discarded. The monolayer was then rinsed with 5 millilitres of phosphate buffered saline (PBS - *Appendix 1g*). This was followed by incubation with 2 millilitres of trypsin (*Appendix 1h*). The flask was left for two minutes at 37 °C to detach the cell monolayer from the flask. The cells were then dislodged by gentle tapping. Appropriate amounts of growth media (total of 10 millilitres for 75cm^2 and 5 millilitres for 25 cm^2 flasks) were added to the cell suspension to inactivate the enzymatic activity of the trypsin. Cell aggregates were dispersed by pipetting up and down to give a single cell suspension. The suspended cells were then aliquoted into new tissue culture flasks. The cells were then incubated at 28 °C for C6/36 cells or 37 °C for all other cell types. The monolayer would reach confluency in two weeks for primary astrocytes or three days for other cell lines and

used for experiments. The production of the primary cell lines is described in *Section 2.3.7*.

2.1.4 Cultivation of Cells in 24 – Well and 96 – Well Tissue Culture Tray

A confluent cell monolayer of BHK 21 in a 75 cm^2 tissue culture flask was used to seed four 24 – well plates (Greiner Bio – One, St. Louis, USA). The cell monolayer was treated as previously described (*Section 2.1.3*) to produce a single cell suspension. The cell suspension was then made up to a final volume of 48 millilitres using appropriate cell culture growth medium (*Appendix 1a to d*). Aliquots of half a millilitre was transferred into each well of the 24 - well plates. The trays were then incubated at 37 °C in a humidified incubator (Thermo Fisher Scientific, Massachusetts, USA) with 5 % carbon dioxide. The monolayers were confluent in 24 hours and ready for use.

2.2 INFECTION OF CELLS

2.2.1 Viruses

The viruses used in this study are given in *Table 4*. The stock viruses previously grown on a Vero cell monolayer were amplified in Vero or C6/36 cells for this study. Viruses were harvested at the appropriate timing post – infection (p.i.) from infected cell monolayers as indicated in *Table 4.*

Table 4: Viruses used in this study

Virus Family	Virus Name	Strain	Source	Virus harvest Time
Flaviviridae	West Nile	Sarafend (WNVS)	A gift from Emeritus Professor Edwin Westaway, Australia	24 hours post infection (Vero or C6/36 cells)
Flaviviridae	Dengue	Serotype 1 (DV1)	Kind gift from Dr. Ling Ai Ee, Singapore General Hospital	7 days post infection (C6/36 cells)
Flaviviridae	Dengue	Serotype 2 NGC (DV2)	ATCC, USA	3 days post infection (C6/36 cells)
Flaviviridae	Dengue	Serotype-4 (DV4)	ATCC, USA	7 days post infection (C6/36)

2.2.2 Infection of Cell Monolayers

Confluent cell monolayers in 75cm^2 or 25cm^2 flasks were used for infection. The cell culture medium was discarded and the monolayer washed with 5 millilitres of PBS (*Appendix 1g*). Virus suspension with a multiplicity of infection (MOI) of 10 was made up to 2 or 1 millilitres with virus diluent (*Appendix 2a*) for 75cm^2 or 25cm^2 flasks, respectively and incubated over the monolayer at 37 °C for an hour with rocking every 15 minutes to ensure even infection. After one hour, unabsorbed viruses were washed off with five millilitres of PBS (*Appendix 1g*) and an appropriate volume of maintenance media (*Appendix 2b to d*) was added to the flask. The infected cells were then incubated at 37 °C or 28 °C, in separate incubators as those used to cultivate uninfected cells, until the appropriate harvest time (*Table 4*).

Mock - infected controls used in this study were prepared as abovementioned except that a similar amount of virus diluent (*Appendix 2a*) was used instead of virus.

2.2.3 Preparation of Virus Pools

Virus pools were prepared using 75 cm^2 flasks. Infection was carried out as described in *Section 2.2.2*. The virus was harvested at specific time points when cytopathic effects were pronounced (*Table 4*). At the end of the incubation period, the infected supernatant was harvested and spun down at 1000 x *g* for 10 minutes (Sigma Laborzentrifugen GmbH, Germany) to pellet any cellular debris. Aliquots of 500 microlitres of the clarified supernatant was pipetted into 1 millilitre sterile cryovials (Nalge Nunc International, Roskilde, Denmark), capped and immediately snap frozen at - 80 °C with denatured ethanol. The frozen ampoules were stored in a - 80 °C freezer (Thermo Fisher Scientific, Massachusetts, USA). Plaque purified virus were not used in any of the experiments to replicate the mixed virus pool naturally found in human infections.

2.2.4 Plaque Assay

BHK cells were seeded onto 24 - well plates at a concentration of 2×10^5 cells per well and were incubated at 37 °C with 5 % carbon dioxide for 24 hours (*Section 2.1.4*). Ten - fold serial dilutions of the virus sample was prepared in virus diluent down to 10^{-8} (*Appendix 2a*). Aliquots of 100 microlitres from each dilution were transferred in triplicates onto confluent cell monolayers in the wells. After an hour of incubation at 37 °C under 5 % carbon dioxide with the plate rocked every fifteen minutes to ensure even distribution of the virus inocula, the diluted virus inocula were removed, and the cell monolayers washed once with PBS (*Appendix 1g*). One millilitre of overlay medium (*Appendix 2e*) was pipetted into each well. The trays were incubated at 37 °C in a humidified carbon dioxide incubator. Plates were incubated two or five days for WNVS or DV, respectively. Formation of plaques was

visualized by staining the monolayer with 0.5 % crystal violet in a 25 % formaldehyde solution (*Appendix 2f)* for at least two hours at room temperature on an orbital shaker (Labnet Intl. Inc., Edison, USA). The excess formaldehyde fixative was removed for proper hazardous chemical disposal, the trays washed under a running tap to remove residual dye, and dried in a well ventilated 60 °C oven for two hours (Memmert GmbH, Schwabach, Germany). Plaques were counted and the titre calculated as PFU per ml supernatant (PFU/ml) or PFU per gram tissue (PFU/g).

For the evaluation of organs from the suckling mice passaging experiments as described in *Section 2.3.6*, two wells from each 24 - well plate used for plaque assay was layered with pre – titred unpassaged WNVS previously grown on Vero cells. The purpose of this is to evaluate the plaque size of the passaged virus. All the wells were processed in the same way and after the plates were stained and dried, a photograph was taken. Regions of plaques as seen in *Figure 4* were then converted to negative colours through the 'Find Edges' function on ImageJ software (v1.37, National Institute of Health, USA). The resulting image, as seen in *Figure 5* was then measured for plaque sizes using the line tool. The diameters of 10 plaques were measured for both passaged virus and control unpassaged virus for each plate. The mean was determined and plotted graphically against the standard plaque size as determined by Vero grown WNVS.

All statistical analysis was done using Minitab 14 (Minitab Inc., Pennsylvania, USA) by Student's t – test, normality test, and standard error. Graphs were plotted with Microsoft Excel 2007 (Microsoft Inc., Washington, USA).

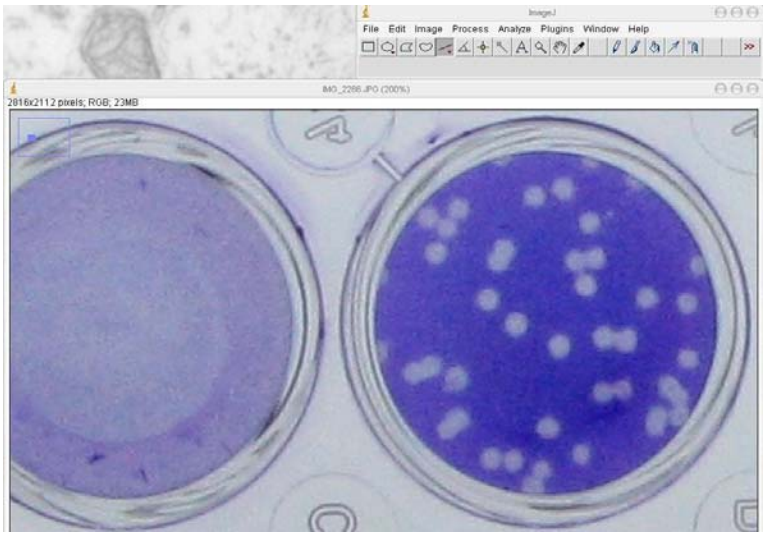

Figure 4: A photograph of two wells of plaque assay.

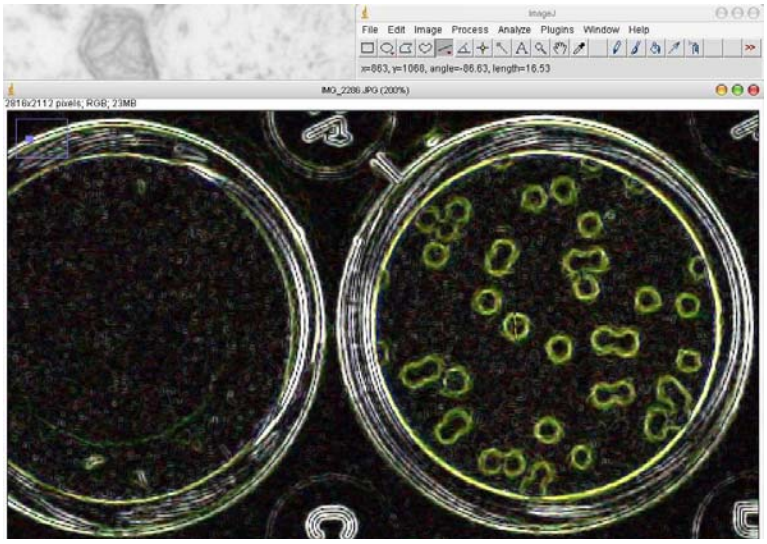

Figure 5: The 'Find Edges' function converts the photograph into negative colours. The same wells were used to measure plaque diameters.

2.3 ANIMAL WORK

2.3.1 Experimental Mice

All BALB/c mice were purchased from the Centre for Animal Resources (CARE), National University of Singapore (NUS) and kept at the Department of Microbiology Animal Holding Facility, NUS, under SPF conditions in microisolator cages (Alternative Design Inc., USA). BALB/c adult mice used were approximately five to

six weeks old while pups experimented on were between two and three days old. The double knockout for interferon α / β and γ receptor mice, AG129$^{-/-}$ (**A**lpha and **G**amma interferon receptor knockout on a **129** mouse background) were obtained from Dr. Woulter Schul of Novartis Institute of Tropical Diseases (NITD), Singapore. AG129$^{-/-}$ mice were housed in a pathogen free environment using a flexible film isolator at the Animal Holding Unit (AHU), NUS. Experiments conducted adhered to the International Guiding Principles for Animal Research and were approved by the NUS Institutional Animal Care and Use Committee (IACUC).

2.3.2 Mice Experiments on Dengue Virus

2.3.2.1 AG129 Mice

Groups of three 10 - week old mice were used to test the efficiency of DV2 infection in adult AG129$^{-/-}$ immunocompromised mice. The virus was diluted to PFU levels of 10^5, 10^6, 10^7, or 10^8 and inoculated intravenously with a tuberculin syringe and a 25G needle (BD Bioscience, New Jersey, USA) and bled at days 1, 2, 3, 4, 5, and 10 post inoculation.

Next, groups of 2 mice were inoculated with 10^7 PFU of DV2 virus and sacrificed at days 1, 2, 3, 4, 5, and 10 post infection via suffocation by purified carbon dioxide in a Perspex chamber (Soxal Pte. Ltd., Singapore). Necropsy of the brain, spleen, and liver was done after ensuring the mice were dead by footpad pressure. The organs were weighed, stored in cryovials (Nalge Nunc International, Roskilde, Denmark), and then snap frozen with ethanol at - 80 ˚C. Organs were stored frozen until used. A portion of tissue was kept for bio – imaging (*Section 2.5*). Tissue homogenates were processed

for plaque assay while sections were stained with haematoxylin & eosin as well as for virus antigen.

2.3.2.2 BALB/c Mice

To test the difference in infectivity between the immunocompromised mouse strain AG129 and immunocompetent BALB/c, adult BALB/c mice were inoculated with concentrated DV1 and DV2 through the tail vein with a 27G ½" needle (BD Bioscience, New Jersey, USA) while restrained by a Mice Tailveiner® (Braintree Sci. Inc., Massachusetts, USA). Supernatant from a 75 cm^2 flask of DV1 and DV2 infected C6/36 cells as described in *Section 2.2.2* was first spun down at 1000 x *g* for 10 minutes to pellet any cell debris. The clarified supernatant was then transferred to a 100000 Dalton pore size Vivaspin (Sartorius – Stedim AG, Germany) and spun at 2500 x *g* for 30 minutes to concentrate the ten millilitre supernatant to 0.5 millilitres. The resultant virus titre increased one log from 6 to 7 log PFU/ml, confirmed by plaque assay (*Section 2.2.4*). Each mouse was inoculated with 100 microlitres of concentrated virus and one mouse from each dengue serotype infection was sacrificed on day 1, 3, 5, and 18 post inoculation, respectively. Blood was collected via cardiac puncture (*Section 2.3.4*) while the brains, livers, and spleens were harvested as described in *Section 2.3.2.1* and processed as detailed in *Section 2.3.5*. A small portion of tissue was kept for bio – imaging purposes (*Section 2.5*).

To test the effect of injecting different dengue strains into the same mouse to mimic a heterologous infection in hope of eliciting a stronger host response against the secondary virus infection, a second experiment was completed. It used two BALB/c mice per group in two groups. The fist group was inoculated with DV1 through the

tail vein at day 0 of the experiment before being inoculated again with DV2 at day 14. The second group of mice received the reverse sequential virus serotype treatment. Mice were sacrificed at day 21 of the experiment and both blood and organs collected.

2.3.3 West Nile Virus Infection in BALB/c Mice

2.3.3.1 Adult Mice

Five-weeks old BALB/c mice were inoculated with WNVS through the tail vein. Supernatant from a 75cm^2 flask of WNVS infected C6/36 or Vero cell monolayer as described in *Section 2.2.2* was spun down at 1000 x *g* for 10 minutes to pellet any cell debris. The clarified supernatant virus titre was approximately 9 log PFU/ml. Each mouse was inoculated with 100 microlitres of virus and 2 mice were sacrificed by carbon dioxide suffocation on days 1, 3, 5, and 18 post inoculation. Necropsy of the brain, spleen, and liver was done after ensuring the mice were dead. A portion of tissue was fixed for bio – imaging purposes (*Section 2.5*).

2.3.3.2 Suckling Mice

Suckling BALB/c pups one to two days old were inoculated intracranially with 5 microlitres of the same WNVS stock as described in *Section 2.3.3.1* using a 50 microlitre gastight glass syringe (Hamilton Co., Nevada, USA) connected to a 30G needle (BD Bioscience, New Jersey, USA). Two mice were harvested every 6 hours from 18 hours post infection for a total experimentation period of 3 days. In addition, groups of 3 – 4 suckling mice were inoculated intracranially with 50000, 10000, 5000, 1000, 500, and 100 virus particles made up to 5 microlitres in virus diluents (*Appendix 2a*). Mice were checked every 12 hours and the brains from dead mice harvested, homogenized, and quantified for infectious virus particles (*Section 2.2.4*).

2.3.4 Blood Collection from Adult Mice

Blood samples were collected from adult mice using two methods; cardiac puncture and submandibular bleeding. Cardiac puncture was performed on deeply anaesthetised mice after carbon dioxide asphyxiation. A 1 millilitre tuberculin syringe was connected to a ½" 26G needle (BD Bioscience, New Jersey, USA) and injected into the thoracic cavity through the diaphragm underneath the sternum at the epigastric region of the mouse on its back. The needle was introduced at a 10 – 30 degree angle from the horizontal axis of the sternum in order to enter the heart. Blood was slowly drawn out from the ventricle of the beating heart until the blood stopped flowing. Approximately 1 millilitre of whole blood could be obtained from each adult mouse.

Submandibular bleeding was done using 4 or 5 millimetre Goldenrod animal lancets (Medipoint Inc., New York, USA) in a class 2A biohazard hood following instructions by the manufacturer as published (Golde *et al.*, 2005). Restrained animals were first swabbed at the cheek area with absolute ethanol. The animals were held by the skin between the shoulder blades and the sharp point of the lancet quickly lunged into the back of the jaw of the mouse, slightly behind the hinge of the jawbones, towards the ear. Once pierced, a serum collection tube was immediately placed under the cheek to collect the blood drippings (BD Bioscience, New Jersey, USA). When 200 microlitres of whole blood has been collected, the flow was stopped by applying direct pressure on the wound site with gauze held for a minute.

In all cases, whole blood was spun down at 14000 x *g* for 10 minutes at 4 ˚C (Sigma Laborzentrifugen GmbH., Germany). The serum was aliquoted into cryovials and

snap frozen in absolute ethanol at - 80 ˚C before being used for plaque assay as outlined in *Section 2.2.4*.

2.3.5 Homogenization of Tissue Samples

Tissue samples collected from all mice necropsies were weighed and homogenized with ice – cold virus diluent (*Appendix 2a*). Buffer was added to the tissue samples in a volume to weight ratio of 2 : 1; microlitre : microgram. All samples were crushed using hand – held 1, 3, or 5 millilitre glass homogenisers with a rated cylinder – plunger clearance of 0.01 to 0.03 millimetres (Sartorius – Stedim AG, Germany). The tissues were crushed until no large particles could be seen in the homogenate, approximately ten to twenty strokes. Cell debris was spun down in a microfuge at 10000 x *g* for 10 minutes at 4 ˚C. The supernatant was aliquoted and stored in cryovials at - 80 ˚C until used.

2.3.6 Passaging Experiments

2.3.6.1 Mouse Only Regime

Stock West Nile virus was subjected to a passaging regime of 10 rounds in suckling BALB/c brains. Virus harvested from *Section 2.2.3* was inoculated into suckling mice brains as described in *Section 2.3.3.2*. Mice were sacrificed after 54 hours and the brains, livers, and spleens were harvested and processed as described in *Sections 2.3.3.2* and *2.3.5*.

The organ homogenate supernatant was tested for number of infective viruses by plaque assay as depicted in *Section 2.2.4*. It was also used to infect a second batch of suckling mice; passage 2. The experiment was carried out as described above and this

process was repeated for 10 rounds for a total passage repeat of ten rounds. Virus supernatant from each stage of passage was kept at - 80 ˚C under lock (Thermo Fisher Scientific, Massachusetts, USA). This passaging regime is labelled as the 'm' series and was carried out in five biological repeats.

2.3.6.2 Mouse – C6/36 Regime

The mouse – C6/36 regime protocol followed closely the mouse only regime detailed in *Section 2.3.6.1* except that after each mouse passage, 500 microlitres of brain homogenate supernatant was used to infect a monolayer of C6/36 cells. Confluent monolayers were incubated with 500 microlitres of brain homogenate supernatant made up to 2 millilitres with virus diluent (*Appendix 2a*) for an hour with rocking every 15 minutes. After one hour, unabsorbed viruses were washed off with 5 millilitres of PBS (*Appendix 1g*) and 10 millilitres of maintenance medium (*Appendix 2b*) were added to the flask. The infected C6/36 cells were then incubated at 28 °C for 24 hours before the supernatant was harvested and stored as described in *Section 2.2.3*. This process was repeated for 10 passage rounds with each passage consisting of a round of virus growth in suckling mice brain followed by virus growth on confluent C6/36 monolayer. This passaging regime is labelled as the 'c' series and was reiterated in five biological repeats.

2.3.7 Isolation of Foetal Mice Brains for Primary Cell Culture

Primary mouse neural cultures were prepared from mouse embryos by the modified protocol of Brewer (1997) and Diniz and group (2006). Pregnant BALB/c mice at approximately gestation day 15 to 16 were sacrificed by carbon dioxide asphyxiation. When the pregnant mouse stopped breathing, it was held by the neck and tilted

downwards. Through the middle of the abdomen of the mouse, the skin of the pregnant mouse was cut open through the abdomen to release the uterus and the embryos. The embryos were removed and each was cut at the neck to remove the head. The heads were collected in a 35 millimetre plastic petri dish (Corning Inc., New York, USA) containing cold virus diluent (*Appendix 2a*). The brains were obtained from the heads after peeling off the skin and the cranium. These were transferred into a clean petri dish with cold virus diluent. The thin layer of membrane covering the brain containing blood vessels was then carefully peeled off using two sharp #7 Jewellers Forceps (Dumont S.A., Switzerland). This was done under an Olympus SZ51 stereomicroscope (Olympus Corp., Japan).

Once all visible membranes had been removed, the whole brain or mid - brain section was taken and washed in another petri dish of cold virus diluent (*Appendix 2a*) before being cut into small pieces approximately 0.2 centimetres in diameter and collected in a 1.5 millilitre microfuge tube. To this, 500 microlitres of papain (Worthington Biochemical Corp., New Jersey, USA) (*Appendix 1i*) was added and the tube kept on a floater in a 37 ˚C GFL water bath for 15 minutes (Gesellschaft für Labortechnik GmbH, Burgwedel, Germany). The tube was gently inverted a few times every five minutes. A 1000 microlitre micropipettor was then very gently used to dislodge the enzyme treated cells as much as possible. This was then left in the water bath for another 15 minutes and the micropipettor was used again to dislodge the cells. Once the cells were seen to be suspended with no large clumps, the tube was centrifuged at 500 x *g* for 10 minutes at 4 ˚C. The pellet from whole brain single cell suspension was resuspended in 20 millilitres of DME growth medium with inactivated serum (*Appendix 1d*) for astrocytes and glial cells or Neurobasal media supplemented with

B27 (Invitrogen Corp., Carlsbad, USA) for cortical neurons derived from mid – brain sections of single cell suspension. After thoroughly mixing the cells, it was plated onto 25 cm^2 tissue culture flasks pre-coated with poly – L – lysine (*Appendix 1j*) and incubated in a 37 ˚C humidified incubator. Cells were left for at least 2 weeks before any experiments were performed. Half the volume of media was removed and replaced with fresh media twice weekly.

2.3.8 Post – Passaging Mouse Experiments

2.3.8.1 Adult BALB/c Mice

A total of five virus samples of passage ten viruses from both *Sections 2.3.6.1* and *2.3.6.2* were used to infect adult five week old BALB/c mice via the intravenous route. A hundred microlitres of virus was injected into the tail vein of 5 mice per virus sample, with a total of 50 mice used. Virus titres are reported in *Section 4.3.1*. Two mice were left for up to 4 weeks to check for mortality and morbidity. These 2 mice were also bled through the submandibular method as described in *Section 2.3.4* every other day. The blood was spun down and the serum tested by plaque assay (*Section 2.2.4*). The remainder 3 mice per group were sacrificed one at a time on days 1, 3, and 5 post inoculation. The mice were bled by cardiac puncture (*Section 2.3.4*), and brains, livers, and spleens harvested and homogenised (*Section 2.3.5*). The resultant supernatant was used for plaque assay (*Section 2.2.4*). A small portion of tissue was kept for bio – imaging (*Section 2.5*).

A second experiment was carried out to test the level of morbidity caused by the different passaged virus by observing if adult mice lost weight as a result of virus inoculation. The experiment was carried out by injecting 100 microlitres of the 10

different passage 10 viruses through the tail vein of the mice. The controls used were mice inoculated with unpassaged virus. Two mice per virus sample were used and the mice were weighed every 12 hours for 20 days with the point of injection represented as 0 hour.

2.3.8.2 Suckling BALB/c Mice

Suckling mice one to two days old were injected intracranially with passage 10 viruses. Each strain of passaged virus was inoculated into 9 suckling mice. This group was divided into 3 subgroups and each subgroup received 50, 500, or 5000 virus particles of passaged virus diluted to 5 microlitres with virus diluent (*Appendix 2a*). The mice were injected using a presterilized 50 microlitre gastight syringe (Hamilton Co., Nevada, USA) connected to a 30G needle (BD Bioscience, New Jersey, USA). The suckling mice were constantly kept in a cage with the dam on soft corncob bedding (Harlan Teklad Laboratories, Madison, USA). Every 12 hours, the mice were inspected and mortality recorded. Brains from dead suckling mice were harvested and homogenised (*Section 2.3.5*) for plaque assay (*Section 2.2.4*).

2.3.8.3 Primary Neural Cell Line

Primary neural cells grown (as processed in *Section 2.3.7*) in 25 cm^2 flasks were infected with passage 10 viruses at an MOI of 10 following the procedure outlined in *Section 2.2.2*. A total of 5 millilitres of maintenance media was added to the flask and every 12 hours for 6 days, 300 microlitres of infected media was removed for plaque assay and replaced with 300 microlitres of fresh media. The extracted media was spun down at 5000 x *g* for 5 minutes to pellet all cell debris and the supernatant stored at -80 ˚C until used for plaque assay (*Section 2.2.4*).

2.4 DIRECT POLYMERASE CHAIN REACTION SEQUENCING

2.4.1 Extraction of Virus Ribonucleic Acid (RNA)

Viral RNA extraction procedure was carried out using QIAmp® Viral RNA extraction kit (Qiagen NV, Venlo, Nederlands). A 140 microlitre aliquot of West Nile virus supernatant (approximately 3 x 10^9 PFU/ml) was added to 560 microlitres of Buffer AVL containing carrier RNA in a 1.5 millilitre RNase and DNase free microfuge tube (Axygen Scientific, Union City, USA). The mixture was incubated at 25 ºC on a heat block for 10 minutes (USA Scientific Inc. Ocala, USA), followed by the addition of 560 microlitres of absolute ethanol (Merck KGaA, Darmstadt Germany). The solution was then transferred to the QIAmp spin column and spun at 6000 x *g* for 1 minute (Sigma Laborzentrifugen GmbH., Germany). The filtrate was discarded. The spin column was spun again at 6000 x *g* for 1 minute after adding 500 microlitres of Buffer AW1. This step was repeated with Buffer AW2. Viral RNA was eluted from the spin column by adding 30 microlitres of Buffer AVE and spun at 6000 x *g* for 1 minute. Viral RNA was stored at - 80 ºC until used.

2.4.2 Reverse Transcription Polymerase Chain Reaction (RT-PCR)

RT-PCR was performed to synthesise cDNA from harvested West Nile virus RNA extracted as described in *Section 2.4.1* using the ImProm – II™ Reverse Transcription System (Promega Corp., Madison, USA). Specific primers were synthesised corresponding to specific locations on the virus genome as detailed in *Table 5* (1st Base Pte. Ltd., Singapore). All primers for this project were synthesised by the same company. The primers were dissolved in DEPC treated water (*Appendix 3a*) to a stock concentration of 10 micromolars.

Table 5: List of RTPCR Primers Used and its Sequences

Original RNA sequence (5' – 3')	First Base	Synthesised Primer (5' – 3')	Name
ACAGCTTCAACTGCTTAGG	962	CCTAAGCAGTTGAAGCTGT	RT10
GTGAAGTTGACATCAGGACA	1801	TGTCCTGATGTCAACTTCAC	RT9
CTGCCACCACTGAAAAAT	2783	ATTTTTCAGTGGTGGCAG	RT8
ATATGTCATTCTCGTTGG	3693	CCAACGAGAATGACATAT	RT7
AGGCGTTTACAGAATCATGA	4671	TCATGATTCTGTAAACGCCT	RT6
CCCCTTTCCAGAGTCTAA	5583	TTAGACTCTGGAAAGGGG	RT5
TGAAGTCATCACAAAGTTGG	6351	CCAACTTTGTGATGACTTCA	RT4
GCGGTGGTCGTCAATCCATC	7471	GATGGATTGACGACCACCGC	RT3
AACATGACAAGCCAGGTA	8383	TACCTGGCTTGTCATGTT	RT2
TGTATTAAATAGTTGTATG	10412	CATACAACTATTTAATACA	RT1
AGTGGAGGACACTGTTTTG	10380	CAAAACAGTGTCCTCCAC	RT13

Four microlitres of experimental RNA was mixed into 1 microlitre of gene – specific primer in an autoclaved, nuclease – free, thin – walled PCR tube and briefly spun down (Abgene Ltd., Epsom, UK). The tube was heated to 70 ˚C for 5 minutes in a thermal cycler (Bio Rad Labs., California, USA) and immediately chilled on ice for another 5 minutes. The tubes were then spun down for 10 seconds in a microcentrifuge to collect the condensate. The transcription mix premixed as described in *Appendix 3b* was then added to the tube on ice to make up a final reaction volume of 20 microlitres.

The tube was capped tightly and placed in the thermal cycler to be equilibrated at 25 ˚C for 5 minutes, then 42 ˚C for 1 hour and lastly 70 ˚C for 15 minutes to inactivate the reverse transcriptase. The products were promptly kept at – 20 ˚C until used.

2.4.3 Polymerase Chain Reaction Amplification (PCR)

PCR was used to amplify specific gene sequences using the respective primers flanking the 5' and 3' end. Amplification was performed using Platinum Pfx DNA Polymerase (Invitrogen Corp., Carlsbad, USA) which has a 3' to 5' exonuclease proof – reading activity to minimise the incorporation of mismatched nucleotides during amplification. Primers were designed and the sequences are as displayed in *Table 6*.

Table 6: Primer Sequences for PCR Amplification

Primer Pair Sequence (Forward and Reverse, 5' – 3')	Genomic Region amplified (BP)	Primer Pair Name
CACAGTGCGAGCTGTTTC ACAGCTTCAACTGCTTAGG	80-962	1
ACGTAGGATATCTCTG GTGAAGTTGACATCAGGACA	584-1801	2
TGAGCAACAGGGACTTCC CTGCCACCACTGAAAAAT	983-2783	3
TATACCGGAAAAGACG ATATGTCATTCTCGTTGG	1951-3693	4
ACCCTCGTGCAGTCGAGAGT AGGCGTTTACAGAATCATGA	3499-4671	5
AGGCAAGGTGGACCAACC CCCCTTTCCAGAGTCTAA	3812-5583	6
TGTCCTTGATTTGCA TGAAGTCATCACAAAGTTGG	5181-6351	7
CGATGAGTACTGCTATGG GCGGTGGTCGTCAATCCATC	6021-7471	8
CAGGTGACTCTGACTGTGAC AACATGACAAGCCAGGTA	7231-8383	9
GTCGACGTTTTCTATAGACC TGTATTAAATAGTTGTATG	8071-10412	10
GTCGACGTTTTCTATAGACC AGTGGAGGACACTGTTTTG	8071-10380	11

PCR Amplification mix was prepared as described in *Appendix 3c*. Twenty microlitres of prepared first strand cDNA from *Section 2.4.2* was added to the Amplification Mix to make up a 50 microlitre reaction. The tube was capped and centrifuged briefly to collect the contents. The template was denatured for 2 minutes at 94 ˚C followed by 30 cycles of PCR amplification in an iCycler (Bio Rad Labs., California, USA) as follows: each cycle consisted of 94 ˚C for 15 seconds, 55 ˚C for 30 seconds and 68 ˚C for 1 minute, which enabled repetitive DNA denaturation, primer hybridization and primer extension, respectively. An extra step of 72 ˚C for 5 minutes allowed final extension to occur and ended with a holding step at 4 °C. Tubes were stored at – 20 ˚C until used.

2.4.4 Agarose Gel Electrophoresis

The PCR amplification products were visualized with agarose gel electrophoresis. A 1.0 % agarose gel was cast as described in *Appendix 4a*. The fluid of agarose mixture was poured into a gel tray where air bubbles were removed using a pipette tip before the gel comb was inserted. The solidified gel was then submerged in the gel – electrophoresis tank (Bio Rad Labs., California, USA) filled with 1 x TBE buffer (*Appendix 4b*). Fifteen microlitres of DNA sample was mixed with 2 microlitres of 6 x gel loading buffer (Bio Rad Labs., California, USA) before loading into a well. Ten microlitres of Bench Top 100bp DNA Ladder (Promega Corp., Madison, USA) was also loaded as a relative molecular size reference. The sample was then electrophorized at 120 volts for 45 minutes. The DNA bands were then visualized under UV light (UV transilluminator, Vilber Lourmat, UK) and a digital photograph of the gel was taken with a ChemiGenius station (Syngene, Synoptics Ltd., Cambridge, UK).

2.4.5 Deoxyribonucleic Acid Sequencing and Analysis

Sequencing PCR was carried out on an ABI Prism 3100 Genetic Analyser using BigDye Terminator v.3.1 (Applied Biosystems, California, USA). Each reaction used 4 microlitres of Big Dye Mix and 1 microlitre of primer from the list given in *Table 7*. Five microlitres of PCR product from *Section 2.4.3* was added to the mix. The total volume of 10 microlitres of solution was added with 2 microlitres of 3 molar sodium acetate (*Appendix 4c*) and 50 microlitres of 95 % ethanol (*Appendix 5c*). The mixed solution was transferred into a new 1.5 ml microfuge tube and incubated on ice for 10 to 15 minutes. The solution was then spun at 14000 x *g* for 20 minutes at four degrees Celcius. The resulting supernatant was discarded. Next, 250 microlitres of 70 % ethanol (*Appendix 5c*) was added to the tube and it was again spun for 20 minutes at top speed. After the liquid was blotted off with a tissue paper, the remaining pellet was dried on a 55 ˚C heat block for approximately 30 minutes or until it was dry. The samples were then processed through the ABI Prism 3100 Genetic Analyser.

Sequences obtained were Blasted against the complete West Nile Sarafend genome sequence found on the Genbank website under accession code AY688948. Regions of differences were noted. Genome editing and assembling were performed using Lasergene 7.2 (DNASTAR Inc., Wisconsin, USA). Sequencing was done only in the forward direction but for each fragment, portions of overlap existed for the whole fragment region, and there was thus a confirmation by using two different forward primers.

Table 7: List of Primer Sequences for Sequencing PCR

Primer Pair Name	Primer Sequence (5' – 3')	First Base Number	Size of Fragment
1	CACAGTGCGAGCTGTTTC	62	388
	CGCCTGTGCTGGAGCTGTGA	450	512
	ACGTAGGATATCTCTG	584	399
2	TGAGCAACAGGGACTTCC	983	421
	GACGACTGTCGAATCAC	1404	397
	TGAGCAACAGGGACTTCC	983	421
	GACGACTGTCGAATCAC	1404	547
3	TATACCGGAAAAGACG	1951	251
	CAGAGGAGCTCAACGA	2202	581
	TATACCGGAAAAGACG	1951	251
	CAGAGGAGCTCAACGA	2202	420
4	GGAAGGAGTCTGTGGCCTGC	2622	382
	TGTGACTCGAAAATCATCGG	3004	495
	ACCCTCGTGCAGTCGAGAGT	3499	194
	ACCCTCGTGCAGTCGAGAGT	3499	313
	AGGCAAGGTGGACCAACC	3812	418
	TACAGAAGTGATGACTGCA	4230	441
5	AGGCAAGGTGGACCAACC	3812	418
	TACAGAAGTGATGACTGCA	4230	318
	CACCTTGGGCCATTCTCC	4548	203
	ATACACTATGGCACACCAC	4751	430
6	TGTCCTTGATTTGCA	5181	402
	TGTCCTTGATTTGCA	5181	412
	GAGTCTAATGCTCCTATC	5593	428
	CGATGAGTACTGCTATGG	6021	330
	CGATGAGTACTGCTATGG	6021	410
7	CTCTGAAGTCCTTCAAAG	6431	420
	AGACTGACAACCAGCTCG	6851	380
	CAGGTGACTCTGACTGTGAC	7231	240

Primer Pair Name	Primer Sequence (5' – 3')	First Base Number	Size of Fragment
8	CAGGTGACTCTGACTGTGAC	7231	423
	GAGAAGCCTGTCCTCAAG	7663	408
	GTCGACGTTTTCTATAGACC	8071	313
	GTCGACGTTTTCTATAGACC	8071	423
9	CTCCTCAATTCTGACACTAG	8494	419
	CCTAGGAGCGATGTTTG	8913	483
	CGAGCTCACGTACCGAC	9396	354
10	GTCAAAGGTCCGCAAAGACA	9750	351
	AGAATGGATGACGACTGA	10101	311
	GTCGACGTTTTCTATAGACC	8071	423
	CTCCTCAATTCTGACACTAG	8494	419
	CCTAGGAGCGATGTTTG	8913	483
	CGAGCTCACGTACCGAC	9396	354
11	GTCAAAGGTCCGCAAAGACA	9750	351
	AGAATGGATGACGACTGA	10101	279

2.5 BIO – IMAGING

2.5.1 Fixation and Processing of Samples

Harvested tissues were immediately cut into approximately 5 millimetre thick sections, and placed in jet cassettes and fixed in 4 % paraformaldehyde for at least 24 hours at 4˚C (*Appendix 5a*). It was then transferred to 4 ˚C PBS (*Appendix 1g*) until further processing. The tissue processor Leica TP1050 (Leica, Microsystems GmbH, Wetzlar, Germany) with an overnight automated embedding program (*Appendix 5b*) was used to fix the sections.

A Leica EG1160 (Leica, Microsystems GmbH, Wetzlar, Germany) tissue embedding centre was employed to embed all the fixed samples into paraffin blocks using stainless steel moulds and embedding rings. Tissue sections were embedded in molten wax and hardened to a block at - 20 ˚C for 2 hours. Blocks were then removed from moulds, trimmed of residual wax and stored at room temperature.

For primary cell lines, the cells were obtained as described in *Section 2.3.7* and layered onto poly – L – lysine coated cover slips (*Appendix 1j*). After 2 weeks in a 37 °C humidified incubator, the cells were washed twice with PBS (*Appendix 1g*) and fixed with 4 % paraformaldehyde (*Appendix 5a*) for 30 minutes at room temperature.

2.5.2 Paraffin Sectioning

Before cutting, paraffin blocks were cooled on ice for an hour. Semi – thin 4 micrometre sections were obtained using a Leica RM2235 rotary microtome and disposable high – profile steel blades (Leica, Microsystems GmbH, Wetzlar, Germany). The wax ribbon was then floated on a 40 ˚C water bath (Medax Nagel, Germany). Positively charged silane coated Histobond slides (Paul Marienfeld GmbH, Germany) were used to pick up the floating sections and slides were left to drip dry by the side of the water bath before being thoroughly desiccated in a covered box overnight at 37˚C. The dried slides were then stored at room temperature awaiting further experiments.

2.5.3 Dewaxing - Rehydration and Dehydration - Clearing Method

Paraffin dewaxing was accomplished using xylene. Slides were soaked in 2 rounds of fresh xylene (Merck KGaA, Darmstadt Germany) for 3 minutes each. Rehydration

followed dewaxing and the slides were put through a decreasing alcohol concentration gradient (*Appendix 5c*) ending with deionised water (Barnstead, New Hampshire, USA). Slides were soaked in each solution for 2 minutes (*Appendix 5d*).

Dehydration and clearing follows the reverse steps of rehydration and dewaxing. Slides were soaked for 2 minutes each starting from deionised water and ending with absolute alcohol following the list in *Appendix 5d* but in reverse order and then for 3 minutes each in 2 rounds of xylene (Merck KGaA, Darmstadt Germany).

2.5.4 Hematoxylin and Eosin Staining

Paraffin – embedded and sectioned tissues on slides from *Section 2.5.2* were heated on an Electrothermal slide drying bench (Barnstead, New Hampshire, USA) at 70 ˚C for 10 minutes before dewaxing as described in *Section 2.5.3*. Slides were then soaked in various reagents or chemicals as noted in *Appendices 5e to g*. A ready – made modified Harris Hematoxylin was used (Sigma-Aldrich, St. Louis, USA). The protocol is outlined in *Appendix 5h*.

Slides were then dehydrated as described in *Section 2.5.3*; cover slips were mounted with Histofluid (Paul Marienfeld GmbH, Germany), and viewed under brightfield microscopy (*Section 2.5.7*). Sections were examined for histopathological signs.

2.5.5 Immunohistochemistry (IHC)

2.5.5.1 Detection of Viral Antigens

Rehydrated sections (*Section 2.5.3*) were washed in running tap water for five minutes. Antigen was retrieved by microwaving for 10 minutes in sodium citrate

buffer, pH 6.0 (*Appendix 6a*), in a EMS 9000 microwave oven (Electron Microscopy Sciences, USA) at 99 °C. The slides were then left to cool for 20 minutes at room temperature before being washed again in running tap water for 5 minutes.

All steps below were carried out in a moist chamber. The slides were subjected to endogenous peroxidase blocking in 0.6 % H_2O_2 in methanol for 15 minutes (*Appendix 6b*) before washing twice in TBS buffer (*Appendix 6c*) for 5 minutes. The sections were then incubated with 1 : 20 dilution of normal rabbit serum (Sigma-Aldrich, St. Louis, USA) for 20 minutes in order to block non – specific antibody binding. Excessive serum was drained and the slides incubated with anti – WNV monoclonal antibody (Microbix Biosystems Inc., Ontario, Canada), at a dilution of 1 : 500, for 2 hours at room temperature. This was followed by washing twice in TBS for 5 minutes. DV – infected samples were incubated with anti – DV envelope protein monoclonal antibody, 4G2, from the American Tissue Culture Collection, USA. The dextran – polymer Envision$^+$ horseradish peroxidase conjugated anti – mouse antibody (Dako A/S, Denmark) was layered on the sections at 1 : 300 dilution at room temperature for an hour. The slides were then rinsed once in TBS for 5 minutes. Sections were developed with the kit provided 3, 3'-diaminobenzidine (DAB) chromogen, incubated for 5 to 10 minutes at room temperature with the timing dependent on the speed of signal development. The sections were rinsed twice at an interval of 5 minutes each in TBS buffer. Slides were washed in running tap water for 5 minutes, counter – stained using Harris hematoxylin for 30 seconds, washed again in running tap water and dehydrated in graded ethanol and xylene as described in *Section 2.5.3*, and mounted with Histofluid mounting medium (Paul Marienfeld GmbH, Germany).

2.5.5.2 Detection of Various Neural Cell Types

Primary cell lines, as plated onto cover slips and fixed in *Section 2.5.1* were tested for purity of extraction as well as for specific cell type. The cover slips were tested for neurons with anti – Neun antibody, astrocytes with anti – GFAP antibody, and oligodendrocytes with anti – CNPase antibody (Chemicon, Millipore, USA). The fixed samples were first blocked with BSA blocking solution (*Appendix 7a*) for an hour before being incubated with the primary antibody diluted to 1 : 500 in PBS (*Appendix 1g*). The coverslips were then washed thrice in PBS for 5 minutes each and then secondary Alexa Fluor 488 rabbit anti – mouse antibody (Invitrogen Corp., Carlsbad, USA) diluted to 1 : 1000 in PBS was added and left to incubate for another hour. The secondary antibody was washed off with PBS thrice for 5 minutes each before the coverslips were counterstained with DAPI (Invitrogen Corp., Carlsbad, USA) for 10 minutes. The coverslips were then mounted onto low autofluorescence glass slides (Paul Marienfeld GmbH, Germany) with Prolong Gold mounting media (Invitrogen Corp., Carlsbad, USA).

2.5.6 Immunogold – Silver Staining (IGSS)

Paraffin – embedded tissue sections were cut to 4 micrometres thick and attached onto silane slides (*Section 2.5.2*) before dewaxing and rehydration (*Section 2.5.3*). The sections were then incubated for 15 minutes in aldehyde blocking solution (*Appendix 7b*). All incubations were performed in a moist chamber at room temperature. Slides were washed in PBS (*Appendix 1g*) twice for 5 minutes each and then blocked with bovine serum albumin (*Appendix 7a*) for 30 minutes. The next washing step using Aurion BSA - C (*Appendix 7c*) lasted 5 minutes and was repeated twice. Primary antibody incubation was performed overnight at 4˚C with monoclonal anti – dengue

virus envelope protein antibody, 4G2, from the American Tissue Culture Collection, USA. The next BSA – C washing step lasted 3 rounds of ten minutes each followed by incubation with secondary antibody conjugated to ultra – small 1 nanometre gold particles (Aurion ImmunoGold, Netherlands) at room temperature for 2 hours. Sections were then postfixed in 2 % gultaraldehyde for 2 minutes (*Appendix 7d*). The BSA – C wash was again performed but for 4 rounds of 10 minutes each. The silver enhancement (Aurion ImmunoGold, Netherlands) took approximately 20 minutes. This was followed by 3 rounds of 5 minutes deionised water washes (Barnstead, New Hampshire, USA). Sections were then counterstained for 10 minutes in Harris hematoxylin (Sigma-Aldrich, St. Louis, USA), dehydrated according to *Section 2.5.3*, mounted on coverslips with Histofluid (Paul Marienfeld GmbH, Germany) and viewed under epi – polarizing light (*Section 2.5.7*).

2.5.7 Microscopy

For brightfield microscopy, an upright microscope CX40 (Olympus Corp., Japan) with achromat objectives attached with a Pixera Penguin 150CL (Pixera Corp., USA) CCD was used. The Penguin is a charged – coupled device (CCD) digital camera with 1.5 million true pixels. Immunogold – silver enhancement was viewed using a Zeiss Axiophot II (Carl Zeiss Inc., Germany). The microscope was equipped with Plan – Neofluar objectives and an epi – polarization reflector block in the filter house consisting of an immunogold – silver filter, polarizer, polarizer emitter, exciter, and UV blocking filter (Carl Zeiss Inc., Germany). The same Pixera CCD camera was used on the Zeiss microscope.

For brightfield and immunogold – silver staining, white balance was performed with a suitable transmitted light level. The light intensity was then fixed at that level throughout the viewing and image acquisition session. For immunogold – silver viewing through the epi – illumination method, all compensation filters including quarter lambda and polarizing plates were removed beforehand. The iris and field stop was adjusted with every objective change to ensure optimal viewing and image capturing condition. The condenser was left open and transmitted light was only added on when the reflected light has been adjusted.

Fluorescence was visualized with an inverted microscope IX81 (Olympus Corp., Japan) fitted with a mercury lamp and suitable filtersets (Omega Optical, USA). Images were acquired by Metamorph v6.2 (Molecular Devices, MDS Inc., USA) with a CoolSnap HQ monochrome camera (Photometrics, Roper Scientific, USA).

2.6 ELECTRON MICROSCOPY

An equal amount of PBS containing 4 % glutaraldehyde and 4 % paraformaldehyde (*Appendix 8a*) was added to the media containing mock or virus – infected primary cells from 25 cm^2 flasks. Fixation was performed overnight at 4 ^oC. Fixed cells were scrapped with a cell scrapper (Nalge Nunc International, Roskilde, Denmark), pelleted at 1000 x g for 10 minutes and washed thrice for 5 minutes each with PBS (*Appendix 1g*) before postfixation in 1 % osmium tetroxide (*Appendix 8b*) at room temperature for an hour. The samples from henceforth were placed on a tissue rotator for better infiltration. A few crystals of potassium ferricyanide (Merck KGaA, Darmstadt Germany) were added to the 1 % osmium tetroxide solution to further enhance the contrast of membranous structures. Subsequently, the cells were washed

thrice for 5 minutes each with E - Pure™ water (Barnstead, New Hampshire, USA) before dehydrated with increasing concentrations of ethanol; 25 %, 50 %, and 75 % ethanol for 10 minutes each, 95 % ethanol for 20 minutes, and thrice of absolute ethanol for 20 minutes each (*Appendix 5c*). The dehydrated cell pellets were then infiltrated with increasing concentrations of a polyhydroxy – aromatic acrylic resin, LR White (LRW), at 3:1, 1:1, and then 1:3 ratio of ethanol to LRW for 30 minutes each at room temperature, followed by 30 minutes of absolute LRW at room temperature. Subsequently, the pellet was left in fresh absolute LRW overnight at room temperature. The next day, absolute LRW was used to further infiltrate the specimen (four times, each for an hour). Embedding and polymerization was carried out at 60 ºC ovens for 48 hours in 00 size gelatin capsules.

The embedded specimens were then trimmed on a EM TRIM specimen trimmer (Leica, Microsystems GmbH, Wetzlar, Germany) and sectioned into 50 – 70 nm – thick sections using an ultramicrotome (Ultracut E, Reichert-Jung, Germany). The ultrathin sections were picked up onto 200 mesh uncoated copper grids (TAAB Lab. Equipment Ltd., England) and stained with saturated aqueous uranyl acetate (*Appendix 8d*) for 5 minutes. Excess stain was washed off using deionized water. This was then followed by secondary staining with Reynold's lead citrate solution (*Appendix 8e*). The sections were allowed to dry on a hot plate before viewing under a transmission electron microscope (JEOL, 1010, USA).

CHAPTER 3
RESULTS

3.0 RESULTS

3.1 INFECTION OF MICE WITH DENGUE VIRUS

3.1.1 Infection of Adult Mice with Dengue Virus

Stock dengue virus was grown on C6/36 cells and titred. The yield of DV1 was 10^7, DV2 were 10^6, and DV4 was 10^4 PFU/ml (*Section 2.2.3 and 2.2.4*). Adult BALB/c mice in groups of twos was first tested for levels of viremia and mortality when injected with 100 microlitres of stock DV through the tail vein (*Section 2.3.2.2*). The two different DV were either used for inoculation individually or in combination, with the inoculation of consecutive virus 2 weeks after the first infection. There were no observed deaths in any of the groups. Mice sacrificed on days 1, 3, 5, and 18 after the first virus inoculation and on day 21 after the post second inoculation (*Section 2.2.4*) were found to be negative for virus in serum, liver, brain, and spleen. Therefore, the wild type DV from the laboratory stock was unable to show any mortality or morbidity in adult BALB/c mice. Moreover, histological sections from mice organs (*Section 2.5.4*) showed no obvious pathology. As there were no detectable virus levels, no immunohistology was done.

3.1.2 Infection of Adult AG129 Mice with Dengue Virus

3.1.2.1 Testing of Various Dengue Virus Doses

As the immunocompetent BALB/c adult mice did not show any signs of mortality or morbidity from the DV inoculation, an experiment was done on immunocompromised mice with double knockout of alpha and beta, and gamma interferon receptors, AG129 (*Section 2.3.2.1*). This was done to see if the virus was able to infect immunocompromised mice. First, the effect of different dengue virus doses on the level

of viremia was tested on adult mice inoculated intravenously with 10^5, 10^6, 10^7, or 10^8 PFU/ml DV2. Three mice were bled on days 1, 2, 3, 4, 5, and 10 post inoculation (*Section 2.3.4*). The 10^{th} day bleed was performed to test for virulence at a late time point. *Figure 6* shows the $\log_{10}$ PFU/ml titres in serum samples. From this it was evident that there was little difference between the 10^7 and 10^8 PFU/ml DV2 inoculated mice. As the 10^8 PFU/ml stock required an additional step of concentration using Vivaspin columns (*Section 2.3.2.2*), it was more economical to proceed with the neat 10^7 PFU/ml virus pool. In addition, the virus was able to persist in mice for at least 5 days unlike in the immunocompetent BALB/c mice. The data also corresponded to approximately the same timeframe during which human dengue patients exhibit viremia in a clinical setting (Sabin, 1952). The virus was not detected at day 10 post infection. It is not known if the cause for this was the inability of the virus to persistently infect the mice or the immune system although deficient, was able to clear the virus. However, this experiment proved that DV could still infect mice although only in the immunocompromised strain.

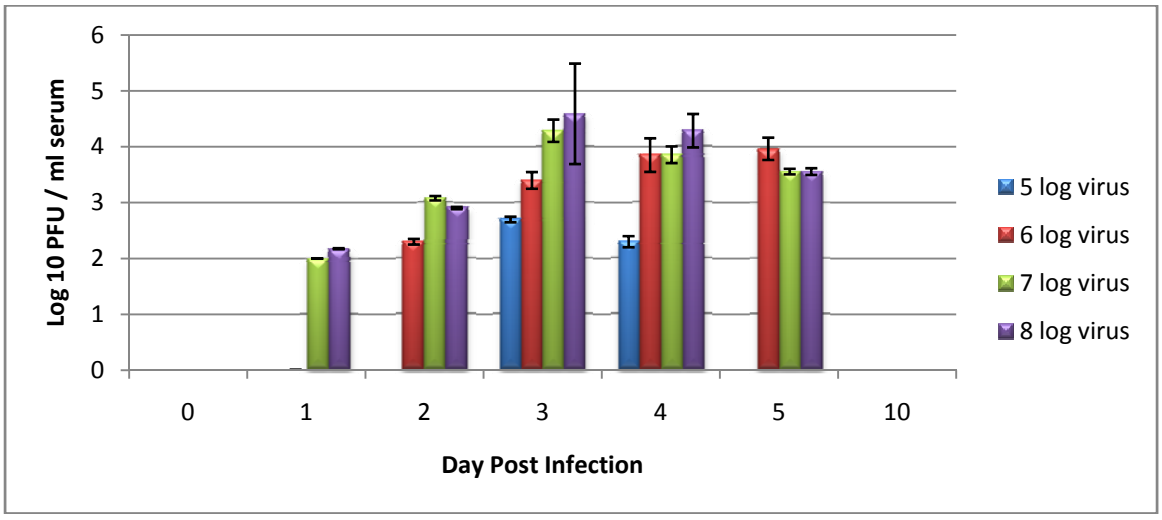

Figure 6: Log_{10} virus yield from sera of AG129 mice inoculated with various doses of DV2 bleed on different days. The results show a dose dependant response and the 7 log virus is the best titre to work with as it does not require any virus concentration step while giving acceptable virus titres as well as the least variation in results in the experimental mice. Error bars represent standard errors.

3.1.2.2 Short Term Virus Infection Study

Adult AG129 mice in groups of two were next infected with 10^7 PFU/ml of DV2 virus intravenously through the tail vein and pairs of mice were sacrificed on each day from days 1 to 5 (*Section 2.3.2.1*). *Figure 7* shows the level of viremia in the sera of mice. In addition, organs were harvested for plaque assay as well as histological analysis. *Figure 8* shows the virus levels in spleens and livers of mice infected with DV2 harvested on various days. The brains showed no virus presence and were thus not shown. Haematoxylin & eosin staining as well as immunohistochemistry was done to detect the pathological changes as well as to detect viral antigens in the organs (*Section 2.5*).

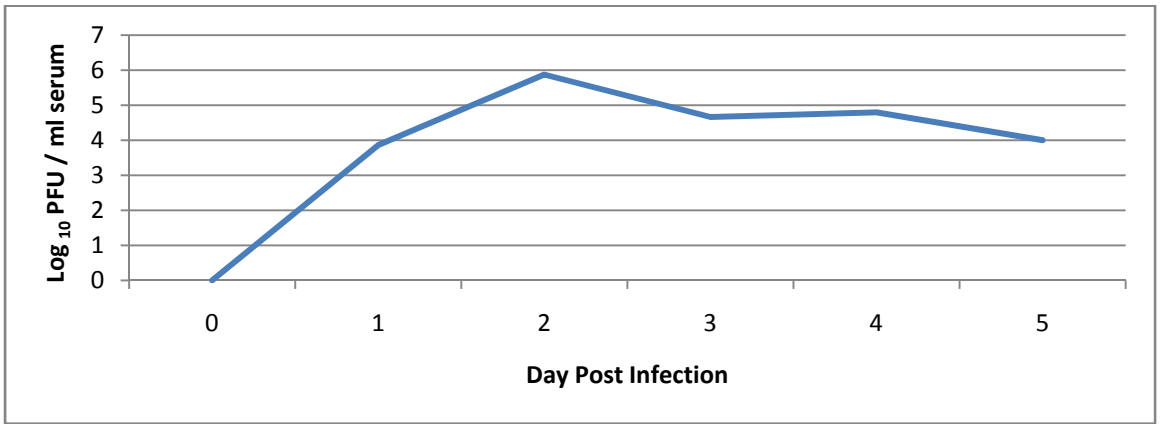

Figure 7: Level of virus in sera of adult AG129 mice inoculated with DV2 *over 5 days. The graph represents means from two mice.*

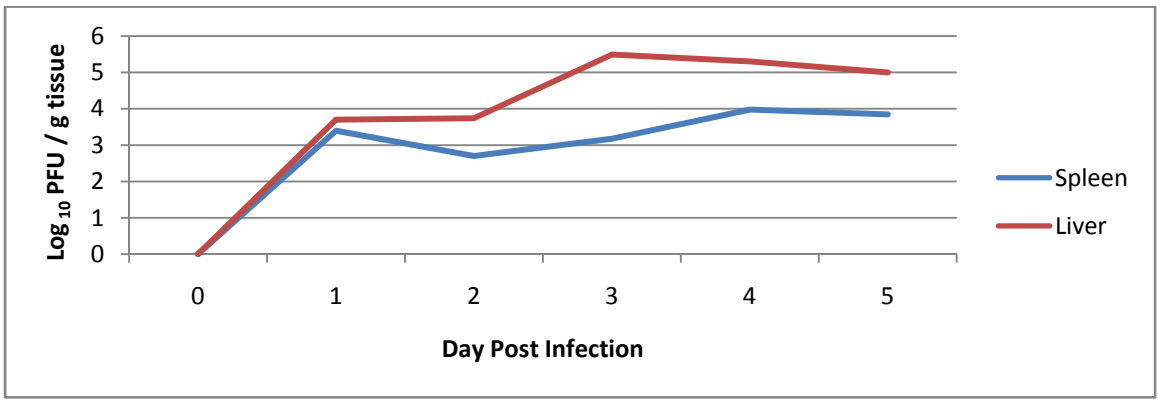

Figure 8: Virus levels in spleens and livers of adult AG129 mice inoculated with DV2 *over five days. Each graph represents the mean from two mice.*

The histological sections from spleens, livers, and brains of mice were stained by haematoxylin & eosin and observed under brightfield microscopy. Overt changes could be seen in tissue sections from mice sacrificed on day 3 post inoculation onwards. *Figure 9b* shows inflammation in the red pulp of spleen in infected mice (white arrows) while the same area was clear of any infiltrating cells (green arrows) in the control sections (*Figure 9a*). The dense infiltrating cells almost obliterated the white pulp markings (orange arrows) making it indistinctive from the red pulp, which is characteristic of inflammation. The gross morphology of the spleens also showed overt splenomegaly as the size of spleens from infected mice were up to 150 % compared to uninfected ones as observed during organ harvesting. Cells infiltrating into the spleen causing the inflammation could be made up of B, T, macrophages, or a combination of these cells.

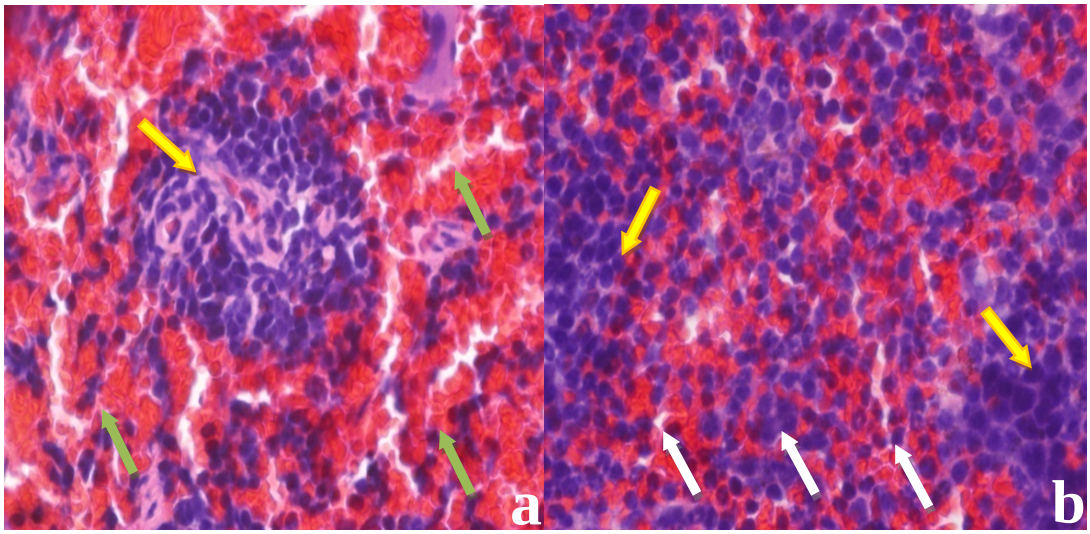

Figure 9: Red pulps of mock – inoculated (a) and DV2 – inoculated (b) AG129 mice spleens at day 3 post infection showing cell infiltration (white arrows) in the red pulp that totally masks the white pulps (yellow arrows). Cell infiltration is absent in the mock infected cells (a) which shows a clear red pulp (green arrows). Original magnification 400x.

The test for viral antigens using the standard immunohistological avidin – biotin complex did not yield any results although plaque assay showed virus titre of 10^3 PFU/g in spleens (*Figure 8*). As such, a more sensitive method was employed in order to detect virus antigens. The immunogold – silver staining (IGSS) method is a very sensitive method using secondary antibodies – conjugated to ultrasmall gold particles which can be magnified with silver deposits that has a natural affinity towards gold (*Section 2.5.6*).

From the same tissue block of *Figure 9,* IGSS was done and the white pulp shown in *Figure 10*. It was very clearly seen that two cells have bright markings indicating the antigen localization (*Figure 10a, yellow arrows*). The staining follows a granular pattern commonly seen in immunofluorescence staining. A macro view (*Figure 10b*) shows the positive – labelled cells along the red pulp sinuses between two white pulps (white arrows). It was suggested that virus – infected cells in the bloodstream or lymph nodes were carried to the spleen where they gathered and were retained, resulting in inflammation. It has not been proven that the spleen cells *per se* were infected as examination of day 10 post – inoculated mice did not show positive labelling for antigens in the different organs. Plaque assay could be a more sensitive assay compared to immunohistochemistry because virus particles could be hidden after paraformaldehyde fixation. Moreover, IHC is only a qualitative assay while plaque assay is a quantitative one.

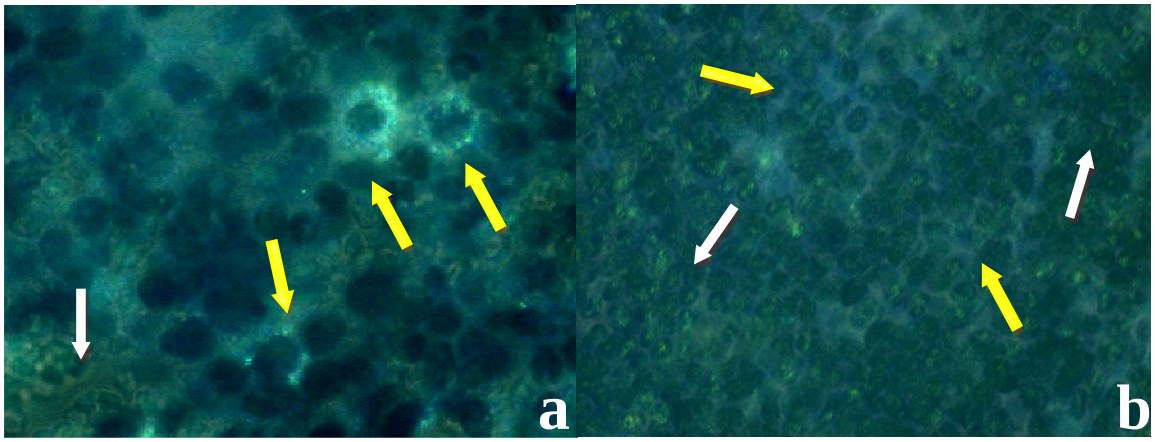

Figure 10: A granular labelling of DV antigens with 4G2 mAb in infiltrating cells in the spleen of AG129 mice inoculated with DV2 *at day 3 post inoculation. The infiltrating cells are localized specifically to the inflamed red pulp (yellow arrows). The white pulp area is demarcated by white arrows. Original magnification 630x (a) and 400x (b).*

The brains of mice sacrificed at day 3 post inoculation did not show any titre by plaque assay. Immunohistochemistry on paraffin sections gave nonspecific staining at blood vessel and meninges regions (*Figure 11*) when the Envision^{+} kit was used (*Section 2.5.5.1*). IGSS returned no false positive results.

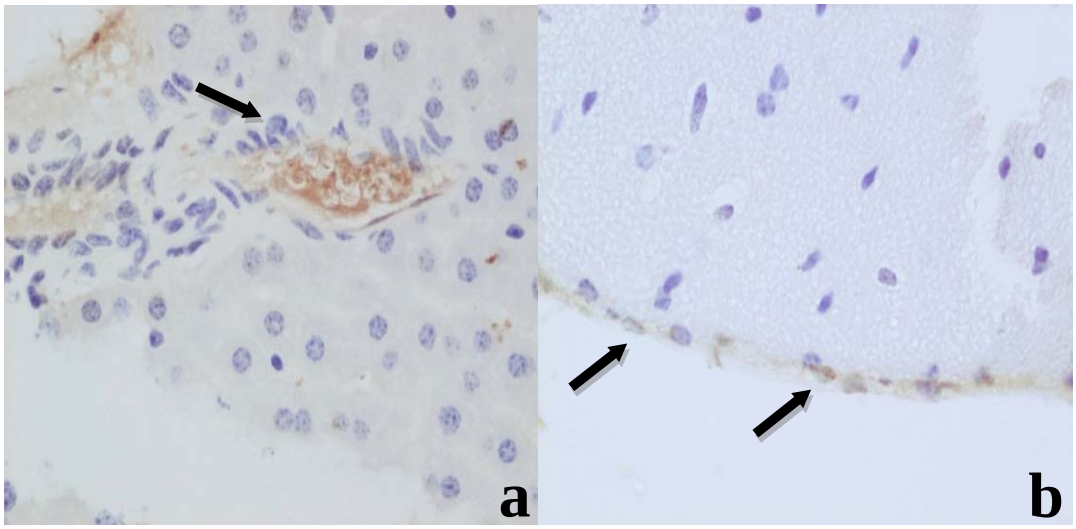

Figure 11: Nonspecific labelling on blood vessels (a - arrow) and meninges (b - arrows) in AG129 mice inoculated with DV2 *and sacrificed on day 3 post inoculation. Original magnification 400x.*

In one of the mice tested, it was found that the brain section was positive for viral antigens (*Figure 12* – red arrows) in cells surrounding a blood vessel that showed perivascular cuffing (black arrows), an inflammatory response where immune cells congregate around a blood vessel which has been activated by chemokines. The neural cells surrounding this blood vessel stained specifically in the cytoplasm and showed distinct granular markings. Other sections of the brain showed no such staining or inflammatory signs. It is possible that no living virus was present in the tissue but viral debris could have been picked up by the surrounding cells or seeped into the organ through the compromised blood vessel.

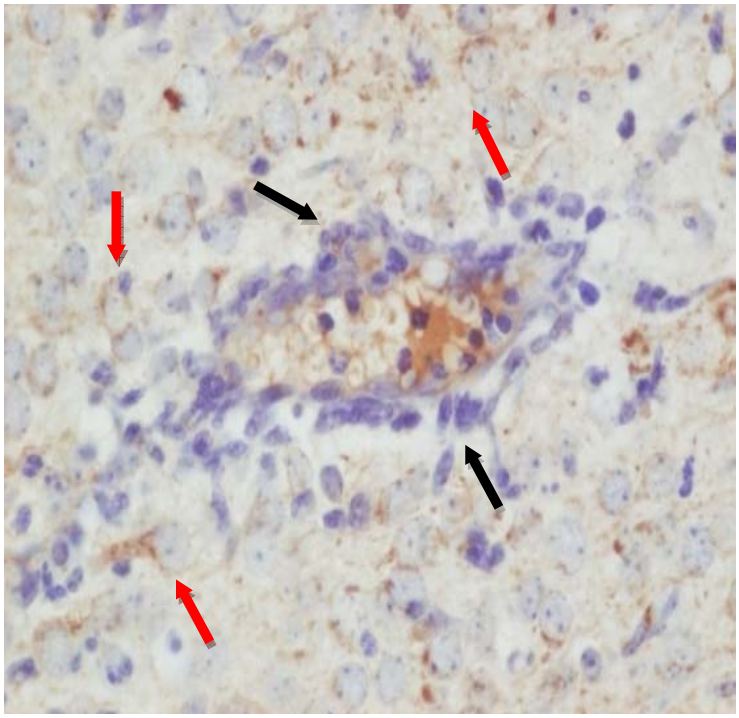

Figure 12: Clear indication of a compromised blood vessel in the brain section; perivascular cuffing (black arrows) and specific labelling of virus antigens nearby (red arrows). The AG129 mouse is inoculated intravenously with DV2 *and sacrificed on day 2 post inoculation. Original magnification 400x.*

The liver sections were closely evaluated for pathological changes and antigen staining but no significant observation was noted. This was unexpected as *Figure 8* clearly shows the liver had an approximate virus load of 10^5 PFU/g on day 3 post infection. As the liver is a major blood reservoir, it could be that the virus load came from the blood trapped in the organ as perfusion of the organs was not done prior to organ harvesting.

3.1.2.3 Long Term Virus Infection Study

To study the long term effects of DV in AG129 mice, virus infection was repeated but with mice sacrificed on day 10 post infection (*Section 2.3.2.1*). By this time, no infectious particles were detected in either serum or organs (*Figure 6*). However, it was postulated that mice could continue to mount an immune response against the virus even after the virus was completely cleared as a result of the initial immunogenic priming. The evaluation of the brain and livers found no significant pathological changes but the spleen showed strong immunological response. In the spleens of two mice sacrificed at day 10 post infection (*Figure 13*), germinal centres in the white pulp were strongly activated (yellow arrows) with inflammation in the red pulp starting to rubside (white arrows).

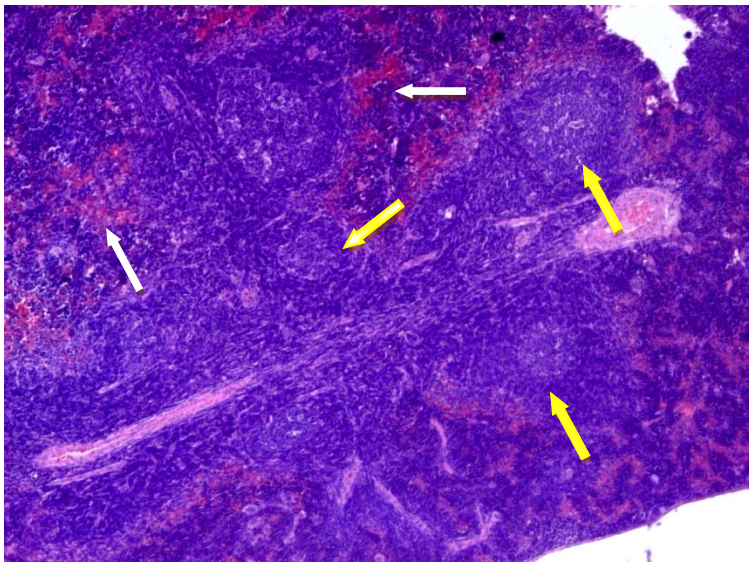

Figure 13: Spleens from AG129 mice inoculated with DV sacrificed at day 10 post infection. Yellow arrows point to B cell germinal centres in the spleen. White arrows point to red pulp areas that are clearing up after being filled with inflammatory cells during the early infection phase in Figure 9. Original magnification 40x.

Areas of T cell proliferation were also appearing indicating that the virus was able to stimulate both arms of the adaptive immune system (*Figure 14 and 15*). B – cell germinal centres in the white pulp and T – cell proliferation areas in the red pulp (yellow arrows) were easily identified. The spleen was still inflamed as seen by the perivascular cuffing (*Figure 15, white arrows*). However, verification using specific T and B cell markers has to be performed in order to confirm this postulation.

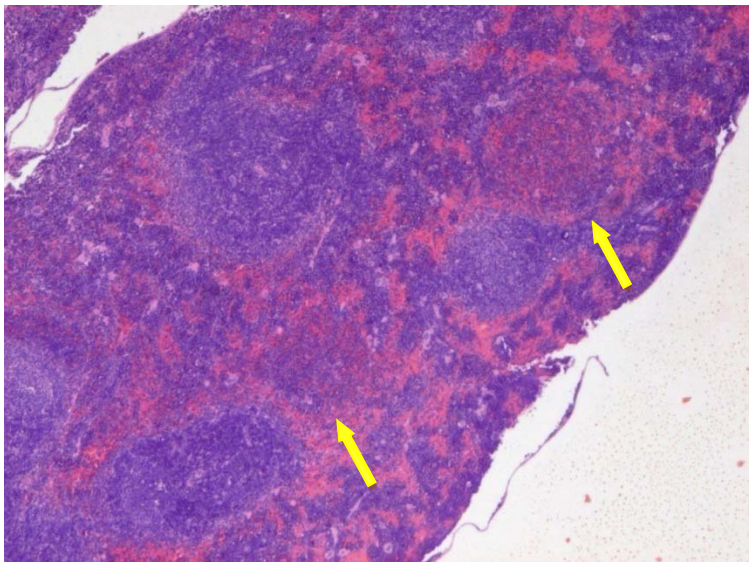

Figure 14: Areas of T cell proliferation (yellow arrows) in AG129 mice inoculated with DV sacrificed on day 10 post inoculation. Original magnification 40x.

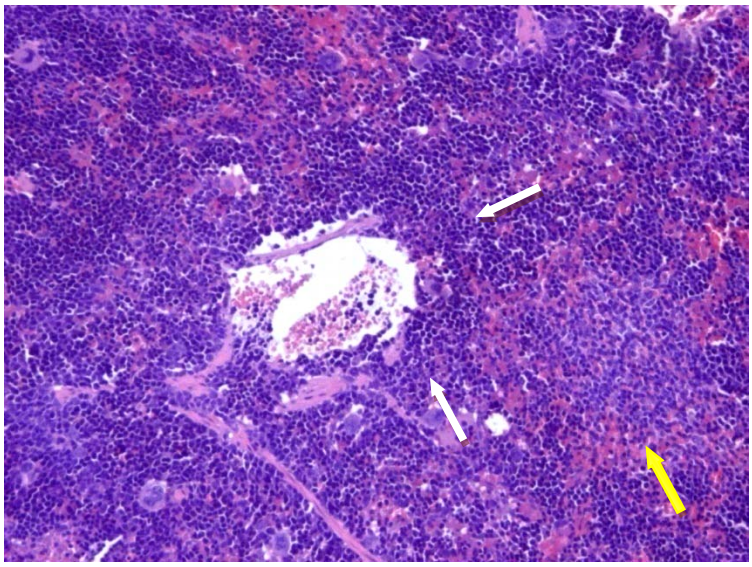

Figure 15: Perivascular cuffing made up of basophilic cells (white arrows) and a germinal centre (yellow arrow) points to a strong immune response in inoculated AG129 mice sacrificed on day 10 post inoculation. Original magnification 100x.

Immunohistology of various organ sections for virus antigens were all negative except for one serendipitous case of a possible phagocytic cell in the brain cortex that displayed positive staining for viral antigen (*Figure 16 – arrow*). It was probable that this phagocyte was clearing up cell debris left by dead cells containing virus proteins.

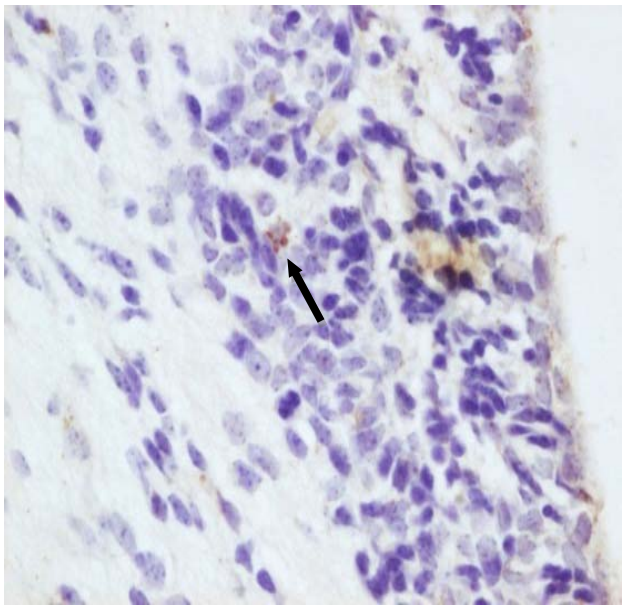

Figure 16: A phagocyte removing cell debris containing virus proteins (arrow). The micrograph comes from a brain section of an AG129 mice inoculated with DV and sacrificed on day 10. Original magnification 400x.

The immunocompetent BALB/c mice inoculated with DV did not show any form of mortality or morbidity. On the other hand, the immuno – deficient AG129 mice inoculated with DV mounted an immune response and had detectable levels of viremia for at least four days in various organs. However, in order to study the full spectrum of a disease and the host reaction to the immunogen, an immunocompetent model is needed. As such, experiments using West Nile virus Sarafend (WNVS) virus was next done to see if this virus could cause more overt signs and symptoms in the BALB/c model. West Nile virus was perceived to be a better model since the virus grows to 10^9 PFU/ml and higher titres could be used for inoculation.

3.2 INFECTION OF MICE WITH WEST NILE VIRUS (SARAFEND)

3.2.1 Infection of Adult Mice with West Nile Virus (Sarafend)

Stock WNVS was grown on C6/36 or Vero cells and titred at 10^9 PFU/ml (*Section 2.2.4*). Adult BALB/c was first tested for levels of viremia and mortality when inoculated intravenously with 100 microlitres of stock WNVS (*Section 2.3.3.1*). The virus was injected through the tail vein with two mice per group and bled on days 1, 3, 5, and 18 post inoculation through the submandibular vein (*Section 2.3.4*). The sera were tested by plaque assay for levels of infective virus particles (*Section 2.2.4*). *Table 8* showed the results of the pilot study for WNVS grown in C6/36 cells while *Table 9* showed the study using Vero cell – grown virus. Similarly, two mice were killed on days 1, 3, 5, and 18 post inoculation; the organs harvested, homogenized and titred for infectious viruses. From *Tables 8 to 9,* only one mouse had residual virus load on day 1 post infection. The rest of the mice cleared all 10^9 PFU/ml of WNVS in less than 24 hours. Histological sections from all timepoints stained with haematoxylin & eosin showed no signs of disease or pathology. This clearly indicated that the WNVS stock similar to the DV (*Section 3.1*) was unable to infect the immunocompetent BALB/c mouse model or cause any form or morbidity.

Table 8: PFU/ml sera or PFU/g tissue of adult BALB/c mice inoculated with WNVS grown on C6/36 cells and bleed on different days to test for viremia. Titres are means from two different mice.

Organ	Day 1	Day 3	Day 5	Day 18
Serum	2×10^1	0	0	0
Liver	0	0	0	0
Brain	0	0	0	0
Spleen	0	0	0	0

Table 9: PFU/ml sera or PFU/g tissue of adult BALB/c mice inoculated with WNVS grown on Vero cells and bled on different days to test for viremia. Results derived from the mean of two mice.

Organ	Day 1	Day 3	Day 5	Day 18
Serum	0	0	0	0
Liver	0	0	0	0
Brain	0	0	0	0
Spleen	0	0	0	0

As the virus was not able to infect adult mice, it was decided to test on suckling mice. Sucklings are more susceptible to infection as the mice immune system is not yet fully developed.

3.2.2 Infection of Suckling Mice with West Nile Virus (Sarafend)

Ten million WNVS particles were injected into the brains of suckling mice and two mice were harvested every 6 hours from 18 hours post infection onwards. The brains were collected for plaque assay and the means shown in a typical growth curve as seen in

Figure 17. It was clear that the maximum virus titre was found at 54 hours post inoculation. This result would be later applied in *Section 3.3*.

The high titre at 18 hours post inoculation could be from the initial inocula and the virus entered into the eclipse phase between 18 to 24 hours post inoculation to begin new cycle of replication. The exponential phase of the progeny virus production was observed from 24 hours post infection onwards. The virus titre plateaued from 30 hours post infection showing a small increase in the titre at 54 hours post inoculation before the decline in virus production.

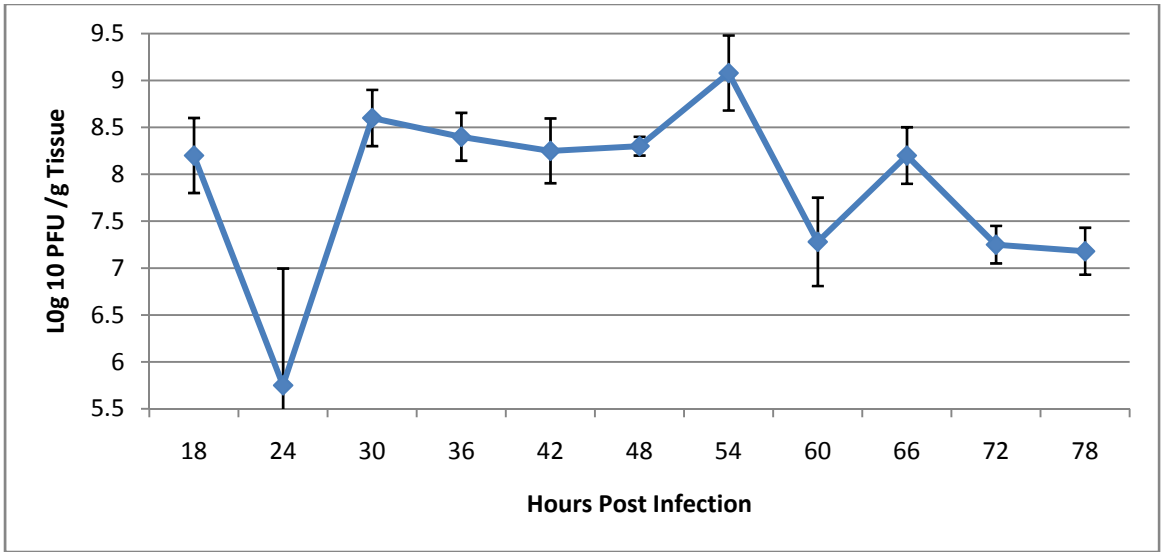

Figure 17: WNVS growth curve in BALB/c suckling mice brain at different periods post infection. At 54 hours post infection the virus titre is found to be the highest. Each point represents the mean of 3 mice. Error bars represent standard errors.

Suckling mice were also tested for survival times with different dosages of stock WNVS inoculated intracerebrally into the brain (*Section 2.3.3.2*). The mice were checked every 12 hours and dead suckling mice were dissected and the brains harvested for homogenization and plaque assay. Groups had either 3 or 4 mice. From *Figure 18*, only

small differences could be seen between the survival times of suckling mice inoculated with different virus doses. Mice started dying on day three post inoculation onwards with a steady drop in the number of surviving mice until day seven to eight post infection. Outliers seen were mice infected with 10000 PFU/100 microlitres – infected mice as the day of most recorded deaths was pushed back to day 10 post infection compared with day 4 post inoculation for the other groups. The brains were harvested for plaque assay and showed consistent virus titre levels of between 10^7 to 10^9 PFU/g tissue sample.

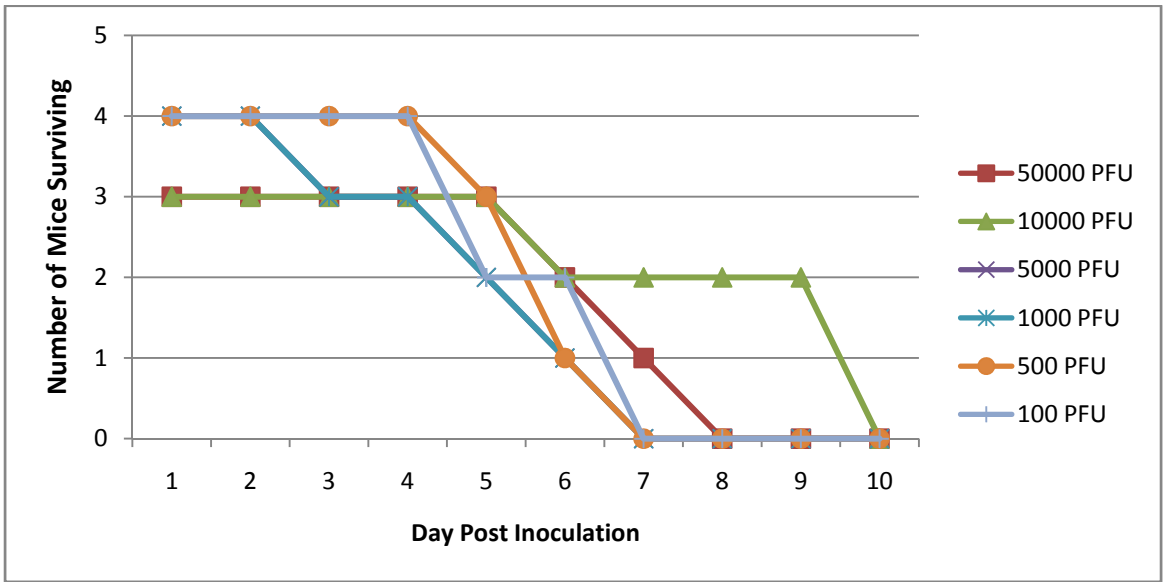

Figure 18: Survival curve of BALB/c suckling mice intracerebrally inoculated with various WNVS loads. All curves except the 10000 PFU line show a strong drop from day 3 onwards.

The different killing trend for the 10,000PFU injected suckling mice could be attributed to error in experimental methods as the group was only made of 3 mice. However, collectively with the different doses tested, a total of 21 suckling mice were used and this overall, as seen in the graph, showed a very narrow deviation in killing pattern.

The results convincingly showed that wild type DV and WNVS from the laboratory were not able to consistently infect and cause any form of mortality or morbidity in adult immunocompetent mice. Suckling mice succumbed to the virus when inoculated intracerebrally with a range of dosages of infectious particles without any dose dependent pattern. Because the immunocompetent adult mice were injected through the intravenous route and not intracerebrally, it was able to clear the virus infection as compared to the suckling mice. The suckling mice also did not have a fully mature immune system. It was therefore not surprising that the virus infection showed such variation when injected into those two mice models using different inoculation routes.

Since the virus had been passaged through cell culture for many years in the laboratory setting, it was postulated that the virus became adapted to infecting specific cell lines and could not establish infection in *in vivo* animal models. It was thus hypothesised that the virus could be re – adapted to infect adult mice should the virus be re – passaged repeatedly in mice. This became the objective of the subsequent study detailing the effects of passaging WNVS in an immunocompetent model.

3.3 PASSAGING OF WEST NILE VIRUS (SARAFEND) THROUGH SUCKLING MICE AND C6/36 CELL CULTURE

The WNVS was chosen for the passaging experiment instead of DV as there are four dengue serotypes. Selecting one serotype, strain, or isolate over the others would be difficult. Moreover, DV is known to show fewer and weaker signs and symptoms in both infected humans and animals. WNVS on the other hand is able to infect immunocompetent mice as reviewed in *Table 2*. As such, it was of interest to study if and

how the laboratory strain of cell culture attenuated WNVS could evolve into a mouse – infecting strain given suitable adaptive conditions.

In nature, WNVS transmits between birds and blood sucking arthropods. To mimic nature while adapting the virus to infect mice, WNVS was passaged through suckling mice brains and C6/36 mosquito cell culture. Stock WNVS was subjected to ten rounds of continual passaging through either only suckling mice brains ('m' series, *Section 2.3.6.1*) or both suckling mice brains and C6/36 cells ('c' series, *Section 2.3.6.2*). Mouse organs were harvested and weighed before being snap frozen at -80 °C. After homogenizing the samples at 50 % w/v (*Section 2.3.5*), it was spun down and the supernatant used for plaque assay (*Section 2.2.4*). Both passaging routines were duplicated 5 times resulting in a total of 10 passaged viruses (*Section 2.3.6*). The resulting viruses generated from each passage level were assayed for infectivity as well as plaque size (*Section 2.2.4*).

To explain the terminology used, the two different passaging regimes used were known as 'm' and 'c' series. Virus passaged through suckling mice brains repeatedly for ten rounds was known as 10m, *i.e.* the tenth passage of the 'm' passaging regime. Conversely, the 'c' series delineates viruses passaged alternately through suckling mice brain and C6/36 mosquito cell line. So the tenth passage of this series was known as 10c. Because both series were repeated five times in tandem, there were ten passaged viruses, five from the suckling mouse brain regime: 10m1, 10m2, 10m3, 10m4, and 10m5; and

five from the suckling mouse brain – mosquito C6/36 cell culture regime: 10c1, 10c2, 10c3, 10c4, and 10c5.

From each round of passaging, the virus was titred by plaque assay (*Section 2.2.4*). In addition, each assay plate had two positive control wells using unpassaged Vero cell grown WNVS. These two wells were used as a benchmark for plaque size. The average of ten plaque diameters of the unpassaged WNVS was compared against the average of ten plaque diameters of the passaged virus on each plate. The results from all 10 different repeats for all 10 consecutive passages were then plotted on a graph and displayed as *Figures 19 to 21* as a plaque ratio curve of the passaged virus against the unpassaged WNVS. The size of unpassaged WNVS plaque was set at an absolute value of 1.

Figure 19 clearly showed an increase in relative plaque sizes for viruses passaged through suckling mice brain at two points; passage number two, and approximately passages five to eight. The synchronisation of increase of plaque size between the different repeats was clearly seen at passage two and less obvious at the larger increase between passages five to eight. It was suggested that with increasing passaging rounds, a wider range of plaque size viruses could be found, giving rise to haphazard cyclic ratio trends towards passage 10. The largest plaque size observed was 40 % larger than the unpassaged virus (*Figure 19* – m2). On average there was a general trend of larger size plaques with increasing passage number.

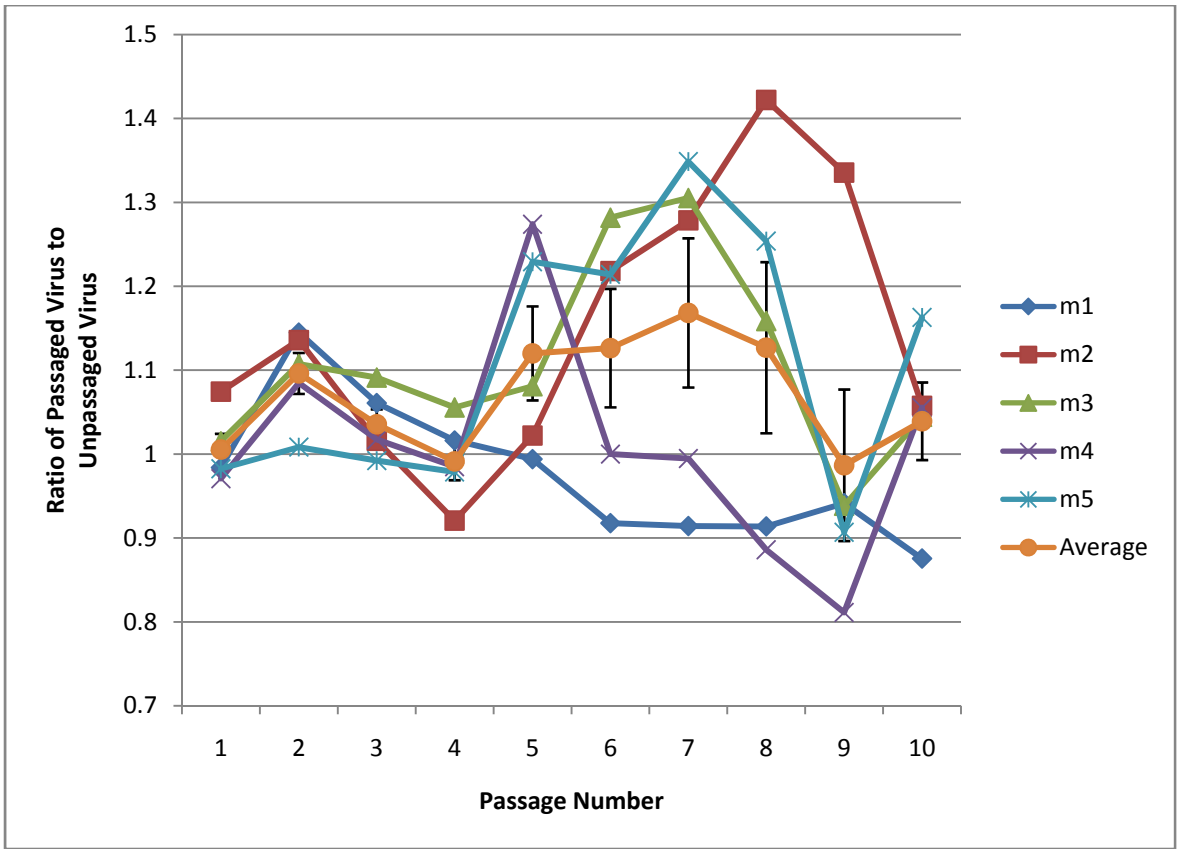

Figure 19: Relative plaque sizes from the mouse - only 'm' passaged viruses over 10 passages. Each point represents the mean from two mice. The ratio of 1 represents baseline value of no difference in plaque size between passaged and unpassaged viruses. Error bars on average curve represents standard errors.

For the mouse – C6/36 'c' passaging series, *Figure 20* showed the virus plaque sizes from the alternate mouse passage while *Figure 21* displayed the alternate C6/36 passaged virus plaque sizes. Compared to the mouse only 'm' passaging regime, the plaque sizes from the mouse – C6/36 passage showed a general decrease in size as compared to the unpassaged virus plaque size. From the average curve, the graph pattern was different compared to the bimodal trend in *Figure 19* as the general size change shown by the average graph indicated a lowering in plaque size with increased passaging. There was also less correlation in the graph pattern when comparing the different repeats. The five

different repeats were less synchronised in cyclic size patterns as compared to the 'm' passaged virus in *Figure 19.*

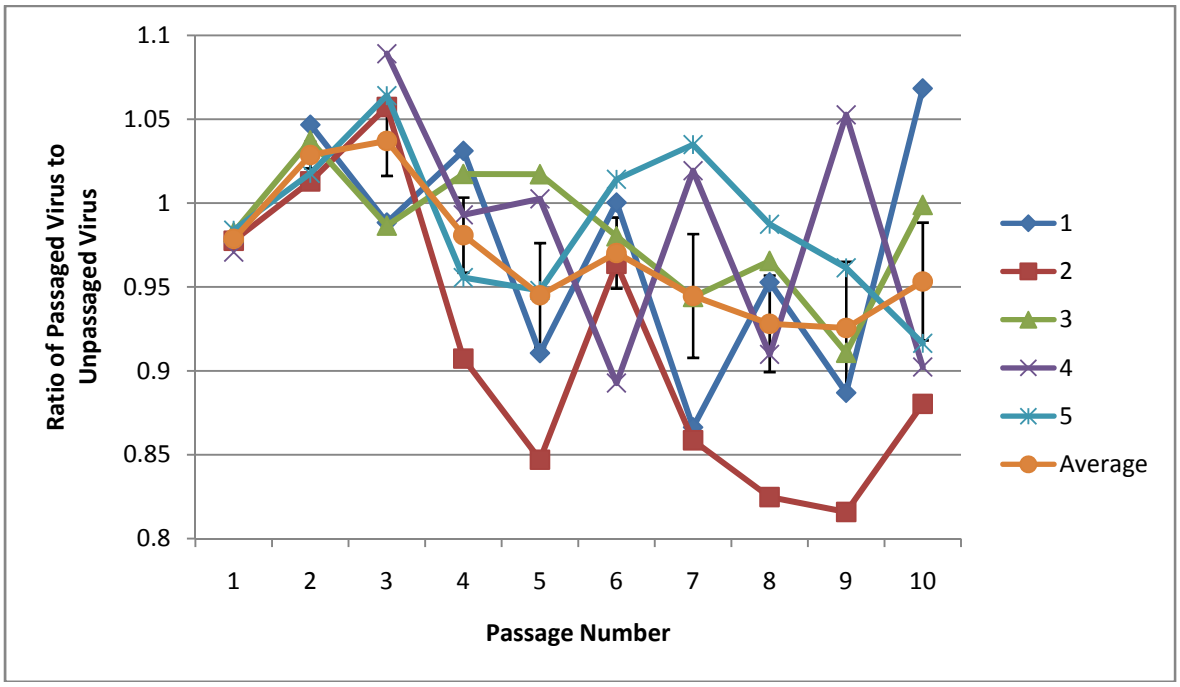

Figure 20: Relative size of virus plaques from the alternate mouse passage of the mouse - C6/36 'c' passaged series. There is a drop in plaque size with increasing passaging. Each point represents the mean from two mice. The ratio of 1 represents baseline value of no difference in plaque size between passaged and unpassaged viruses. Error bars on average curve represent standard errors.

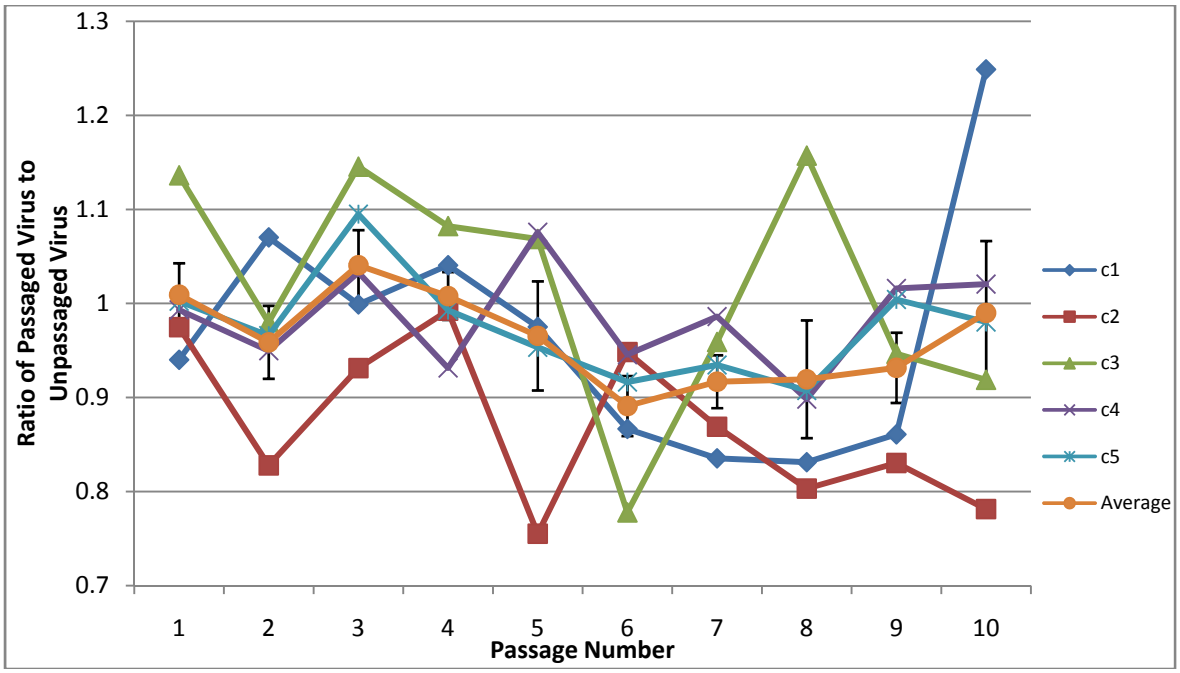

Figure 21: Relative size of virus plaques from the alternate C6/36 passage of the mouse - C6/36 passaged series. The average trend shows the plaque size dropping with increasing passaging. Each point represents the mean from two mice. The ratio of 1 represents baseline value of no difference in plaque size between passaged and unpassaged viruses. Error bars on average curve represent standard errors.

Standard deviations from ten plaque sizes were calculated and displayed as a graph (*Figures 22 to 24*). The standard deviation of plaque sizes was a representative figure of how varied the plaque sizes are. A larger standard deviation indicated a more diverse range of plaque sizes. The average standard deviation hovered between 1 and 3.5 units throughout the passaging. There was a peak in average standard deviation for both the 'm' and 'c' series passages at different passage numbers. Higher standard deviations were seen during the mouse passages for both the 'c' and 'm' series.

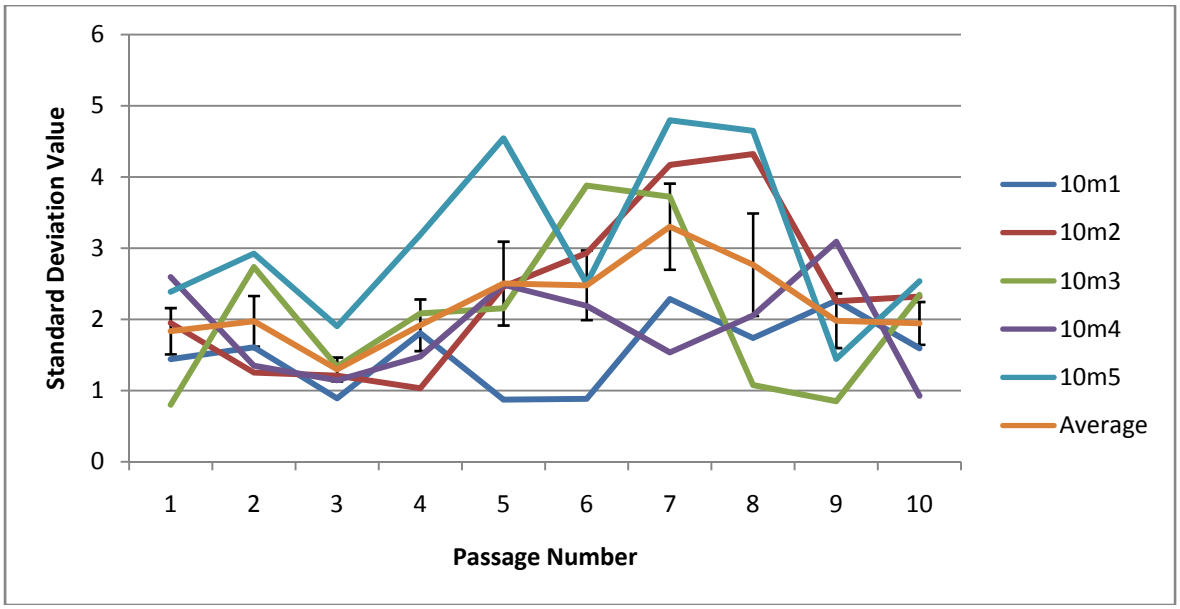

Figure 22: Standard deviation of plaque sizes of the different passage repeats for the mouse – only 'm' passaged viruses over 10 pasages. The average graph shows a peak in virus size variation at passage seven. The average errors are higher than the 'c' series. Error bars represent standard errors.

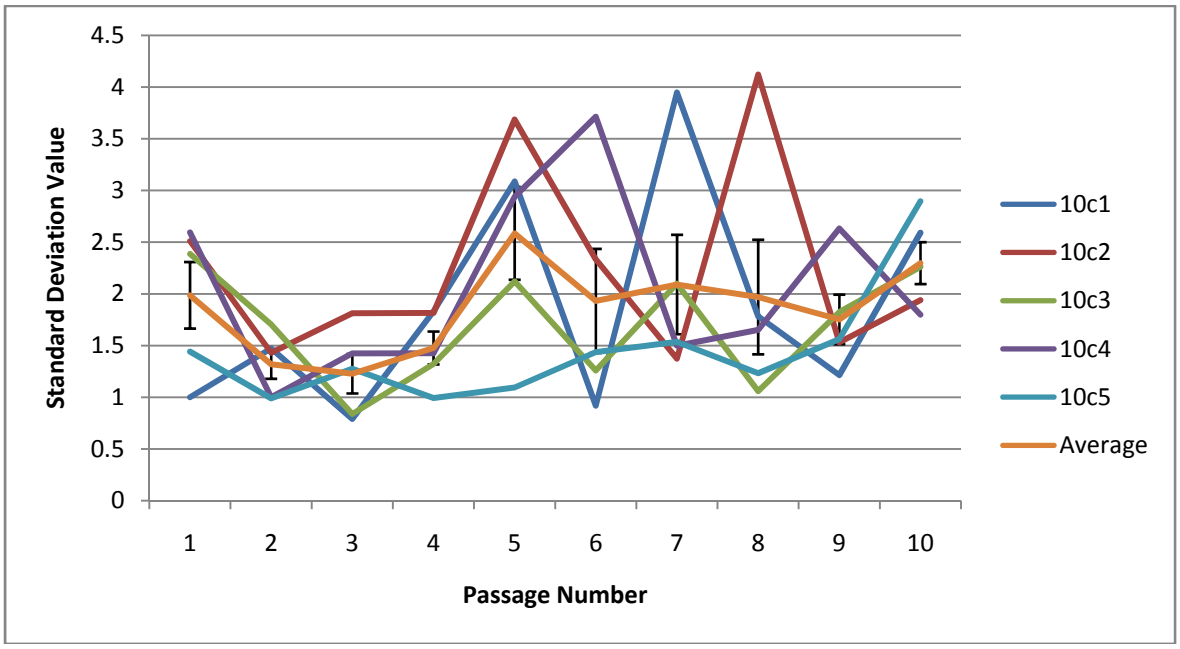

Figure 23: Standard deviation of plaque sizes of the different passage repeats from the alternate mouse passage of the mouse - C6/36 'c' passaged series. The average line fluctuates greatly during passages five to eight. There is a peak in average plaque size variation at passage five with 3 of 5 repeats showing a peak on that passage. No statistically significant points are detected on the average graph. Error bars represent standard errors.

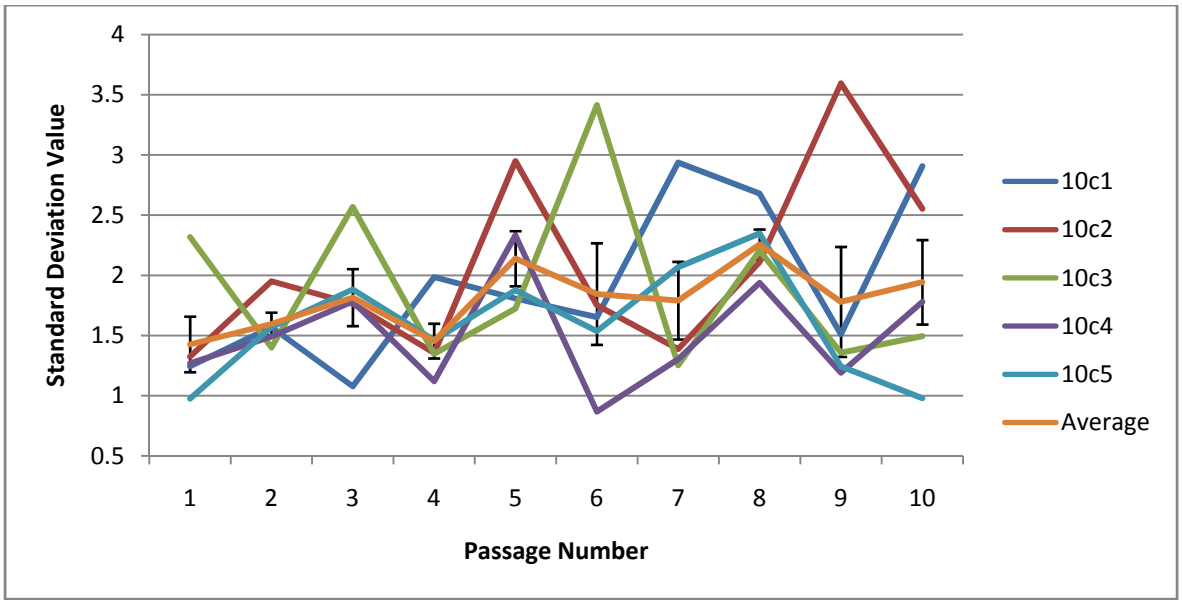

Figure 24: Standard deviation of plaque sizes of the different passage repeats from the alternate C6/36 passage of the mouse - C6/36 'c' passaged series. The average line is relatively linear and has the least variation compared to the other graphs (Figures 22 and 23). The average graph shows a gentle cyclical increase in standard deviation with passaging. Error bars represent standard errors.

Throughout the passaging process, virus titres remained relatively consistent; the plots (*Figures 25 to 30*) showed the log virus titres from various organs of the suckling mice for each virus passage from the mouse 'm' only passages. Virus titres in the brains were highest at an average of 10^8 PFU/g tissue (*Figures 25 to 26*) while the livers were on average one log lower at 10^7 PFU/g tissue (*Figures 27 to 28*) and in spleens a further log lower at 10^6 PFU/g tissue (*Figures 29 to 30*). No blood was collected from the suckling mice as there was insufficient volume to complete the experiments. The virus inoculated into the brains of suckling mice could migrate and proliferate in both livers and spleens of the inoculated mice showing that the blood – brain barrier was still underdeveloped in the sucklings. It was also noted that the suckling mice inoculated with the virus at late passage numbers (passage eight to ten) showed less severe symptoms of illness at 48 hours post infection unlike the earlier passages (passage one to seven) where the pups

stop suckling, lost weight and were mostly inactive. The virus at late passages thus appeared to become attenuated. The viruses were still neurovirulent at passage 10 as significant virus titres were obtained from the brains of suckling mice. No error lines were shown for the line graphs as it is the average from only 2 mice.

The different titre levels of virus in different organs were a reflection of virus tropism and infectability. Suffice to say WNVS retained its ability to infect and cause severe disease in suckling mice throughout the whole passaging period. Starting titres from all tested samples were comparable to titres at passage 10 indicating the virus was replication – competent throughout the ten passages.

Bar graphs (*Figures 26, 28, and 30*) showed the more erratic mean virus titers found in the brains, livers, and spleens of sacrificed suckling mice from the mouse 'm' only passaging method as compared to the latter mouse – C6/36 'c' passaging experiments (*Figures 31 to 36*). The graphs for livers and spleens (*Figures 28 and 30*) seemed to show a bimodal distribution with a drop around passage five. The standard error bars showed some variations in the virus titer but compared to the line graphs, one can conclude that the titers from each organ were quite conserved over different passages. This gave some confidence to suggest that the data was not a random occurance.

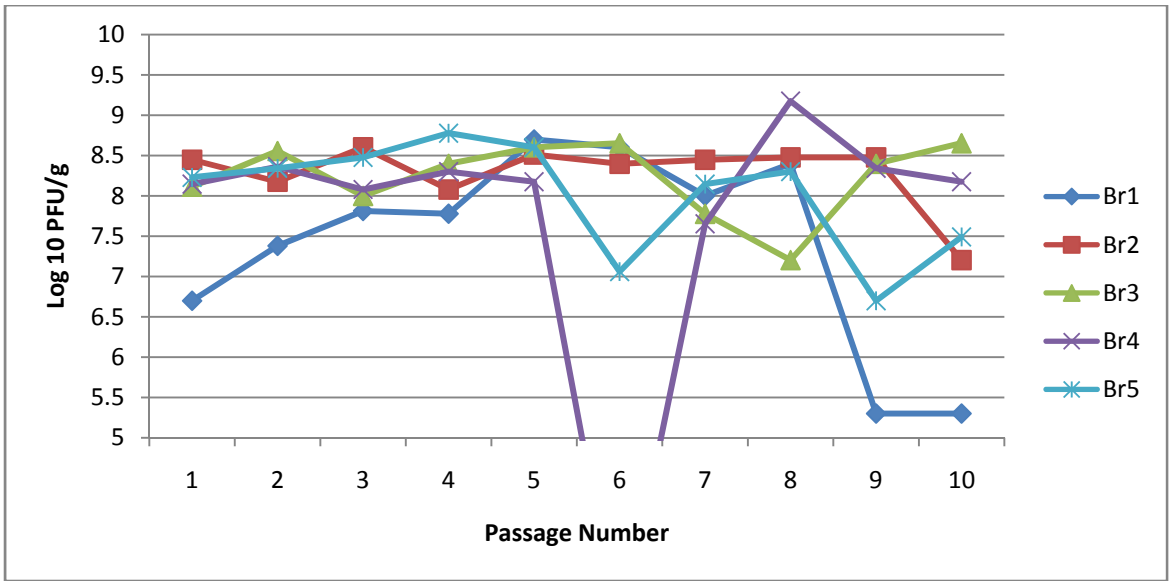

Figure 25: Log_{10} PFU/g tissue sample of virus in suckling mice brains from different passages of the mouse only passaging series 'm'. Each point represents the mean from two mice. A null titre in Brain 4 passage 6 was due to ethanol seeping into the cryovial during the snap freezing process and virus was not recovered.

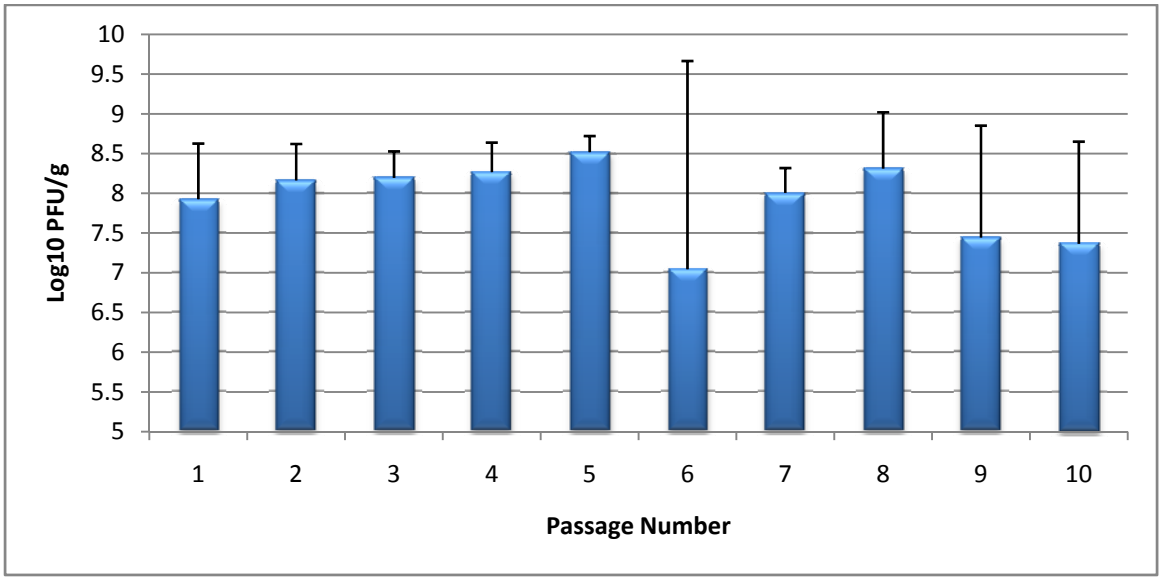

Figure 26: Average Log_{10} PFU/g tissue sample of virus in suckling mice brains from the 5 repeats of different passages in the mouse only passaging series 'm'. Although the absolute titre for one repeat dips significantly in passage 6 (Figure 25) the average graph does not show any statistically significant variation between the titres of passage 6 as compared to the other passages ($p<0.05$). Error bars represent standard errors.

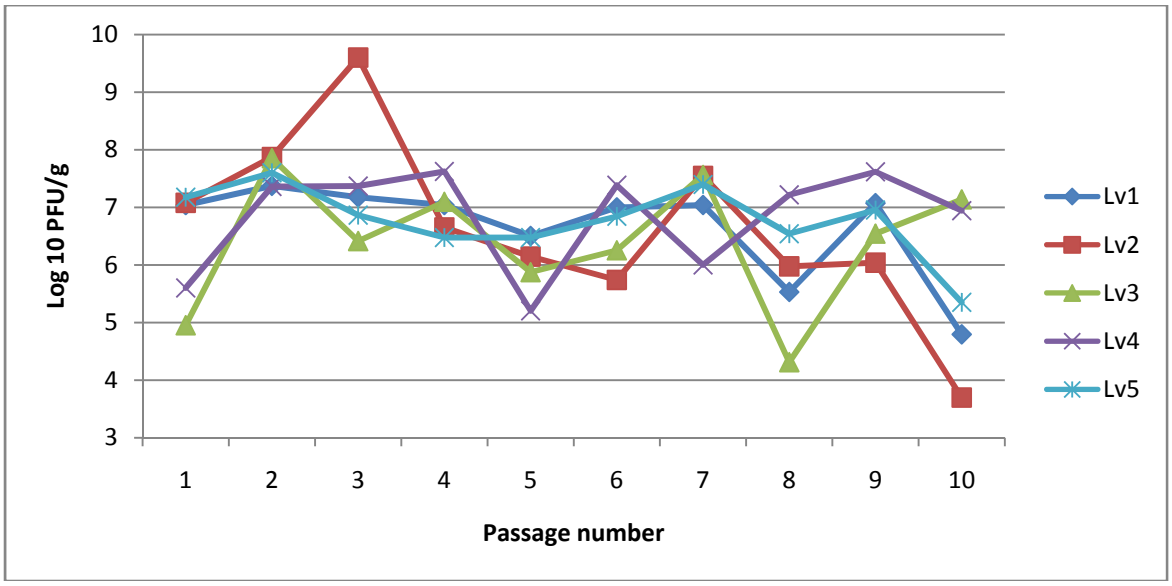

Figure 27: Log_{10} PFU/g tissue sample of virus in suckling mice livers from different passages of the mouse 'm' only passaging series. Each point represents the mean from two mice.

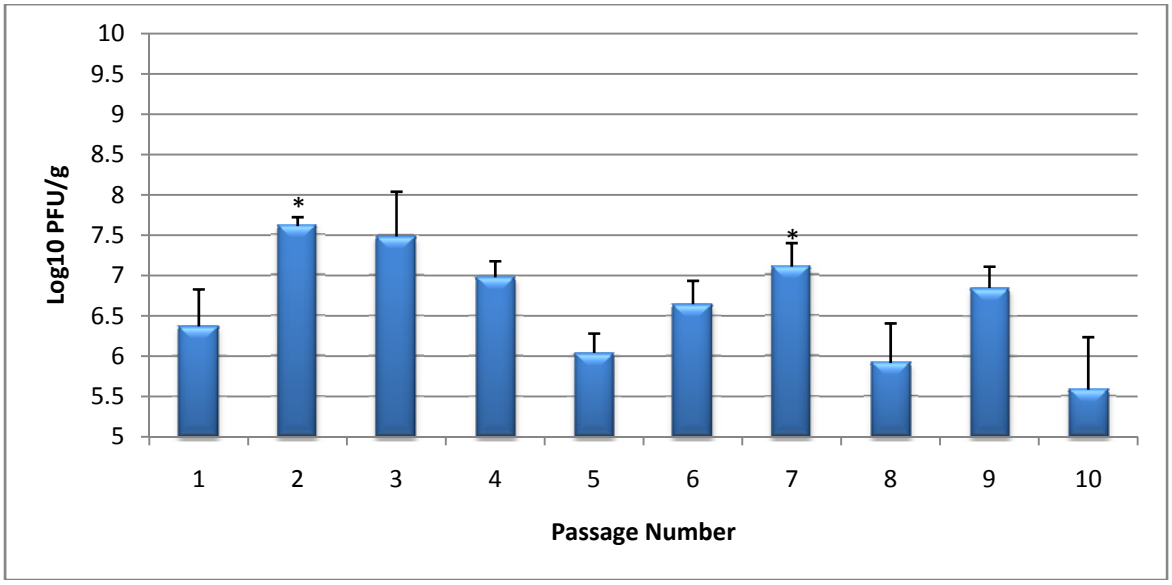

Figure 28: Average Log_{10} PFU/g tissue sample of virus in suckling mice livers from the 5 repeats of different passages in the mouse 'm' only passaging series. A bimodal distribution can be seen with peaks at passage 2 and 7. Asterisks indicate significant virus titre ($p<0.05$) difference against passage 5 titre. Error bars represent standard errors.

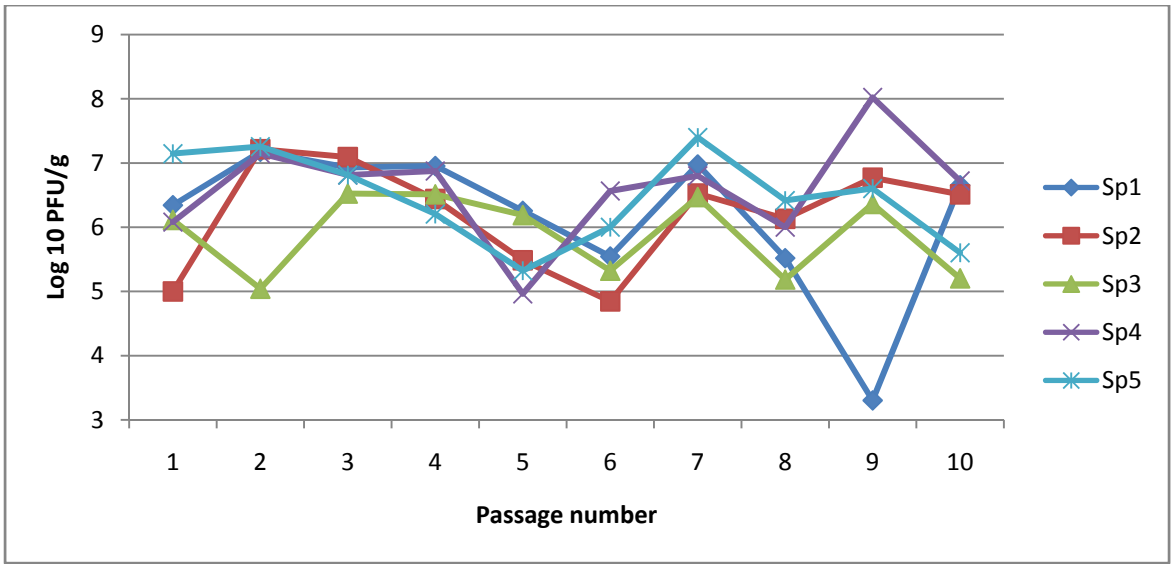

Figure 29: Log_{10} PFU/g tissue sample of virus in suckling mice spleens from different passages of the mouse 'm' only passaging series. Each point represents the mean from two mice.

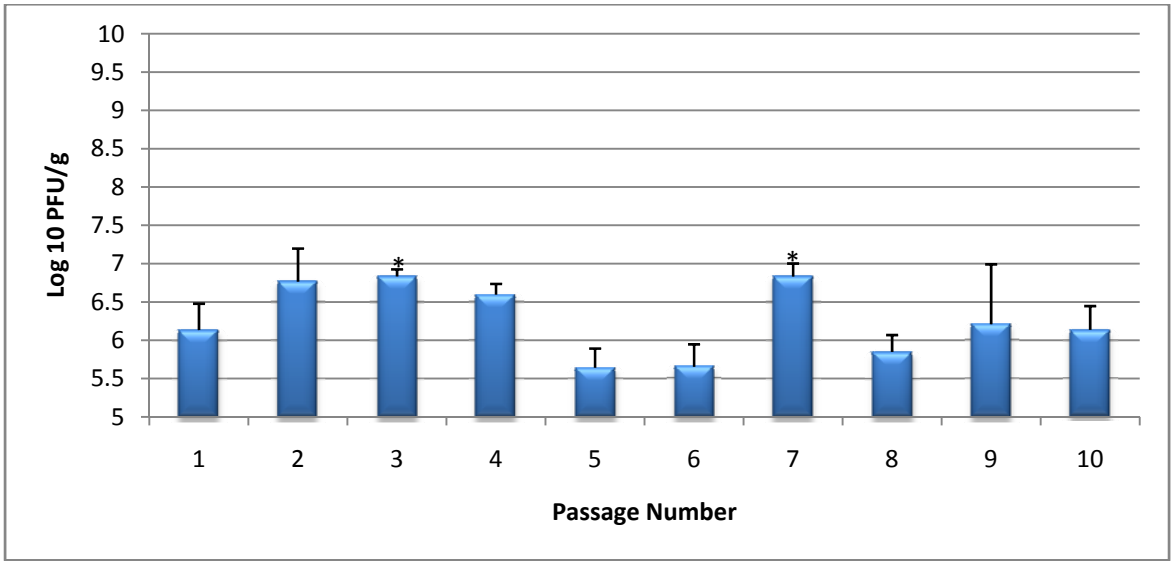

Figure 30: Average Log_{10} PFU/g tissue sample of virus in suckling mice spleens from the 5 repeats of different passages in the mouse 'm' only passaging series. There is a bimodal distribution with average virus peaks at passage 3 and 7. Asterisks indicate significant ($p<0.05$) virus titre difference against passage 5 titre. Error bars represent standard errors.

Virus levels from the mouse – C6/36 'c' passaging regime yielded titres not unlike the mouse 'm' only passaging method. *Figures 31 to 36* showed the log virus titres in brains, livers, and spleens at various passages. The difference between organs was approximately

one log. No trend could be spotted from the graphs as the virus yield remained relatively constant throughout the passaging rounds. Statistical analyse comparing each passage virus titre against other passage numbers detected no significant titre change ($P < 0.05$).

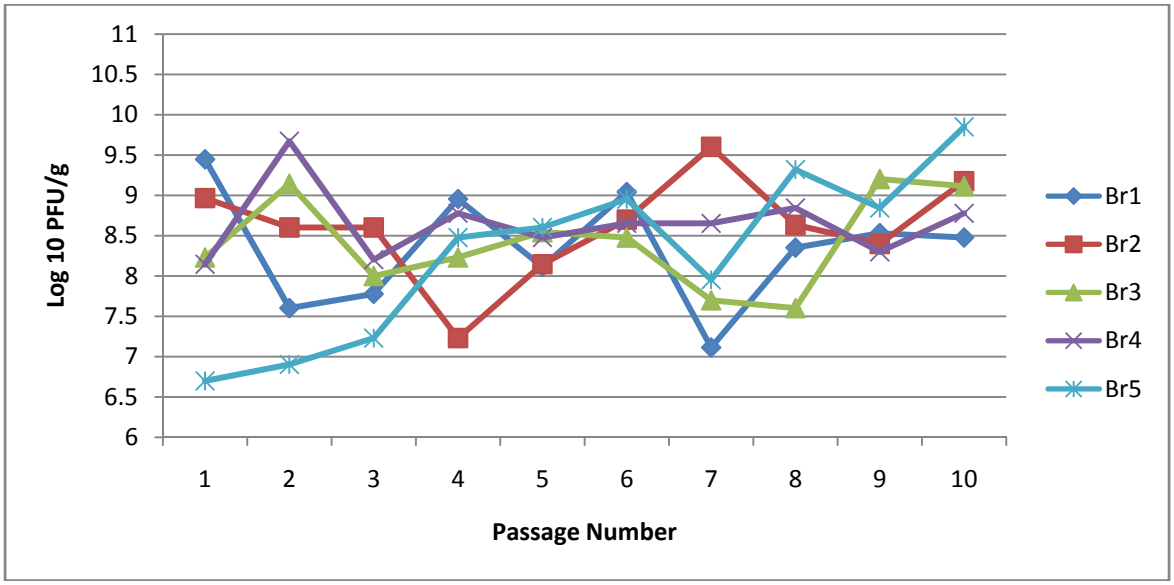

Figure 31: Log_{10} PFU/g tissue sample of virus in suckling mice brains from different passages of the mouse – C6/36 'c' passaging series. Each point represents the mean from two mice.

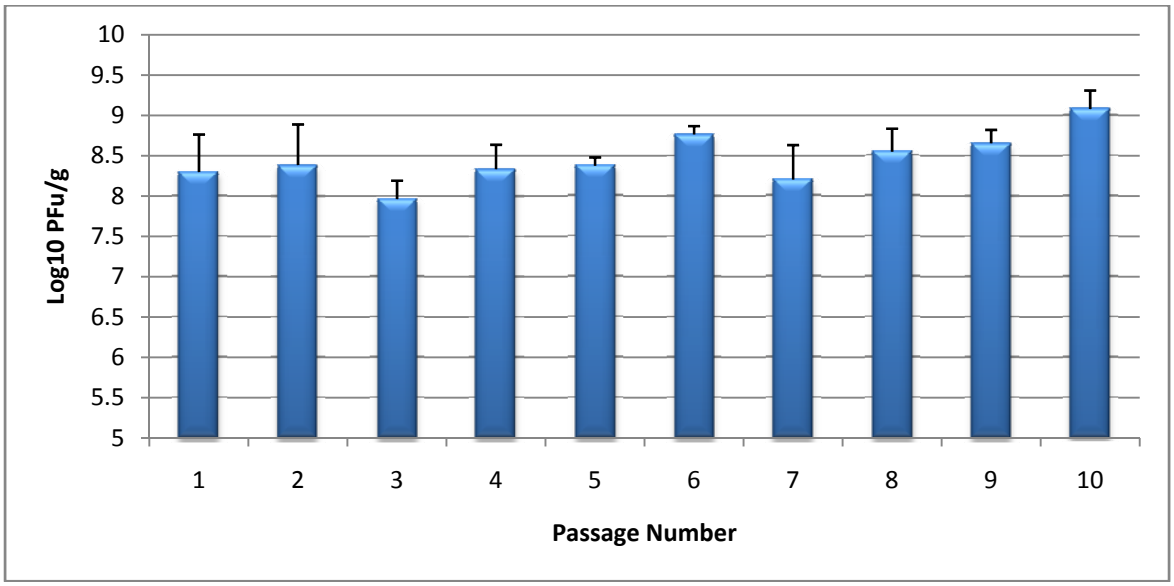

Figure 32: Average Log_{10} PFU/g tissue sample of virus in suckling mice brains from the 5 repeats of different passages in the mouse – C6/36 'c' passaging series. The average graph shows little variation in virus titres. No statistically significant variation in titres between passages are noted ($p<0.05$). Error bars represent standard errors.

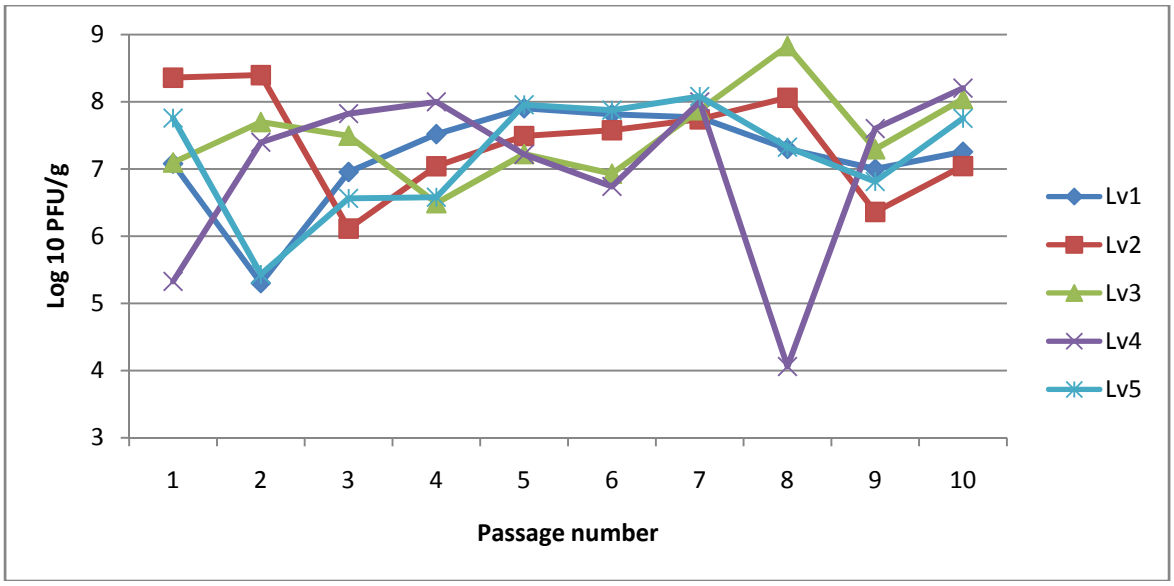

Figure 33: Log_{10} PFU/g tissue sample of virus in suckling mice livers from different passages of the mouse – C6/36 'c' passaging series. Each point represents the mean from two mice.

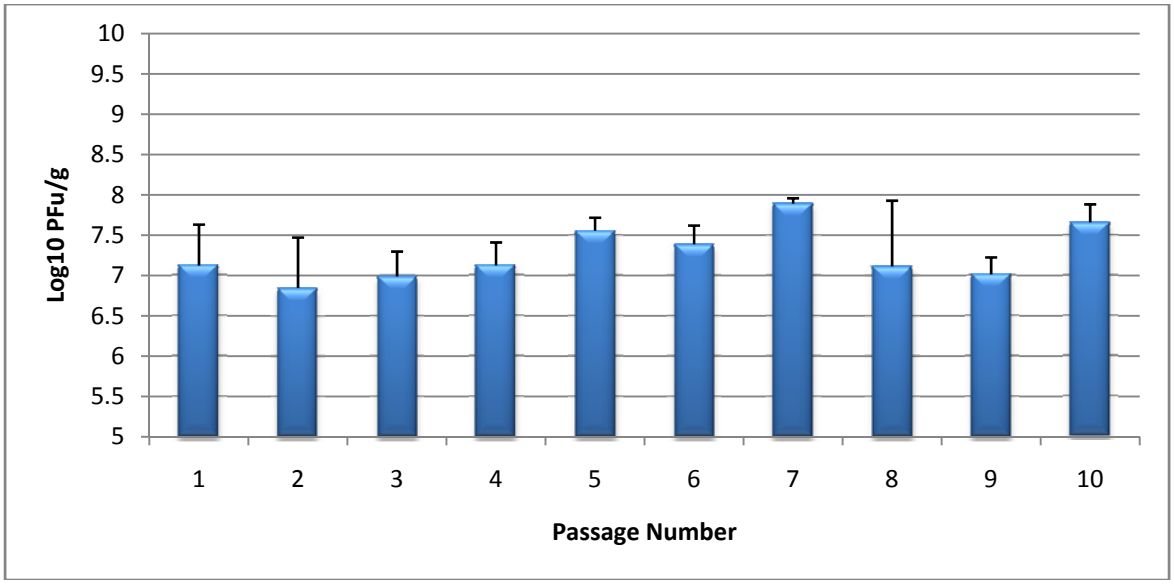

Figure 34: Average Log_{10} PFU/g tissue sample of virus in suckling mice livers from the 5 repeats of different passages in the mouse – C6/36 'c' passaging series. There is a unimodal distribution with a peak at passage 7. No statistically significant variation in titres between passages are noted ($p<0.05$). Error bars represent standard errors.

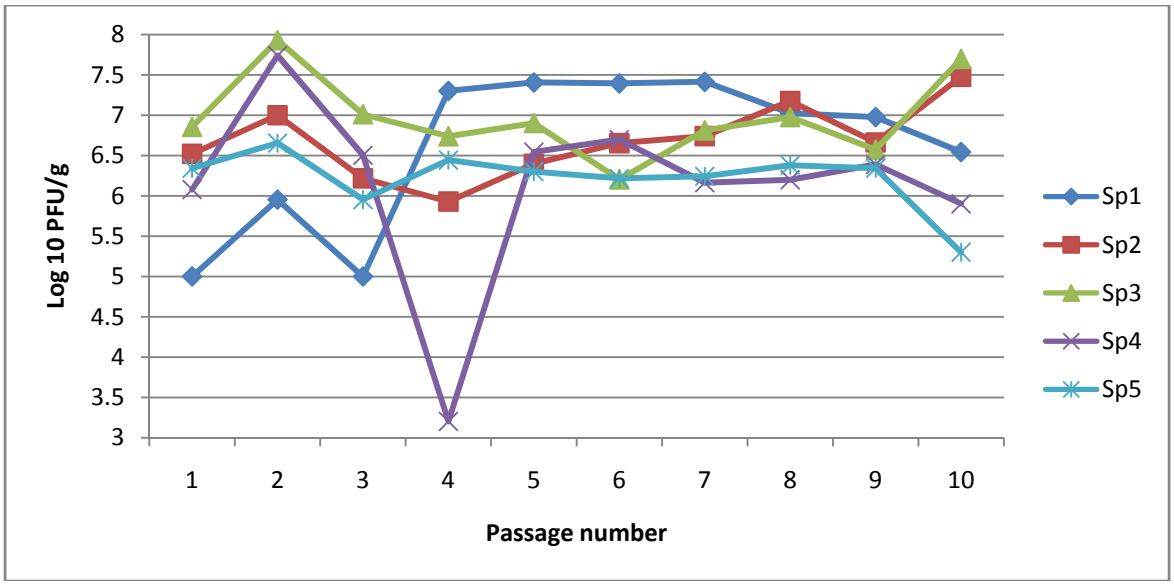

Figure 35: Log_{10} PFU/g tissue sample of virus in suckling mice spleens from different passages of the mouse – C6/36 'c' passaging series. Each point represents the mean from two mice.

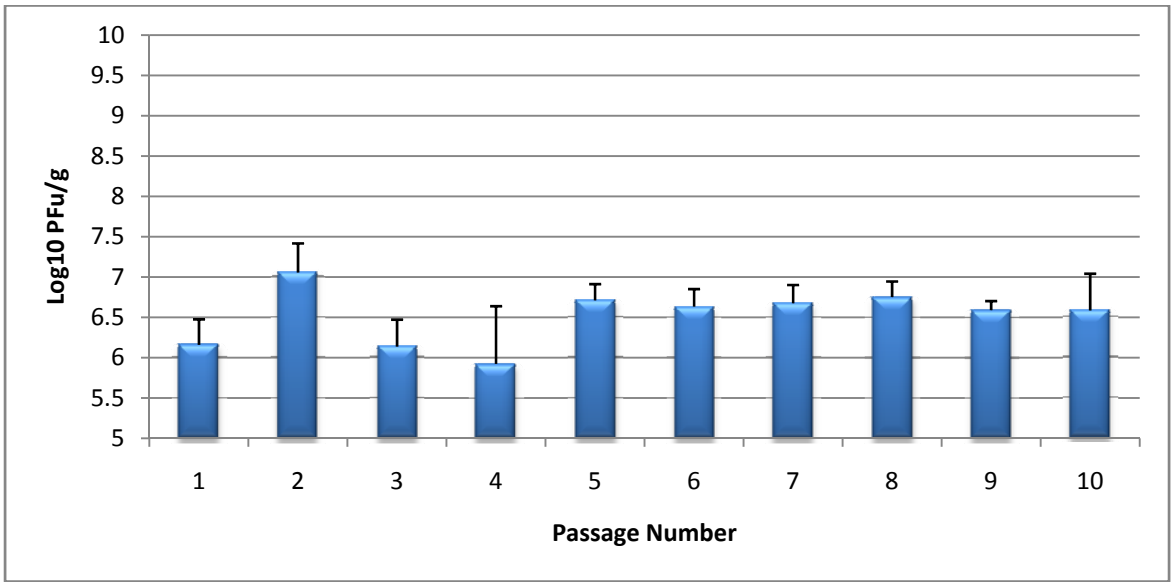

Figure 36: Average Log_{10} PFU/g tissue sample of virus in suckling mice spleens from the 5 repeats of different passages in the mouse – C6/36 'c' passaging series. A bimodal distribution is present with virus peaks at passages 2 and 8. No statistically significant variation in titres between passages are noted ($p<0.05$). Error bars represent standard errors.

As for the C6/36 alternate passages from the mouse – C6/36 series, the virus titre remained at approximately log 9.5 PFU/ml (*Figures 37 to 38*). There was a sudden drop

in virus titres at passage number five when four out of five repeats experienced a sharp decline with an average decrease of about 1.25 $\log_{10}$ PFU/ml or a 17 fold reduction taking the average 5^{th} passage titre as comparison. This could be biologically significant as it was observed in four out of the five repeats. However, this decrease was only momentary. At passage six the virus titre reverted to that of passage four with an increase of 1.0 $\log_{10}$ PFU/ml or an 11.5 fold increase on average. Statistical analyses comparing passage five virus titres against all other passage numbers showed significant change in virus titre ($p < 0.05$). A bimodal distribution was seen in this group with a drop of about one log virus titre at passage number 5 (*Figure 38*).

The passage 4, 5, and 6 viruses were used to re – infect C6/36 cells to reproduce the drop in virus titre seen. However, the drop seen in passage 5 could not be reproduced. Evaluation of supernatants from the re – passaged stocks was performed for viral RNA levels by real – time PCR, viral protein levels by Western blotting, and infectious virus levels by plaque assay. None of the methods showed a drop in virus levels at the fifth passage upon re – infection in C6/36 cells. This was repeated twice, with similar results.

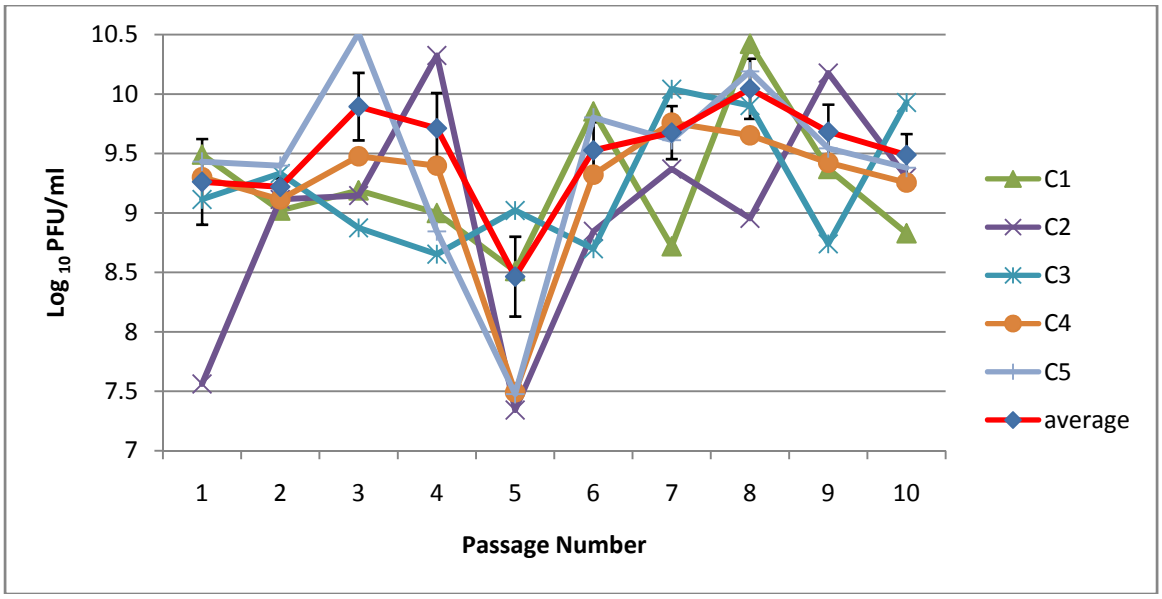

Figure 37: Log_{10} PFU/ml of virus from C6/36 cells from different passages in the mouse – C6/36 'c' passaging series. Each sample represents one flask of cells, no repeats are done. Error bars on average curve represent standard errors.

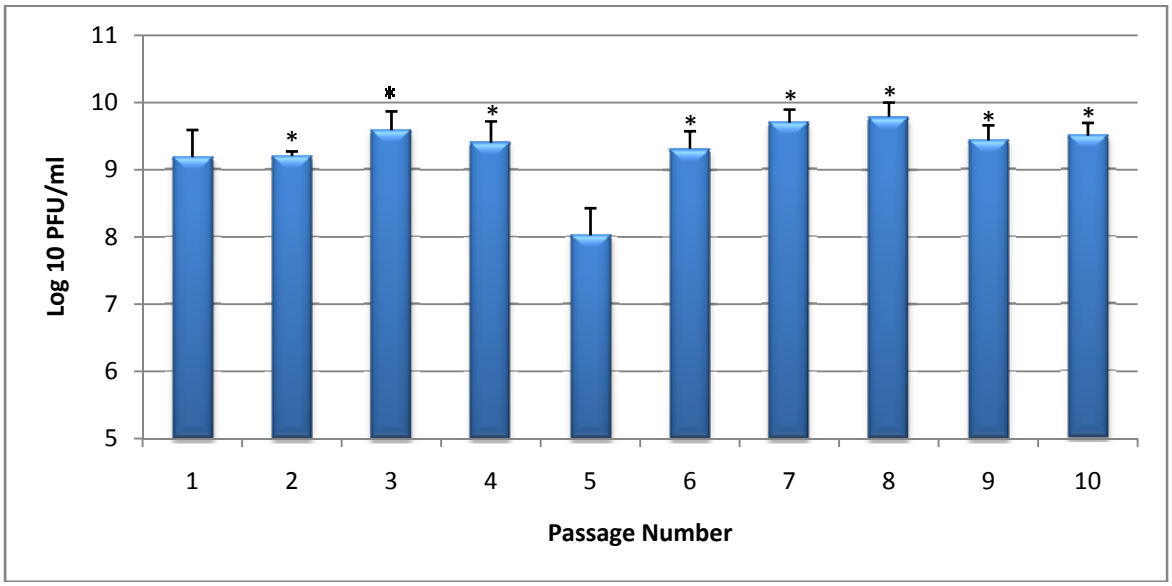

Figure 38: Average Log_{10} PFU/ml of virus from C6/36 cells from the 5 repeats during the different passages in the mouse – C6/36 'c' passaging series. A bimodal distribution is seen with titre peaks at passage 3 and 8. All the passage titres are statistically different from the passage 5 titre ($p<0.05$) except passage 1 as indicated with asterisks. Error bars represent standard errors.

CHAPTER 4
RESULTS

4.0 RESULTS

4.1 EVALUATION OF POST PASSAGING VIRUS STRAINS

The ten rounds of ten different passaged virus strains were evaluated through different means described below to determine for any phenotypic changes between the unpassaged and passaged viruses. The virus was tested for infectivity in both adult and suckling BALB/c mice. The mice were evaluated for virus loads in different organs by plaque assay as well as time of death. Furthermore, adult mice inoculated with the virus were weighed every 12 hours for 20 days to observe if the virus caused any inhibition in animal growth. The organs from the infected mice were also processed for histopathology. From the observed results, a further experiment was carried out to map the growth kinetics of the unpassaged and passaged virus on primary mouse neural cultures. First the various viruses were grown in an astrocyte/oligodendrocyte mixed culture and subsequently in neuronal primary cell culture. All the experiments suggested that passaged WNVS were more pathogenic and neuroinvasive compared to unpassaged WNVS.

4.2 INFECTION OF SUCKLING BALB/C MICE TO EXAMINE THE VIRULENCE OF PASSAGED WEST NILE VIRUS (SARAFEND)

Testing the ten passaged viruses on suckling mice was done by injecting 50, 500, or 5000 virus particles in 5 microlitres intracranially into suckling mice and observing for mortality (*Section 2.3.8.2*). Groups of 9 suckling mice were used for each of the 10 passaged viruses. *Figures 39 to 40* showed the results from this experiment. The time of

death after infection for each group was counter intuitive as it did not follow any dose dependent trend. The initial hypothesis was a higher dose of virus would lead to shorter survival times. Only the group 10c1 had a trend following this hypothesis and there was thus insufficient evidence to support it.

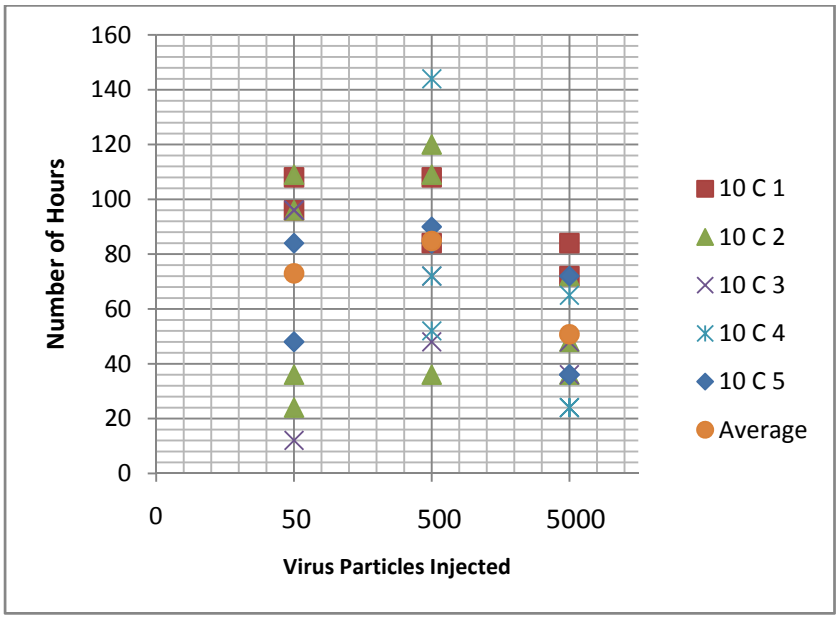

Figure 39: Mortality levels of suckling mice inoculated with passaged viruses from the 'c' regime. The x – axis shows the amount of virus particles injected (50, 500, or 5000 virus particles in 5 microlitres) while the y – axis shows the hour of mortality post inoculation. Each point refers to one mouse. Only 10c1 follows the initial hypothesis that a higher virus dose would cause an earlier time of death. All other viruses do not show any clear distribution pattern. The three groups of mice are not statistically different from each other ($p<0.05$). Each point is representative of one mouse. Each virus has two mice per group. Averages represent mean survival times of each virus titre group.

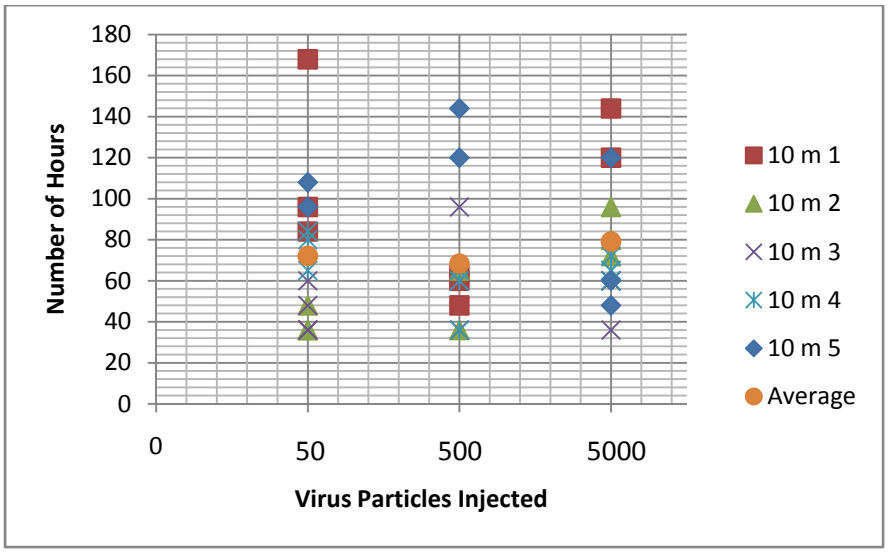

Figure 40: Mortality levels of suckling mice inoculated with passaged viruses from the 'm' regime. The x – axis shows the amount of virus injected (50, 500, or 5000 virus particles in 5 microlitres) while the y – axis shows the hour of mortality post inoculation. Each point refers to one mouse. None of the viruses show any dose – dependent killing potential. Each virus has two mice per group. Averages represent mean survival times of each virus titre group.

Comparing *Figures 39 to 40* to the survival curve of unpassaged virus (*Figure 18*), unpassaged virus generally caused the death of mice at around 96 hours post inoculation. However, from *Figures 39 and 40*, suckling mice inoculated with passaged virus started dying as early as 12 hours but the median was at 36 hours post inoculation. There was a substantial time difference between the two sets. For the unpassaged virus group, the last suckling mouse died at 192 hours post inoculation (*Figure 18*) but for the passaged virus group, the last mouse died at 168 hours. Removing this mouse that died at 168 hours as an outlier, the difference in time between the death of mice from the passaged (144 hours) and unpassaged (192 hours) virus strain infection was more than 48 hours. In other words, the passaging caused the virus to be better adapted to infecting suckling mice.

However, between groups of suckling mice inoculated with different titres of virus from the same passaging regime, there was no discernable difference. *Figures 39 and 40* showed no trend or significant difference in mean survival times of suckling mice for the various virus doses infections; 50, 500, and 5000 virus particles. For suckling mice infected with unpassaged viruses in *Figure 18*, again no observable difference could be noted between the mean survival times of suckling mice inoculated with various virus doses; 100, 500, 1000, 5000, 10000, and 50000 virus particles. This was contrary to the hypothesis that virus infective dose played a role in virus replicative ability and thus also survival times.

4.3 INFECTION OF ADULT BALB/C MICE WITH PASSAGED WEST NILE VIRUS (SARAFEND)

4.3.1 Levels of Viremia in Various Organs Post Inoculation

From this point, further investigations were done to examine the infectivity of passaged virus in adult mice (*Section 2.3.8.1*). From previous observations, unpassaged laboratory strain of WNVS grown in Vero cells did not cause any mortality or morbidity. Virus could not be detected in the liver, spleen, brain, or serum of the mice 24 hours after inoculation (*Tables 8 to 9*). For WNVS propagated in C6/36 cells, intravenous inoculation resulted in the presence of virus in serum after 24 hours at 10^1 PFU/ml. However, this dropped to zero on day 2 (*Section 3.2.1)*.

Adult mice were injected intravenously with 100 µl of passaged virus at 10^8 PFU/ml (*Section 2.3.8.1*). It was noted that passaging had a profound effect on the levels of infectious virus particles in sera over time. Using passaged viruses as the inocula, the organs from the infected mice also showed presence of viruses on day 1 and 3 post inoculation, as shown in *Figures 41 to 44*. Tests on mice at day 5 post inoculation found that virus presence was not sustainable as all samples from sera, brain, liver, and spleen homogenates were negative for viruses. The passaged virus 10c3 was most virulent for the 'c' series as it yielded the highest virus titres in livers and spleens at day 1 post inoculation and in sera on day 3 post inoculation. 10m4 virus was the most virulent for the 'm' series with all organs from mice inoculated with this virus showing highest virus titres on day 1 post inoculation compared to other 'm' viruses.

The highest virus levels were detected in sera and spleens. The same two organs were the sites of most sustainable virus infection. Livers were seen to be easily infected at day 1 post inoculation but in both the 'c' and 'm' series, the virus titres quickly dropped to zero on day 3. Not surprisingly, spleens were the most infectable organ with 16 out of 20 suckling mice inoculated with passaged viruses showing presence of virus on day 1 post inoculation. The spleen is a key organ in host immunological response against pathogens, an important site for antigen presentation, and crucial for B cell maturation. It is thus expected that the virus will congregate in this organ, either brought by professional antigen presenting cells, the bloodstream, or by natural tropism of the virus for this organ. This high and sustainable virus titre in *Figures 41 to 44* was also co – relatable to pathology in *Section 4.3.3.*

Of interest in *Figure 42* were the high titres of virus in brains of suckling mice inoculated with ‘c’ series passaged viruses and sacrificed at day 3 post inoculation. When compared to the null titres in the brains of adult mice inoculated with ‘m’ series virus in *Figure 44*, the higher neurotropism of the ‘c’ series passaged virus became obvious. The ‘c’ series passaged virus was able to initially establish itself in the brain of adult mice after passing through the blood brain barrier on day 1 post inoculation, and for viruses 10c3, 10c4, and 10c5, replicated to higher titres on day 3 post inoculation as compared to day 1 (*Figures 41 and 42*). The same phenomenon was not seen in the ‘m’ series (*Figures 43 and 44*) leading to the conclusion that WNVS passaged through suckling mouse brain and C6/36 cells repeatedly became more adapted to infecting immunocompetent adult mice compared to WNVS passaged only through suckling mice brains. This proved that the insect cell line alternate passage was of importance for virus adaptation. Moreover, when comparing the virus titres in organs from both ‘c’ and ‘m’ virus series on day 3 post inoculation, ‘c’ resulted in more organs showing higher virus titres in more mice compared to the ‘m’ series.

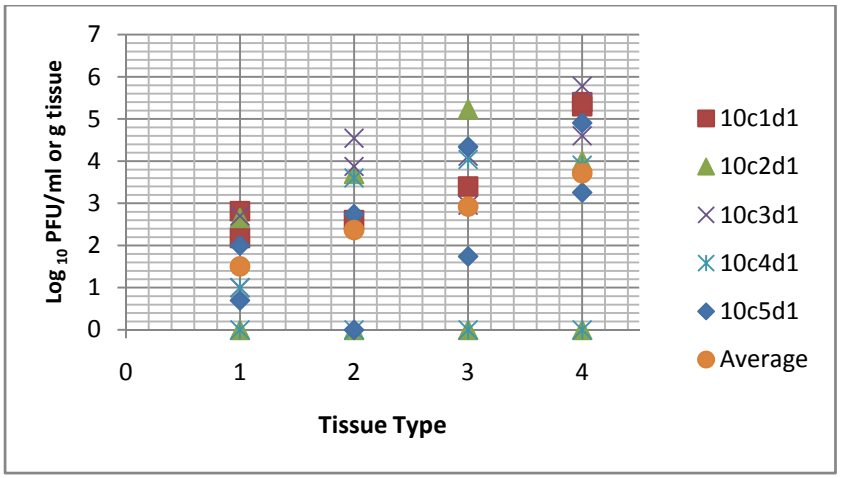

Figure 41: Virus titres from adult mice inoculated with the mouse – C6/36 passaged virus 'c' sacrificed on day 1 post inoculation. 1:Brain, 2:Liver, 3:Spleen, 4:Serum. The 10^8 PFU/ml virus inoculated through the tail vein is detected in the brains as well as spleens, a site involved in immunological response. This shows that the passaged virus is neuroinvasive, being able to cross the blood – brain barrier to infect the brains from the blood stream. Average points indicate serum as the most infectable followed by spleens, livers, and lastly brains. 10c3 virus shows the highest titres in serum and livers while 10c1 is highest for brains and 10c2 virus in spleens. Each virus has two mice per group. Each point is representative of one mouse.

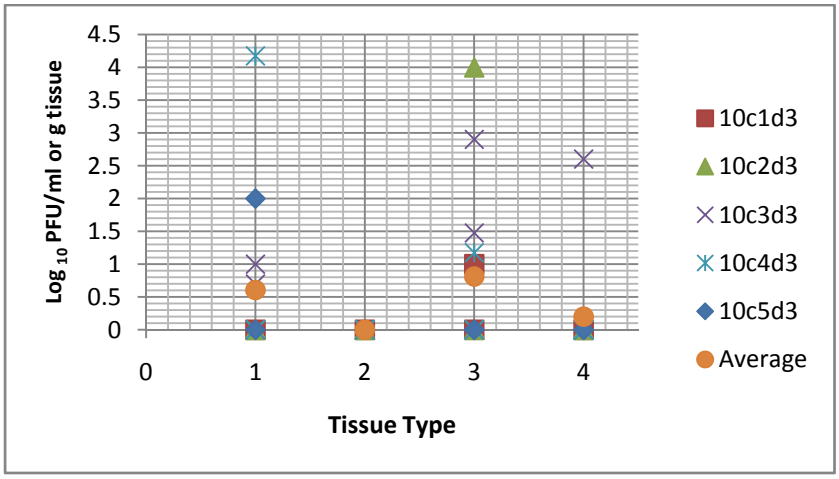

Figure 42: Virus titre levels from adult mice inoculated with the mouse – C6/36 passaged virus 'c' sacrificed on day 3 post inoculation. 1:Brain, 2:Liver, 3:Spleen, 4:Serum. The virus quickly clears from the livers but persists in other organs at lower PFU/ml. The virus titres are notably high in brain and spleen. 10c3 virus shows the highest titres in serum while 10c2 is highest in spleen and 10c4 virus in the brains. Each virus has two mice per group. Each point is representative of one mouse.

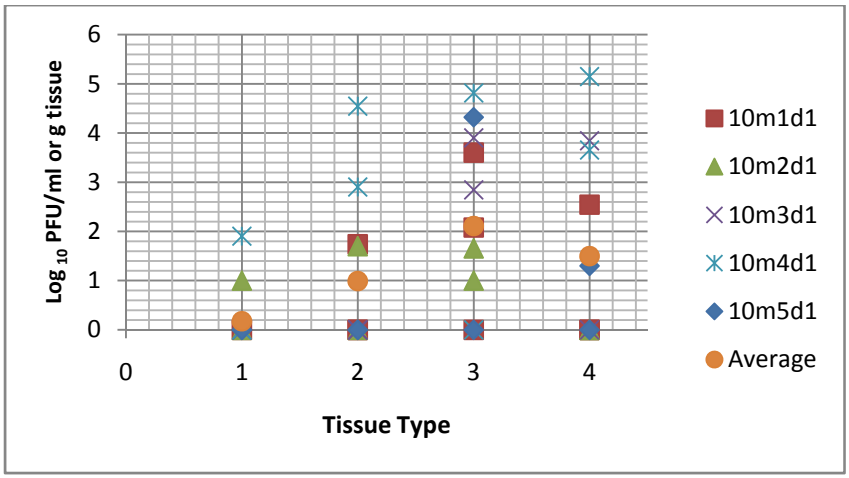

Figure 43: Virus titres from adult mice inoculated with mouse brain passaged virus 'm' sacrificed on day 1 post inoculation. 1:Brain, 2:Liver, 3:Spleen, 4:Serum. Overall, there are fewer animals showing viremia in fewer organs and at lower levels as compared to the mouse - C6/36 passaged virus (Figure 41). The spleens are the most infectable organ with 8 out of the 11 mice showing some level of viremia. The brains are the least infectable with only 2 out of 11 animals showing low levels of virus load. 10m4 virus is the most virulent passaged virus as it gives the highest titres. Each virus has two mice per group. Each point is representative of one mouse.

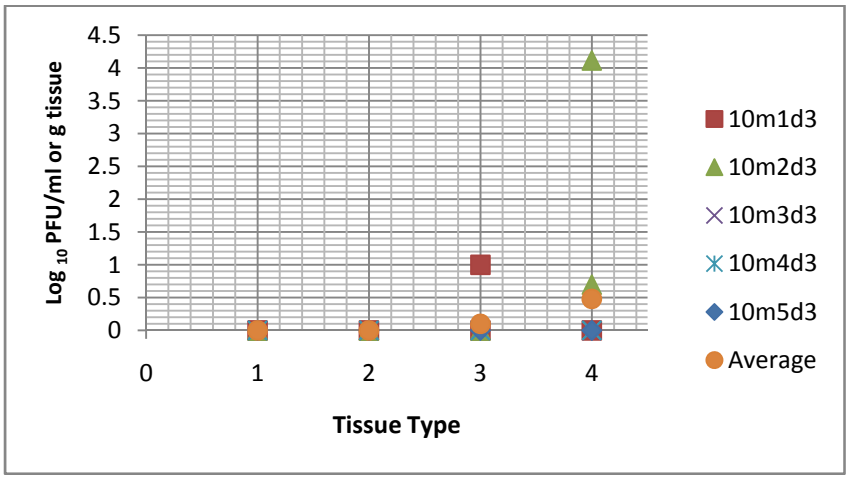

Figure 44: Virus titres from adult mice inoculated with mouse brain passaged virus 'm' sacrificed on day 3 post inoculation. 1:Brain, 2:Liver, 3:Spleen, 4:Serum. All animals have null virus levels except three mice each with one organ showing viremia. One mouse has a positive virus titre in the spleen while two others are positive in the sera. The brains and livers are totally devoid of virus. Each virus has two mice per group. Each point is representative of one mouse.

4.3.2 Effects of Passaged Virus Inoculation on Adult Mice Weight

Besides inoculating the virus into adult mice to test for virus loads in different organs, mortality and morbidity as a result of virus infection was also studied (*Section 2.3.8.1*). The animals were observed daily for signs of illness, including ruffled fur, paralysis, and other general indications of illness. There was no observed mortality in any of the mouse groups injected with passaged virus for all 10 respective passaged viruses kept for 20 days. This group of animals were also weighed every 12 hours for the whole period to detect for any overt change in health as sick mice will not feed well and this leads to weight loss.

Figure 45 shows the raw data of mean weights of mice taken from 0 hours before virus inoculation to day 20 post inoculation. Each group consisted of two mice. There was no observable difference in weights after the inoculation of various passaged virus compared to the control mice inoculated with PBS. Mice used for the 10c1, 10c2, and 10c5 groups were obviously underweight at the start of the experiment. The animals were bought from a supplier and specific instructions for five week old mice were given. However, it was to be expected that there would be some variations in the mice weights. *Figure 46* represented the least square regression lines from the curves obtained in *Figure 45*. The slopes from the three underweight mice gained the most as compared to the other mice. All the animals inoculated with passaged virus gained more weight over the 20 day period compared to the PBS inoculated mice (*Figure 47*). There was no indication of any illness in any of the mice tested.

Mice inoculated with viruses, both passaged and unpassaged, gained more weight as compared to mice inoculated with PBS (*Figures 45 to 47*). Comparing the levels of weight gained to virus titres in inoculated mice (*Figures 41 to 44*) and pathological signs in inoculated mice (*Table 10*), no correlation was found between virus titres, survivability, and histopathology. However mice that displayed the highest virus organ titres in organs (10m4 and 10c3 viruses) represented mice with the least weight gained (*Figure 47*). Comparing the graphs in *Figure 45*, only mice inoculated with passaged viruses 10m2, 10m5, and 10c2 registered a drop in weight of any proportion within the first 72 hours after inoculation compared with its original weight at time zero. The same mice had the highest weight gain when mice weights at day 0 and day 20 were compared (*Figure 47*). It can be concluded that the passaged virus at this point although showing virus presence and histopathology in various organs of inoculated adult mice, had yet to be able to cause any noticeable effect on the inoculated animal's general health including encephalitis or any other overt signs of illness.

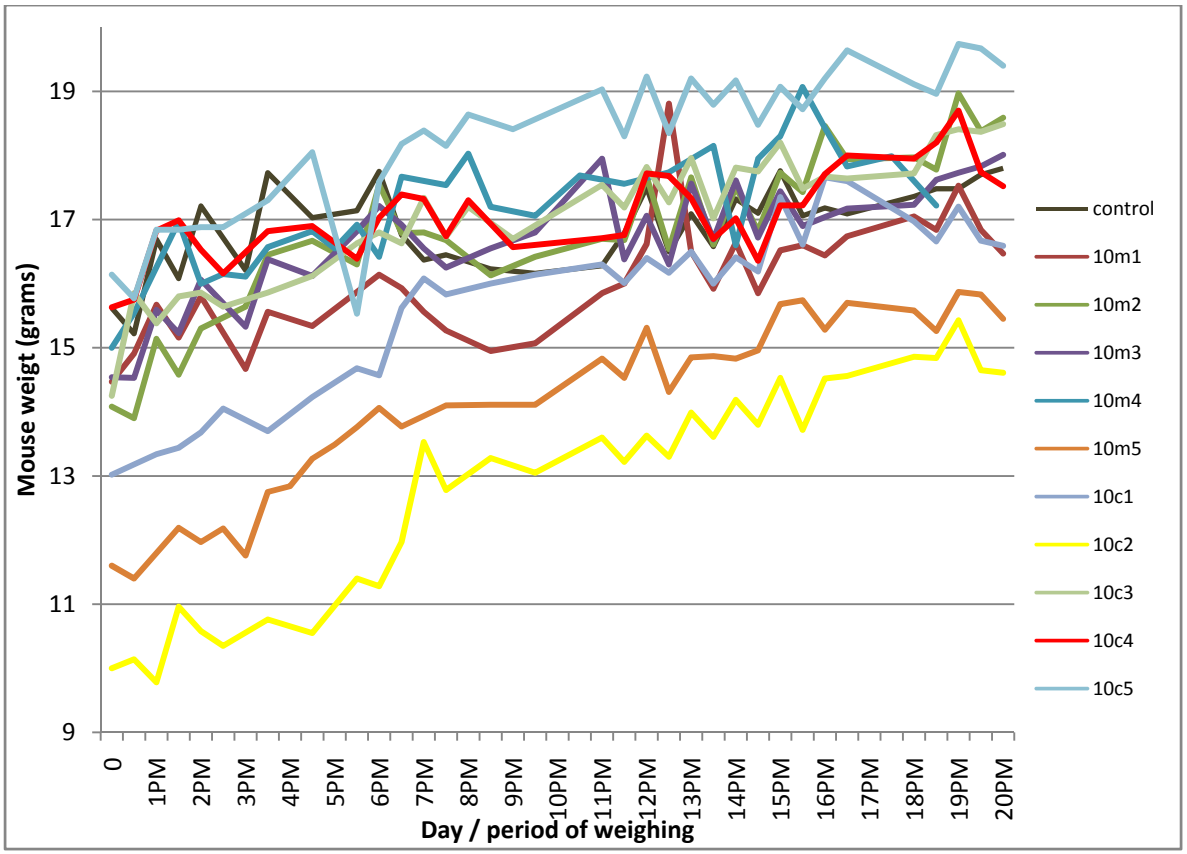

Figure 45: Mice weights over 20 days as a test for morbidity. Adult 5 week old mice are weighed at day 0 before being inoculated with 10^8 PFU/ml of passaged virus. Mice are then weighed every 12 hours and the values plotted as a graph. Each group is made up of two mice.

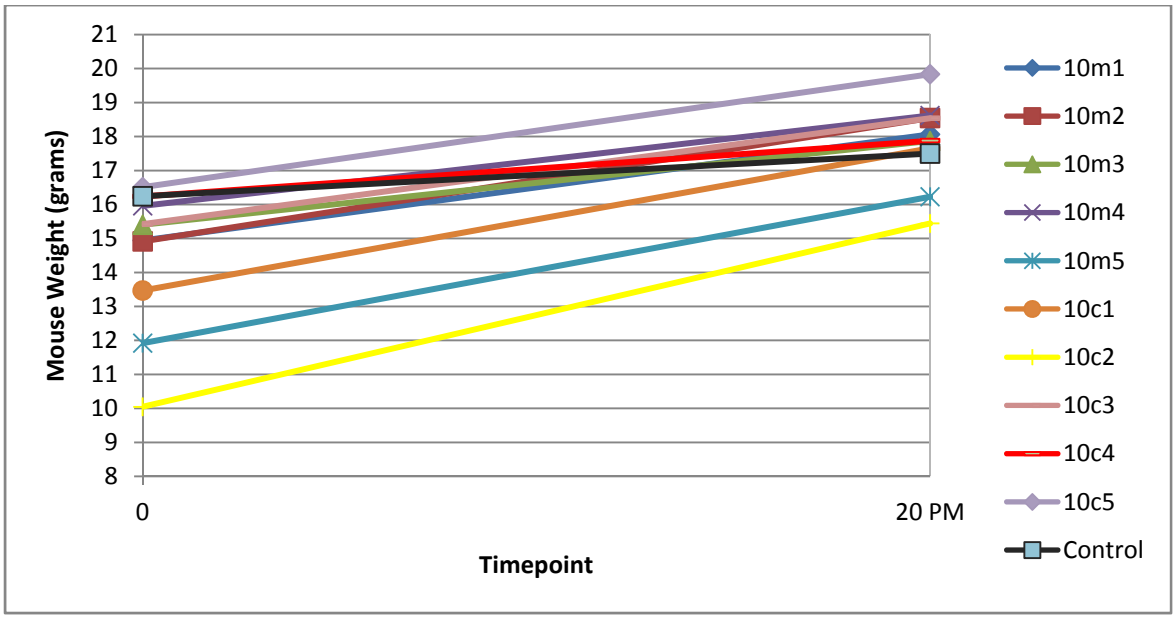

Figure 46: Least square regression lines of mice weights over 20 days. Outliers in terms of starting weight can be identified as 10c5, 10c2, and 10c1 virus – infected mice. These underweight mice have higher growth rates and quickly caught up with the other animals over the 20 days observation period. Virtually all experimental animals have higher weight gain rates as compared to the control animal as seen by the steeper gradient of the passaged viruses compared to the control group. Gradients from all curves are tested for normality and no outliers are observed.

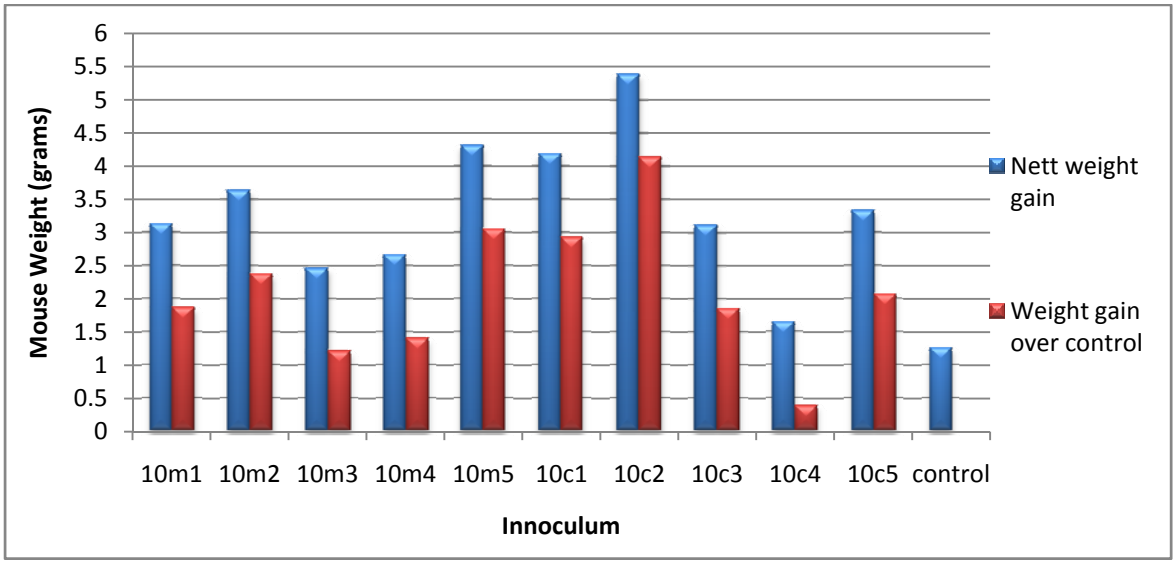

Figure 47: Mice nett weight gained after 20 days and the weight gained when normalised to the control mouse growth. All experimental mice gain more weight compared to control mice over the same time period with the lightest mice gaining the most weight (10c2, 10c1 virus infection). The 'c' series mice on average gain more weight than the 'm' series mice. The virus inoculated affects the mice weights positively over 3 weeks.

4.3.3 Histological Effects in Mice Inoculated with Passaged Virus

Histological sections of brains, livers, and spleens of adult mice sacrificed on day 1 and 3 post inoculation (*Section 4.3*) were prepared and stained with haematoxylin and eosin (*Section 2.5.4*). Tissue sections were observed for signs of pathology. It was seen that the tissue sections showed inflammation in the spleen with infiltration of immune cells into the red pulp, foci of necrosis and inflammation in livers, as well as pyknotic cells and encephalitis in brains.

The most obvious change was in mice spleens. The red pulps became filled with infiltrating cells and were inflammed from day 1 regardless of the passage regime (‘c’ or ‘m’), a common response to infection. By day 3 post inoculation, all except for 10m2 and 10m5 virus - infected mice showed signs of splenomegaly, a result of immune hyperplasia (*Figure 48*). The ‘c’ virus passages seemed to be able to elicit a stronger immune response as seen in spleens. In livers, small areas showed grouped plasma cells or lymphocytes, most likely Kupffer cells, as these are the resident macrophages found in the liver. Kupffer cells were found around blood vessles and could be defined as perivascular cuffing. Again, this was more common in the ‘c’ passaged virus infection as compared to the ‘m’ passaged virus infection with three out of five ‘c’ virus infections having some form of pathology at day 3 post inoculation compared to only 2 viruses from ‘m’. Besides this, no other overt sign of infection or inflammation could be detected in the liver (*Figure 49*). In the brains (*Figure 50*), only one instance of meningoencephalitis was detected in mice from day 1 and 3 post inoculation in mice inoculated with 10m1

passaged virus. No other mouse brain showed pathology except for an occasional pyknotic cell. The results were summarised in *Table 10*.

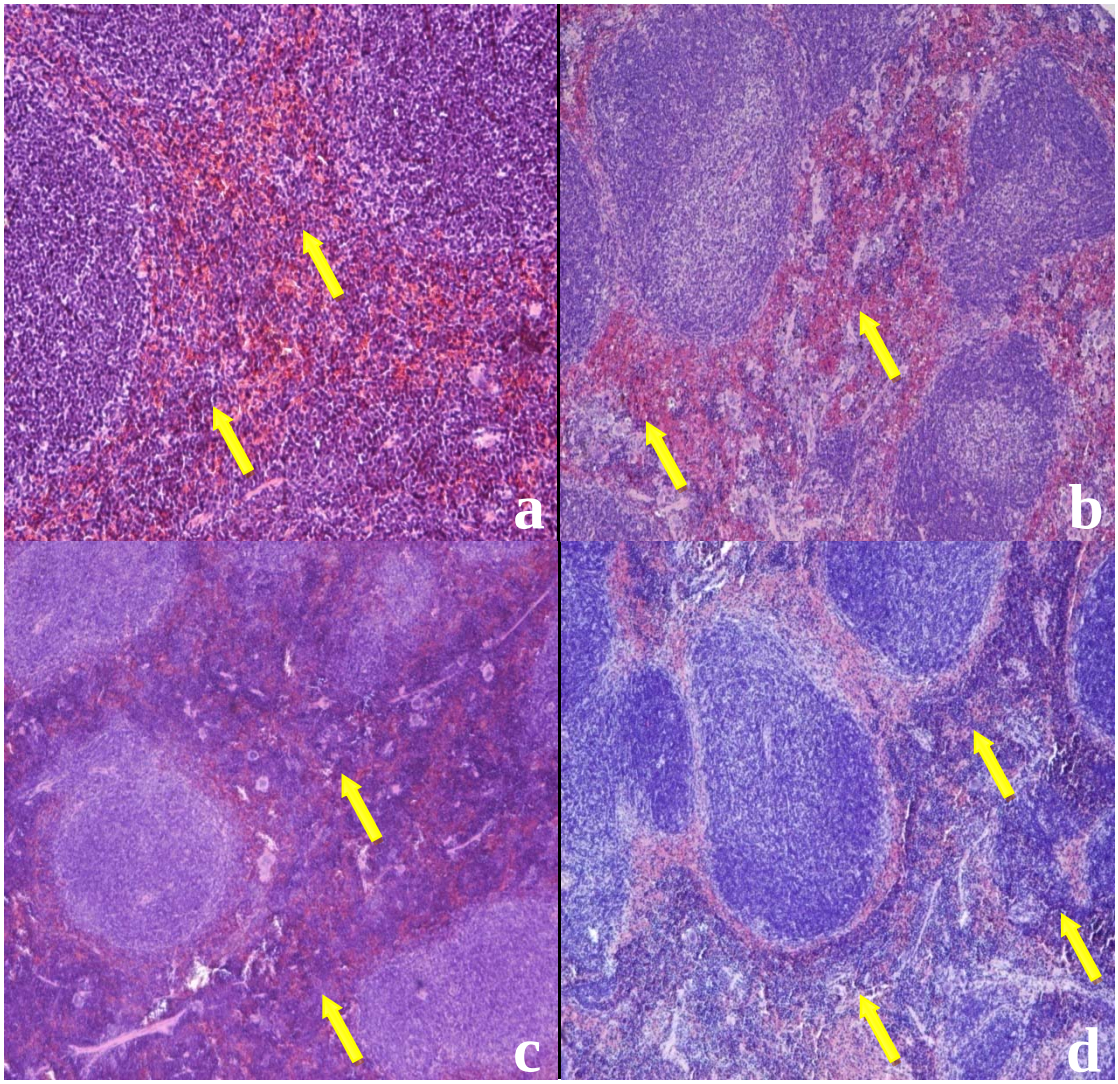

Figure 48: A representative spleen from a day 1 post infected - mouse showing relatively clear red pulps (arrow, a) from 10m2 virus infection. The same is seen for mock - infected animals (arrow, b). By day 3 post infection, most animals start to show varying levels of inflammation (arrows, c and d) in the spleens. (c) a slide from 10m3 virus - infected mouse while (d) is from 10c1 virus - infected mouse. Original magnification 10x.

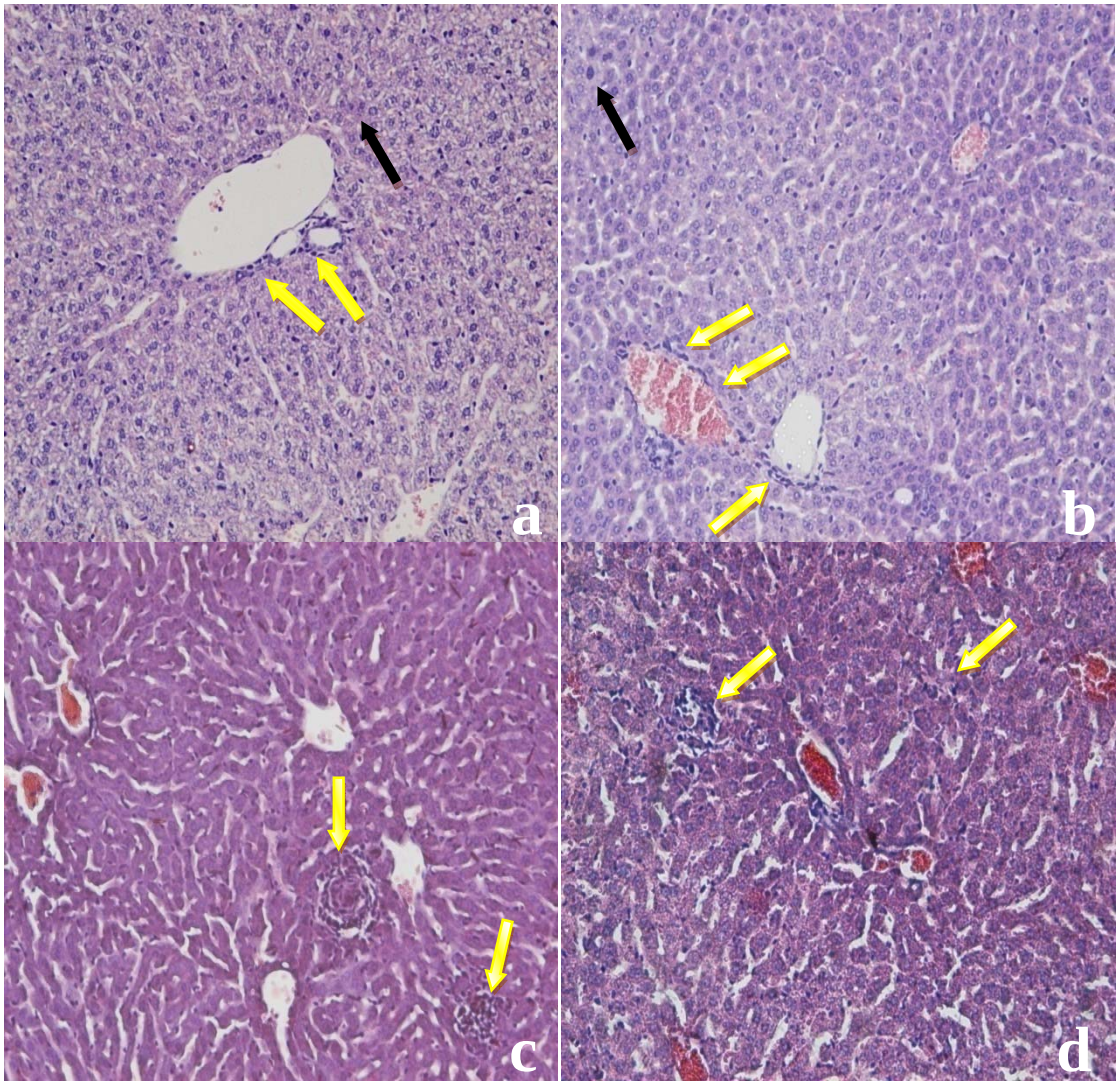

Figure 49: Kupffer cells and other inflammatory cells in the livers of various mice injected with passaged virus. (a) shows a slide from 10m1 virus infection at day 3 with yellow arrows pointing to signs of perivascular cuffing around a portal tract, (b) 10c3 virus inoculation at day 1 also exhibits perivascular cuffing (yellow arrows), (c) 10c1 virus infection at day 3 with arrows showing focuses of dense inflammatory cells in a roselle pattern with apoptotic cells in the middle of the focus area, and (d) 10c3 virus infection at day 1 with arrows pointing to an area of focal inflammation. Evidence of an inflammatory response is usually associated with pyknotic cells (a and b, black arrows). All photomicrographs at 10x original magnification.

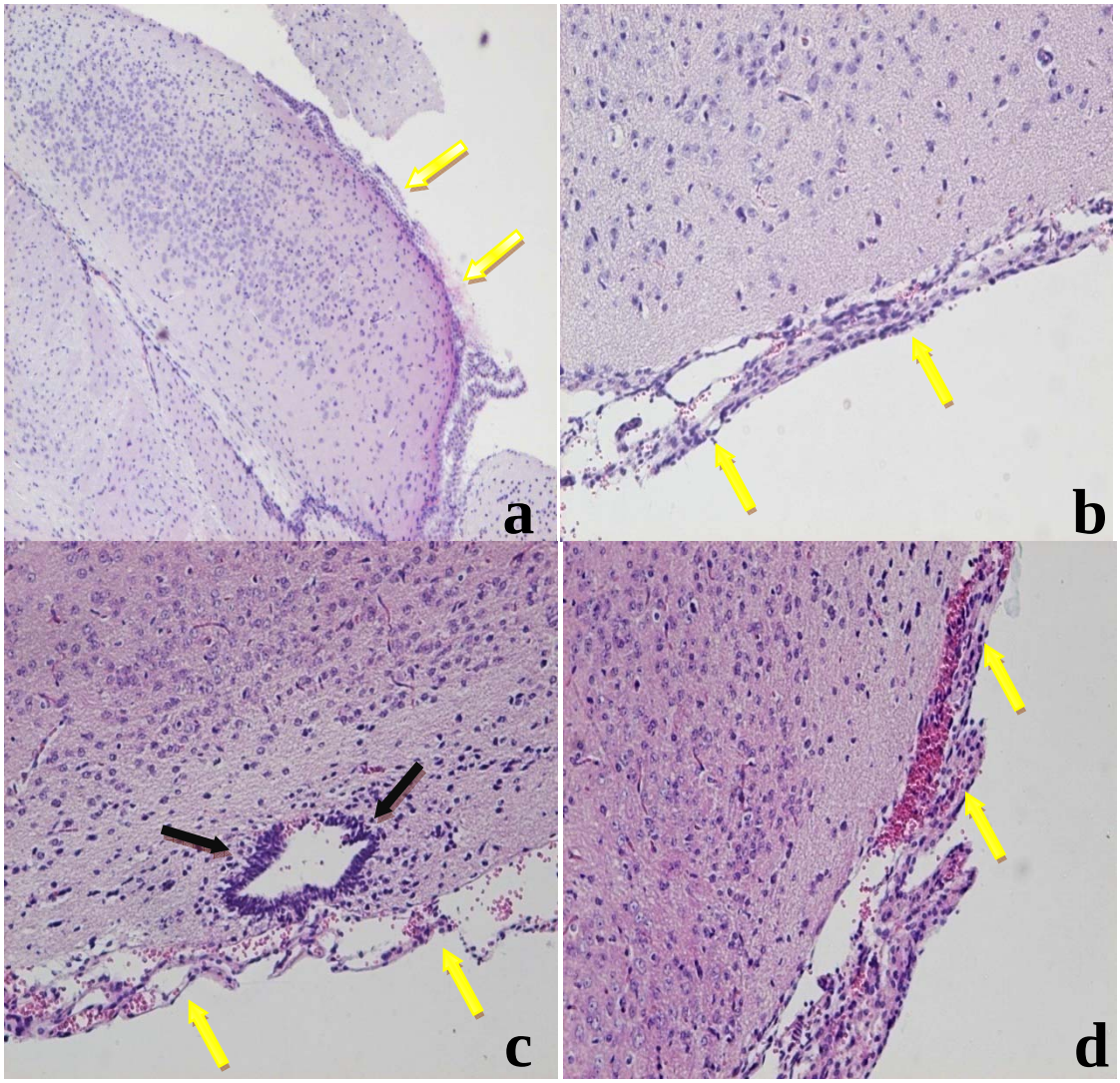

Figure 50: Meningoencephalitis in the pair of mice injected with 10m1 passaged virus. (a) shows a section from mice sacrificed on day 1 post inoculation with thickened membranous structures (arrows). (b) to (d) shows the same experiment on day 3 post inoculation. The leptomeningitis is more severe and contains red blood cells (yellow arrows). Also, there is perivascular cuffing around a blood vessel near the brain surface. There is a large recruitment of inflammatory cells to the thickened membranous structures and blood vessels (c – black arrows) indicating severe infiltration of brain parenchyma. All other brain slides from the same mouse do not show any other forms of pathology. Original magnifications 4x(a) and 10x(b to d).

Table 10: Summary of histopathological findings from haematoxylin and eosin stained tissue sections of brains, livers, and spleens from mice inoculated with passaged virus 'c' and 'm' series sacrificed at day 1 and 3 post inoculation. The 'c' virus series is seen to cause more pathological effects in the mice although only virus 10m1 is able to cause noticeable meningoencephalitis.

	Brain		Liver		Spleen	
Inoculum	**Day 1**	**Day 3**	**Day 1**	**Day 3**	**Day 1**	**Day 3**
10c1	No pathology	No pathology	Perivascular cuffing, Pyknotic cells, Focal necrosis	Perivascular cuffing, Pyknotic cells, Focal necrosis	Inflammation	Inflammation
10c2	No pathology	Pyknotic cells	No pathology	No pathology	No pathology	Inflammation
10c3	No pathology	No pathology	Perivascular cuffing, Pyknotic cells, Focal necrosis	Perivascular cuffing, Pyknotic cells, Focal necrosis	Light inflammation	Inflammation
10c4	No pathology	Pyknotic cells	No pathology	Perivascular cuffing, Pyknotic cells	No pathology	Inflammation
10c5	No pathology	No pathology	No pathology	Perivascular cuffing, Pyknotic cells	No pathology	Inflammation
10m1	Meningoencephalitis	Meningoencephalitis, Perivascular cuffing, Pyknotic cells	Perivascular cuffing, Pyknotic cells	Perivascular cuffing, Pyknotic cells, Focal necosis	No pathology	Inflammation
10m2	No pathology	No pathology	No pathology	Pyknotic cells	Light inflammation	No pathology
10m3	No pathology	No pathology	No pathology	No pathology	No pathology	Inflammation
10m4	No pathology	No pathology	No pathology	No pathology	No pathology	No pathology
10m5	No pathology	Pyknotic cells	No pathology	Pyknotic cells	No pathology	Inflammation

4.4 INFECTION OF PRIMARY CELLS

Results thus far showed that passaged viruses inoculated into both adult and suckling mice displayed higher virus levels for longer periods. This is especially true for the brains of adult mice as seen in *Figures 41 to 44*. As such, it is of interest to investigate the growth kinetics of passaged and unpassaged viruses specifically in the brain tissue. As it is impossible to closely monitor virus titre in live mice, primary neural cells were chosen as the closest *in vitro* model to mimic the whole brain mouse *in vivo* model (*Section 2.3.8.3*).

4.4.1 Isolation of Primary Cells

Primary neural cells were isolated from embryonic BALB/c E16 (*Section 2.3.7*) and cells grown in either Neurobasal media or DMEM. The cells in Neurobasal media were largely neuronal cells (neurons) whereas cells in DMEM with FBS were a mix of neural cells containing astrocytes and oligodendrocytes. Anti - NeuN, CNPase, and GFAP antibodies were used to test for exact neural cell composition of the mixed culture. *Figure 51* showed the identification of the neural culture as a mixed oligodendrocyte – astrocyte culture by immunofluorescence. There were thus two batches of primary neural cells tested, a neuronal culture of pure neurons and a mixed neural culture containing a mix of astrocytes and oligodendrocytes.

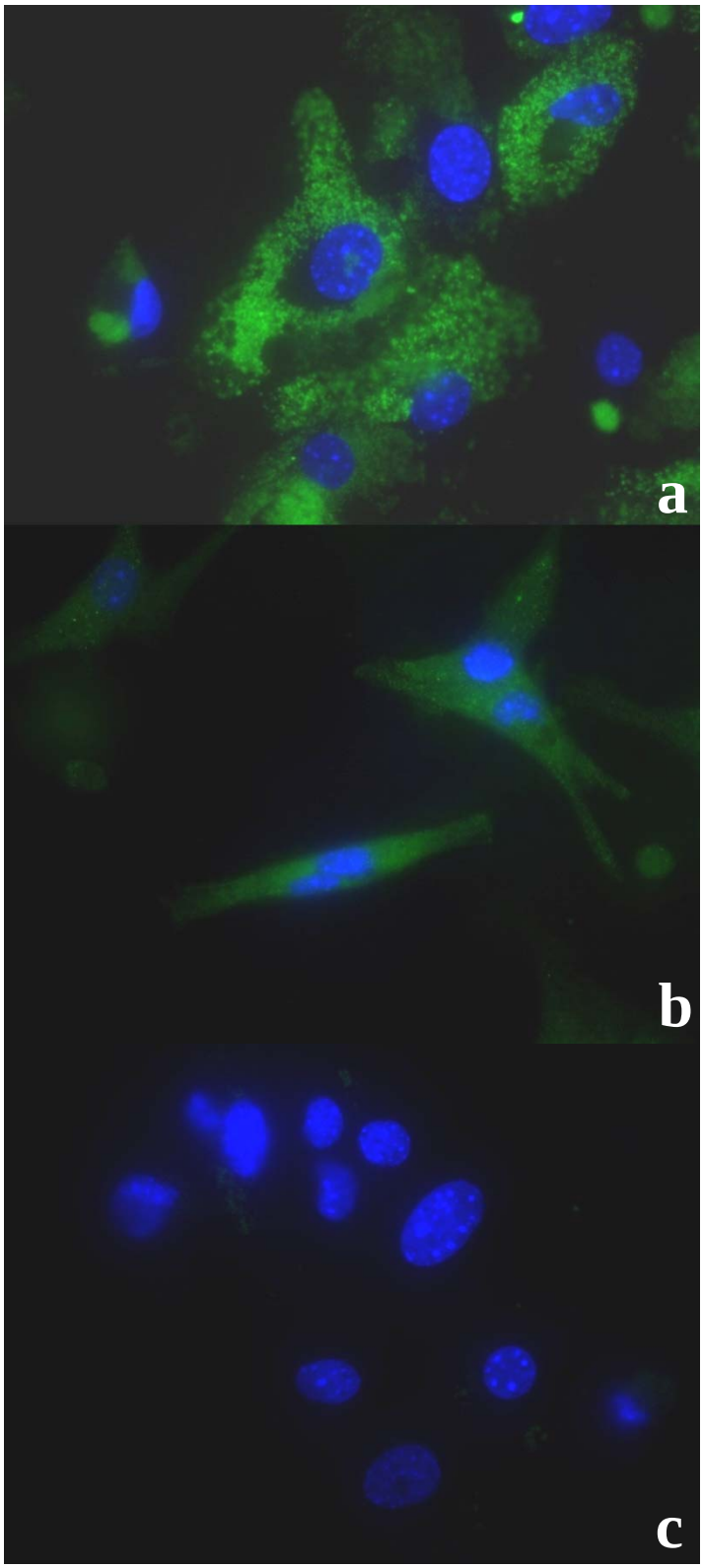

Figure 51: Positive labelling of primary neural cells with primary antibodies against GFAP labelling for astrocytes (a) and CNPase labelling for oligodendrocytes (b) conjugated to Alexa Flour 488. Antibodies against NeuN (c) for neurons do not show any specific labelling. This shows that the primary culture is an astrocyte – oligodendrocyte mixed culture. All photographs are taken with the same exposure time and light intensity. Original magnification 1000x.

4.4.2 Levels of Virus Production on Infected Primary Astrocytes/Oligodendrocytes

Primary cells were infected with PBS (mock), passaged, and unpassaged viruses as described in *Section 2.3.8.3*. The supernatant was collected at various time points and tested by plaque assay for infective virus particles (*Section 2.2.4*). Most of the infections started producing viruses at 12 hours post inoculation with titres ranging from 10^5 to 10^8 PFU/ml. The viruses from the 'm' series passaging started off notably on a lower virus titre ranging from 10^0 to 10^6 PFU/ml (*Figure 53*) whereas the 'c' series passaging started between 10^6 and 10^8 (*Figure 52*). All the viruses except for 10m2 had a slow drop in virus titre over the 132 hour-period.

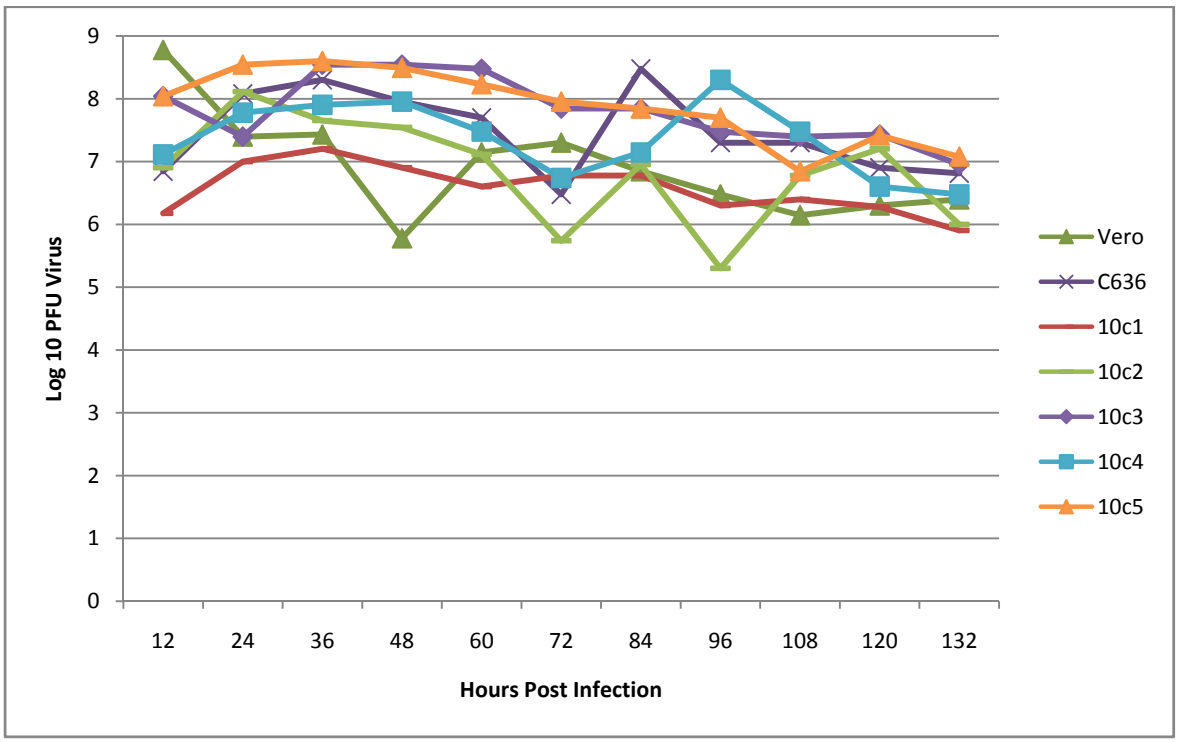

Figure 52: Growth curves of unpassaged (Vero cell and C6/36 cell – grown) and 'c' passaged virus series on mouse primary neural culture. The 'c' series passages has a starting PFU/ml of 10^6 to 10^8.

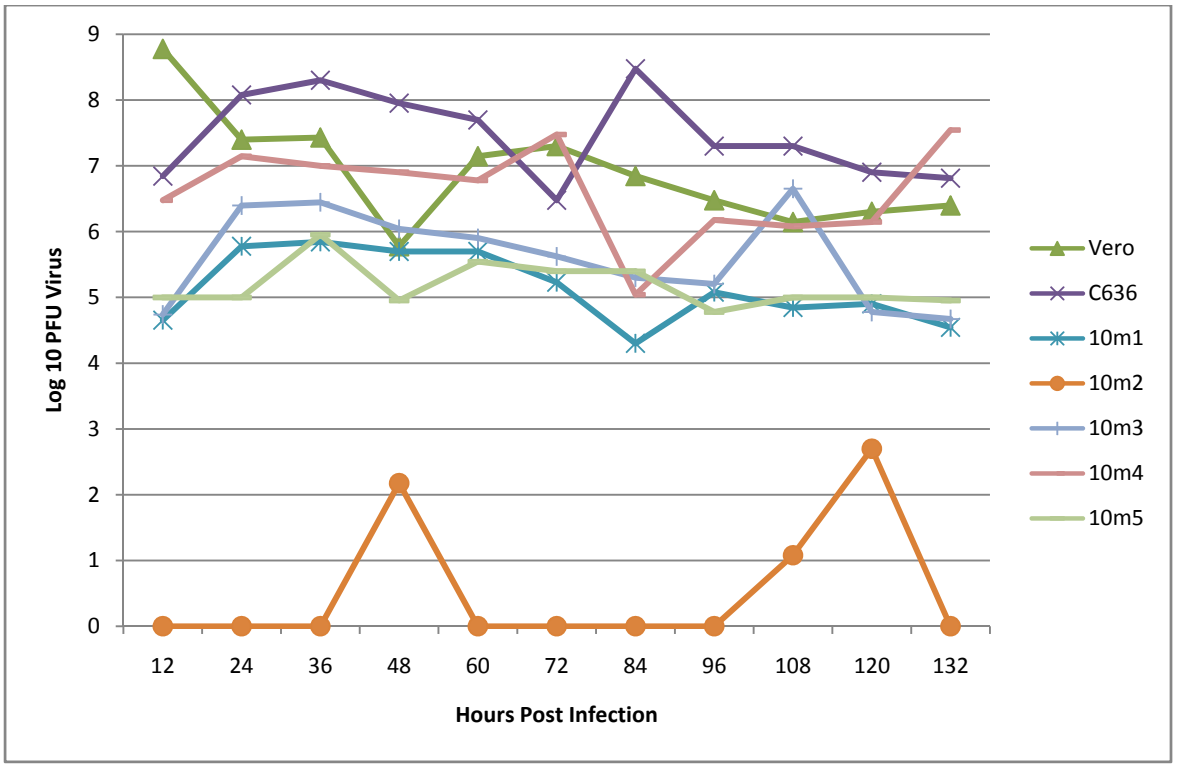

Figure 53: Growth curves of unpassaged (Vero cell and C6/36 cell – grown) and 'm' passaged virus series on mouse primary neural culture. 10m2 virus has an atypical growth pattern. The 'm' series passages has a starting virus yield of 10^0 to 10^6 PFU/ml at 12 hours post inoculation while the 'c' series passages has a starting PFU/ml of 10^6 to 10^8 (Figure 52).

4.4.3 Persistent Virus Infection in Primary Neural Culture with 10m2 Virus

From *Figure 53*, it was obvious that there was an abnormality in the 10m2 passaged viruses. The initial photomicrographs for the early time points for 10m2 virus infection showed no difference compared to mock - infected control flasks. It was thus left to grow beyond 132 hours post inoculation. Titred every week after that, it was seen that the virus titre was consistently at 10^4 PFU/ml, as seen in *Figure 54*. A persistent infection was established with this infected culture. After 8 weeks (1428 hours), the total supernatant was removed and the cell monolayer washed twice with PBS. Fresh media was then added and after three days, an aliquot of the supernatant was taken. The virus titre was

found to be 3.6 x 10^4 PFU/ml. This proved that it was new virus progeny that was being released into the media and not original viruses that remained in the culture. Fifty percent of the media was changed every 3 days from week 8 onwards (1344 hours).

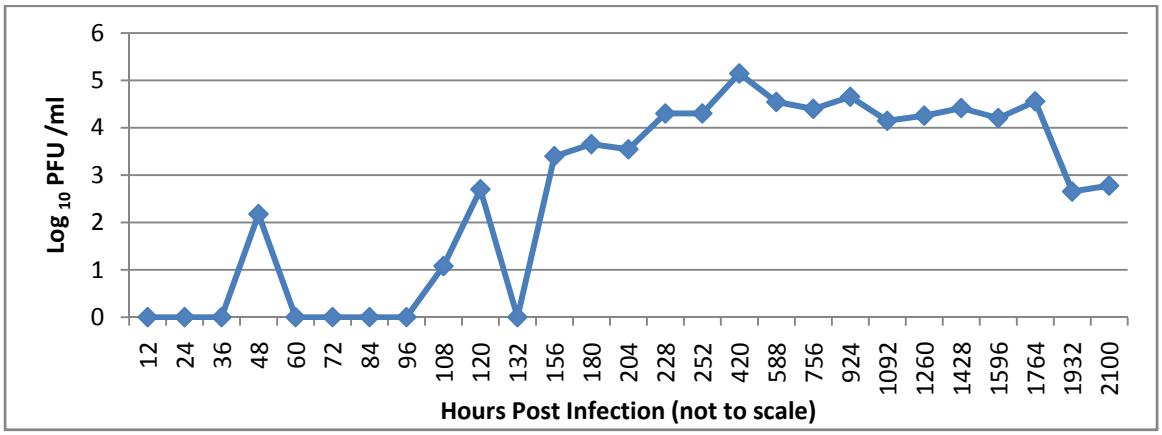

Figure 54: Growth curve for 10m2 virus infection on primary neural cell culture over a total period of 2100 hours (12.5 weeks). The virus titre remains low until 120 hours (day 5) post inoculation when it rises steadily to a peak of 10^5 PFU/ml. The titre drops from 2100 hours (week 12.5) to below 10^3 PFU/ml (Figure 55).

Primary cells persistently – infected with 10m2 virus were found to be confluent after 12 weeks (2016 hours) and at this point, the virus titre dropped to 10^2 PFU/ml. The flask was then subcultured 1 : 2 following protocols outlined in *Section 2.1.3*. The virus titre was continually titred every week from both flasks and the results detailed in *Figure 55*. The virus titres started dropping from week 10.5 (1764 hours) post inoculation (*Figure 54*) and at week 16 (2688 hours) post - inoculation, the experiment was terminated (*Figure 55*). The cells from both flasks were fixed for electron microscopy (*Section 2.6*) and processed.

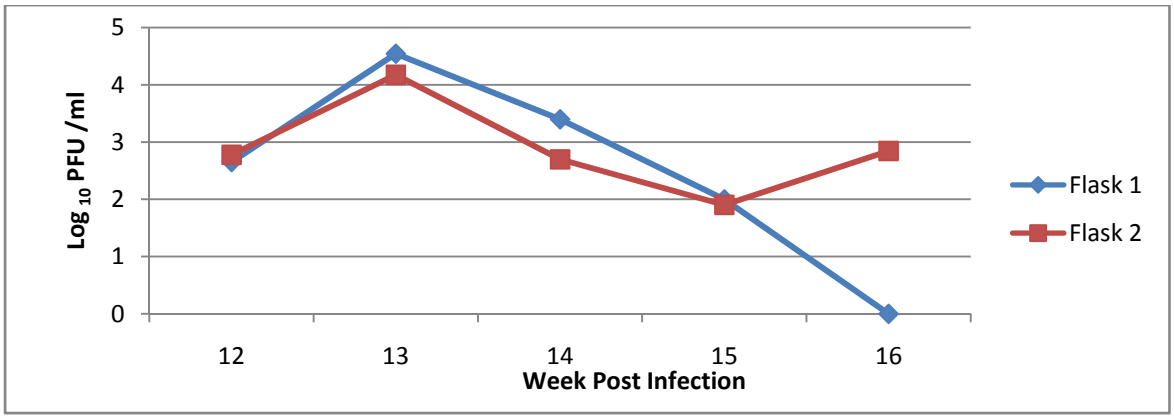

Figure 55: Titres of 10m2 virus from subcultured persistently - infected primary neural cells. The experiment ends on week 16 post - inoculation and cells are processed for electron microscopy.

4.4.4 Gross Phenotypic Changes During Infection of Primary Astrocytes/ Oligodendrocytes

Photomicrographs of the primary astrocyte/oligodendrocyte culture were taken at various time points to give a visual representation of the infection. Comparing the different slides, it was observed that the initial infection by WNVS grown in Vero cells or C6/36 cells showed differences in gross morphology of the infected cells. The three images (*Figure 56*) displayed representative micrographs of primary neural cells infected at MOI of 10 with Vero cell grown WNVS at 48 hours (2 days), 132 hours (5.5 days), and 3 weeks post inoculation. The following three micrographs from *Figure 57* showed photomicrographs at similar timepoints of cells infected with WNVS grown from C6/36 cells. The final set (*Figure 58*) showed control cells mock - infected at the same timepoints. The Vero cell - grown virus was able to infect and disrupt the monolayer but did not fully kill all the cells. On the contrary, the C6/36 cells grown virus caused complete cytopathic effect of the infected monolayers.

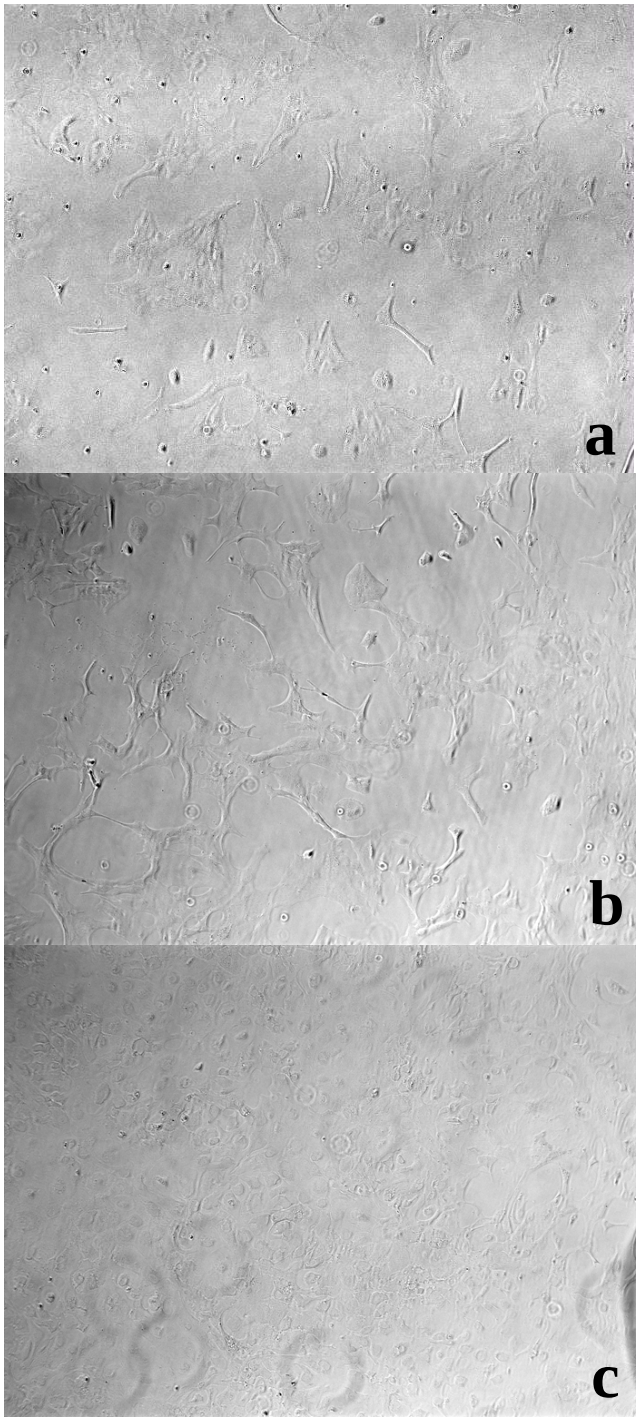

Figure 56: Micrographs of neural cells infected with WNVS previously grown in Vero cell culture at 48 hours (a), 5.5 days (b), and 3 weeks (c) post - inoculation. After an initial high level of cell death, the remaining cells recover in three weeks and the cell monolayer becomes confluent again. Original magnification 10x.

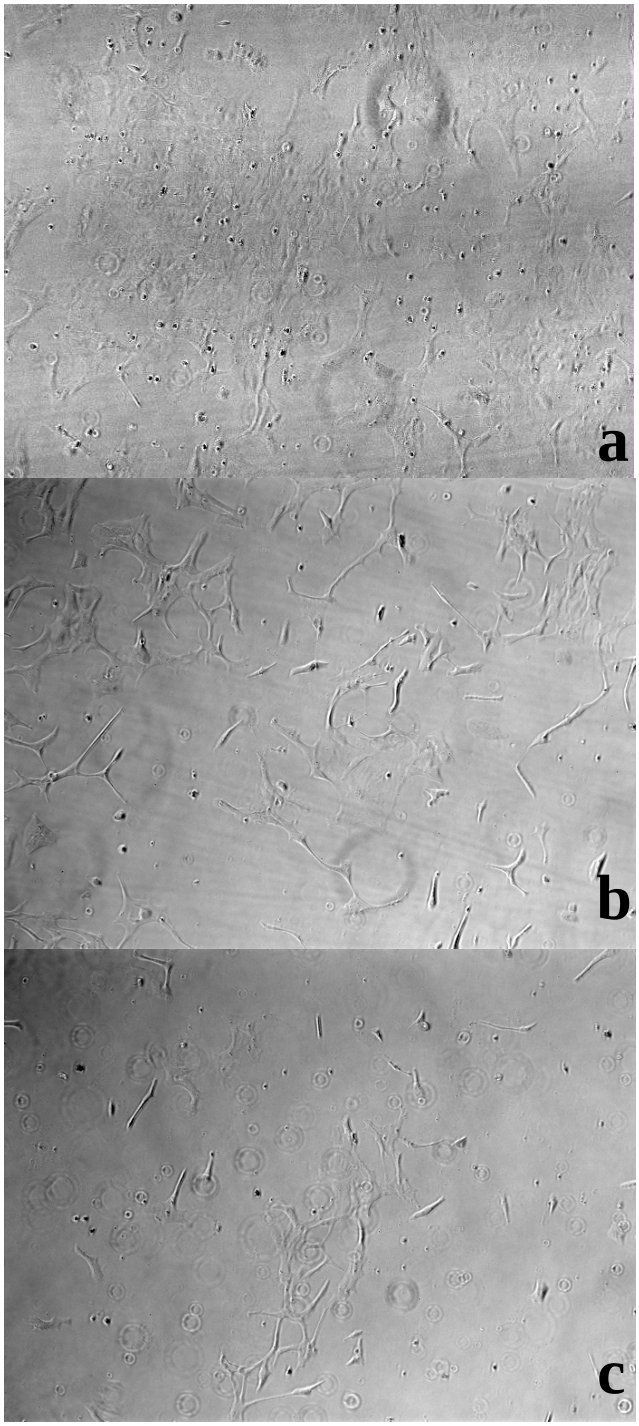

Figure 57: Micrographs of neural cells infected with WNVS previously grown in C6/36 cell culture at 48 hours (a), 5.5 days (b), and 3 weeks (c) post - inoculation. The infected - monolayer shows progressive cytopathic effects ending with total cell death of the cell monolayer. Original magnification 10x.

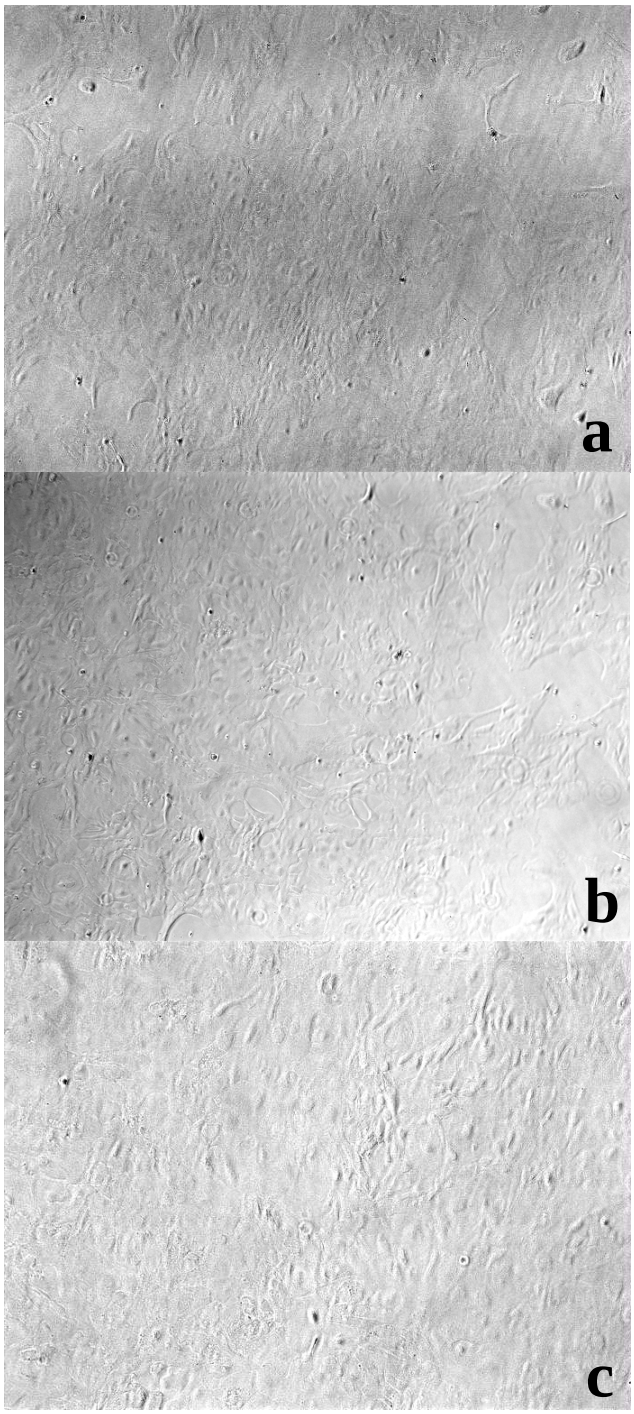

Figure 58: Micrographs of neural cells mock - infected at 48 hours (a), 5.5 days (b), and 3 weeks (c) post - inoculation. The monolayer remains confluent throughout the study. Original magnification 10x.

All ten passaged viruses caused cytopathic effects in infected cells in the first few days with cell rounding and lifting. By the end of day 7, cell attrition stopped and from that point until week 3, the remaining cells on the flask surface were observed to re – colonise the flask. *Figure 59 and 60* showed micrographs representative of the ‘c’ series passaged virus, 10c1 and 10c5, whereas *Figure 61 and 62* represent the ‘m’ series passaged virus 10m2 and 10m4. The observable difference between these two viruses was the levels of relative cell death. The ‘c’ series passaged viruses caused more neural cell death as compared to the ‘m’ series passaged viruses.

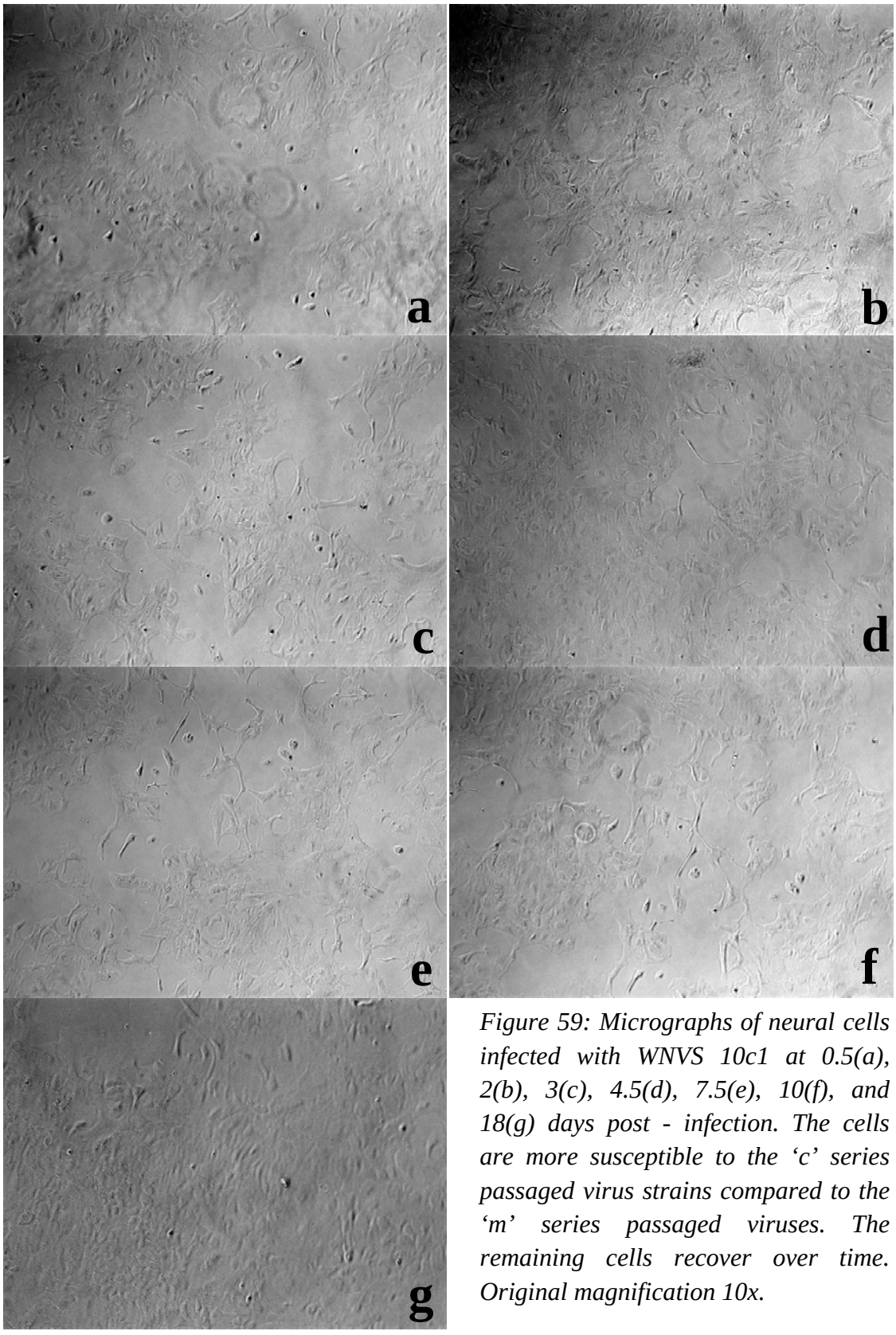

Figure 59: Micrographs of neural cells infected with WNVS 10c1 at 0.5(a), 2(b), 3(c), 4.5(d), 7.5(e), 10(f), and 18(g) days post - infection. The cells are more susceptible to the 'c' series passaged virus strains compared to the 'm' series passaged viruses. The remaining cells recover over time. Original magnification 10x.

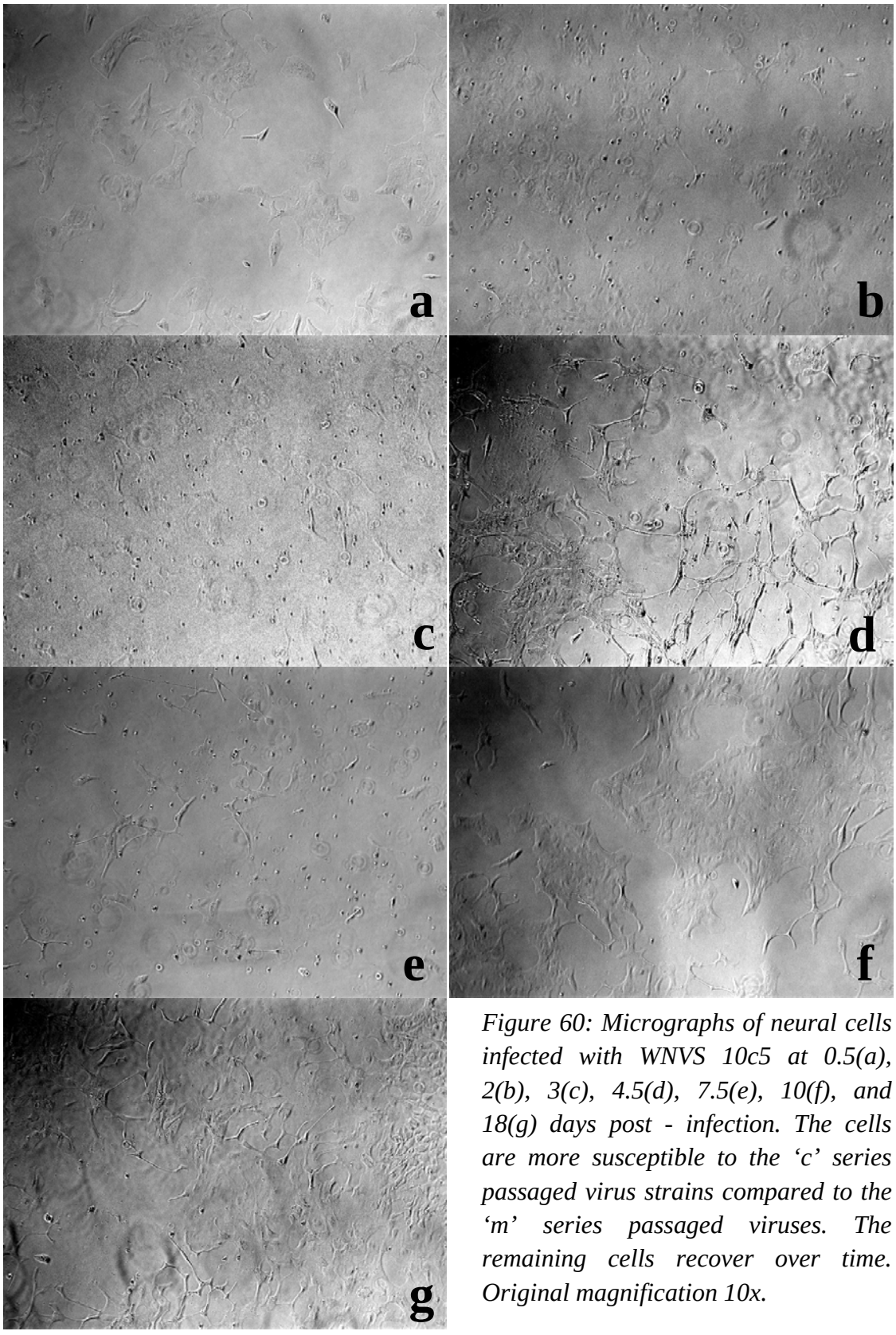

Figure 60: Micrographs of neural cells infected with WNVS 10c5 at 0.5(a), 2(b), 3(c), 4.5(d), 7.5(e), 10(f), and 18(g) days post - infection. The cells are more susceptible to the 'c' series passaged virus strains compared to the 'm' series passaged viruses. The remaining cells recover over time. Original magnification 10x.

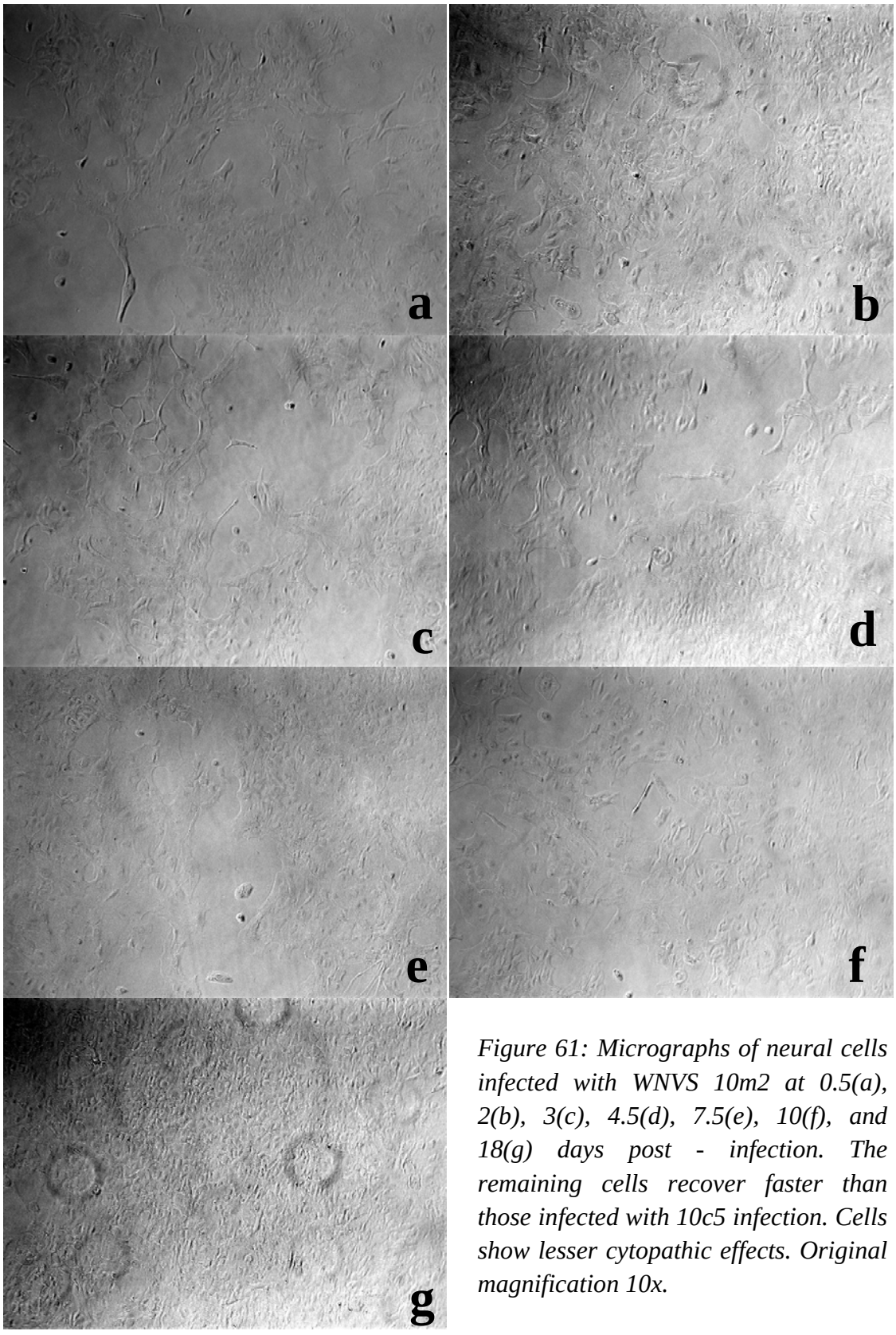

Figure 61: Micrographs of neural cells infected with WNVS 10m2 at 0.5(a), 2(b), 3(c), 4.5(d), 7.5(e), 10(f), and 18(g) days post - infection. The remaining cells recover faster than those infected with 10c5 infection. Cells show lesser cytopathic effects. Original magnification 10x.

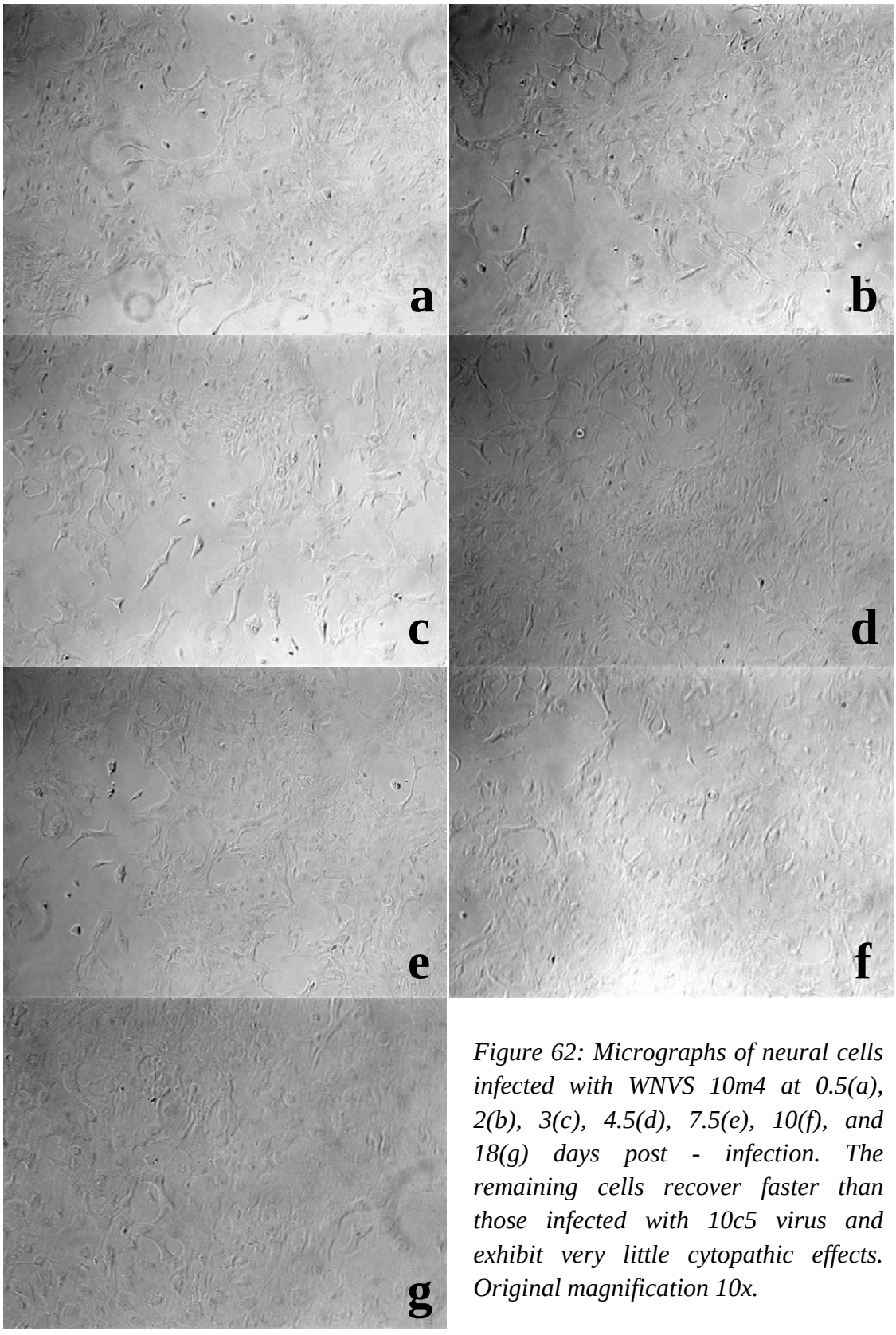

Figure 62: Micrographs of neural cells infected with WNVS 10m4 at 0.5(a), 2(b), 3(c), 4.5(d), 7.5(e), 10(f), and 18(g) days post - infection. The remaining cells recover faster than those infected with 10c5 virus and exhibit very little cytopathic effects. Original magnification 10x.

4.4.5 Electron Microscopy Evaluation of the Persistently - Infected Primary Astrocytes/Oligodendrocytes

Primary neural cells persistently - infected with 10m2 passaged virus (*Section 4.4.3*) was fixed and processed for electron microscopy (Section 2.6). Ultrathin sections were viewed under a transmission electron microscope and images were captured at various magnifications. Most cells seen were thin, rod - shaped with distinct nucleus, and dark myelin bodies in the cytoplasm (*Figure 63*). These cells were identified as light oligodendrocytes with long processes responsible for the myelination of CNS axons. These cells are known to be capable of cell division and are active in myelin sheath growth and maturation (Young and Heath, 2006). From the previous section, it was seen that cells in flasks showing low cytopathic effect could re – colonise the flask (*Figure 59 to 62*). Because astrocytes are incapable of myelenation or cell division, the cells seen through the electron microscope could only be oligodendrocytes. This led to the deduction that astrocytes were preferentially infected by WNVS. Most cells under the electron microscope looked unhealthy with compromised membranes and oversized vacuoles (*Figure 64*). These were easily differentiated from healthy cells which had dense vacuoles and organised cytoplasm (*Figure 63*). The identification of remaining cells as oligodendrocytes also excluded the possibility of primary cell culture contamination with epithelial cells.

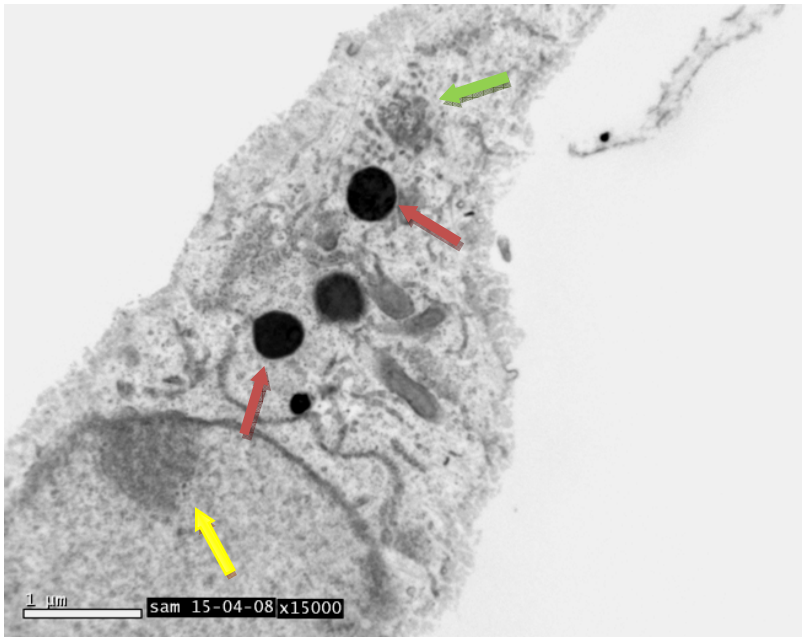

Figure 63: A typical oligodendrocyte with prominent nucleoli (yellow arrow), myelin sheaths (red arrows), and Golgi stacks (green arrow). Original magnification 15000x.

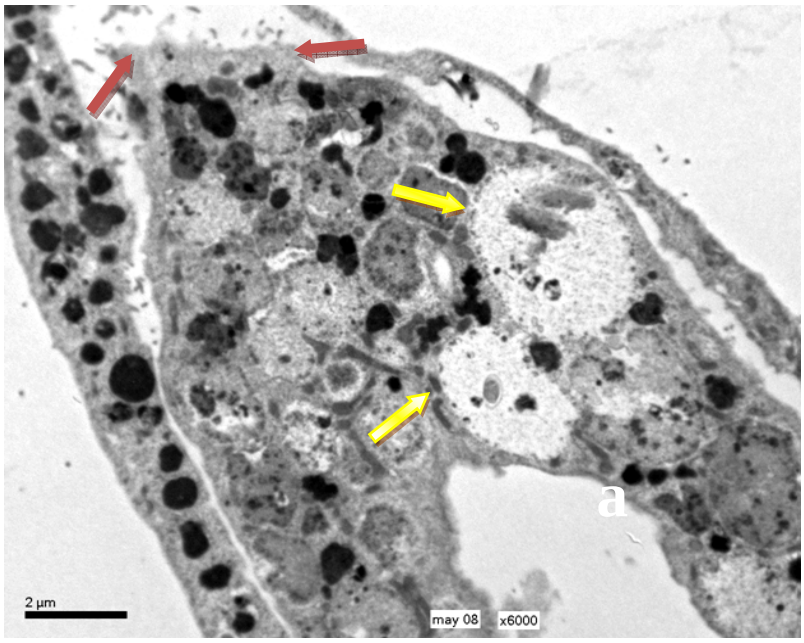

Figure 64: A compromised oligodendrocyte cell with enlarged vesicles (yellow arrows) and disrupted membrane (red arrows). In addition, there is a large increase in the number of myelin sheaths. The areas of myelin sheath growth do not show normal layered structure but is instead grainy. Original magnification 6000x.

4.4.6 Levels of Virus Production in Infected Primary Neurons

The same passaged and unpassaged viruses in *Section 4.4.2* were used for infecting a monolayer of primary mouse neurons isolated from E16 mice at an MOI of 10. From *Figures 65 and 66* below, it could be seen that the level of peak and overall virus production from the unpassaged (*Figure 65*) and passaged (*Figure 66*) viruses were different. The maximum virus titres from cultures infected with passaged viruses were generally higher than the unpassaged viruses. This showed that the passaging affected the virus neurovirulence by increasing the maximum virus titre during infection as well as causing peak virus infection to occur at an earlier time – point.

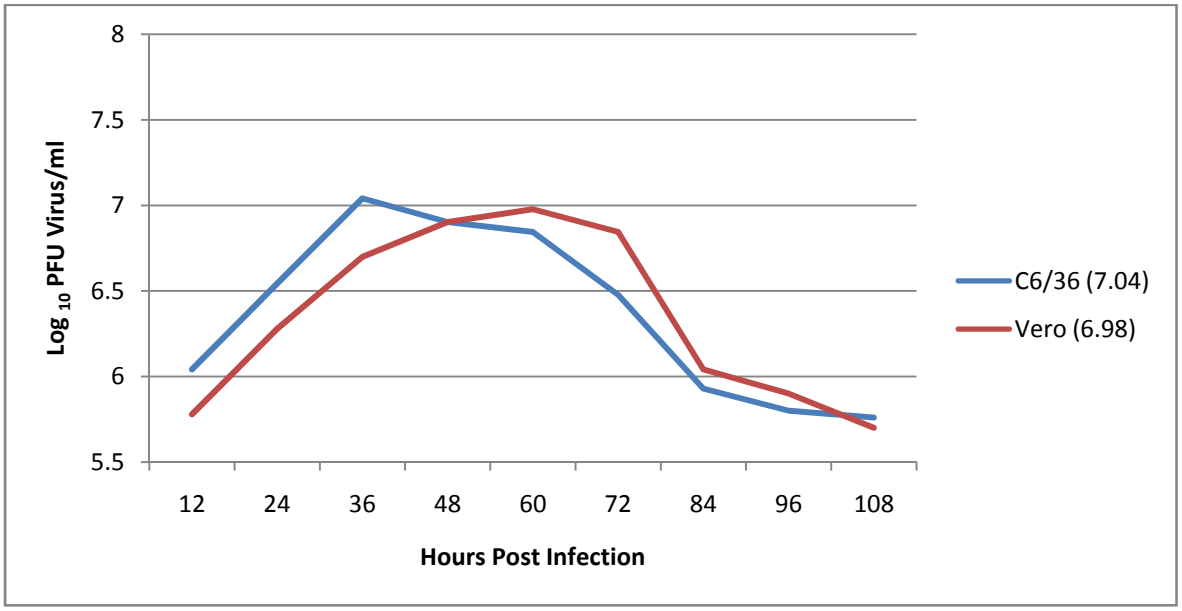

Figure 65: Growth curves of unpassaged viruses on mouse primary neural brain culture. Virus titre peaks at 36 hours post inoculation for the C6/36 cell – grown WNVS while the Vero cell – grown WNVS peaks later at 60 hours post inoculation. For both virus inoculations, there is an exponential rise in the virus titre from 12 to 36 hours post inoculation. The virus titres start to decrease after 60 to 72 hours. The numbers in brackets indicate peak virus titres (Log_{10} PFU/ml).

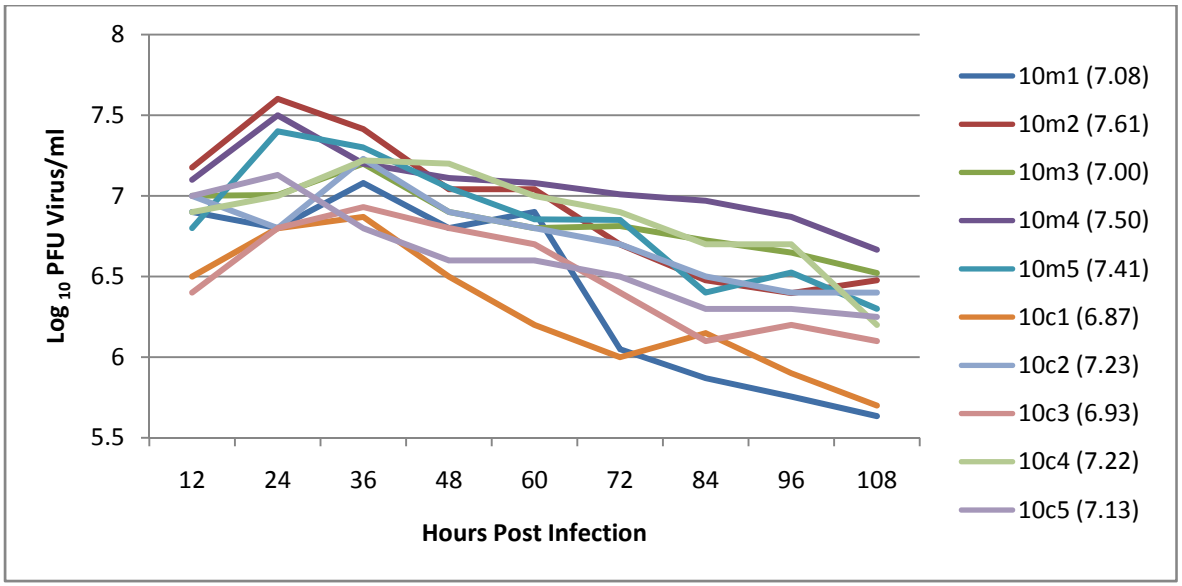

Figure 66: Growth curves of the ten passaged viruses on primary neuronal mouse brain culture. Virus titres generally peak early at 24 hours post inoculation and then slowly drift downward over the days. The curves for passaged and unpassaged virus are different. All of the passaged viruses except 10m3, 10c1, and 10c3 achieve peak virus titre that is higher than the peak virus titre of unpassaged viruses as seen when comparing the numbers in brackets which represent peak virus titres (Log_{10} PFU/ml). No difference in virus titre between 'c' and 'm' series at any time point can be detected unlike in Section 4.4.2 where the 'c' series passaged viruses gives higher PFU/ml levels as compared to the 'm' series passaged viruses at 12 hours post inoculation.

4.4.7 Gross Phenotypic Changes During Infection of Primary Neurons

The phase contrast micrographs taken at 24 hour intervals showed the rapid dying of cells with the onset of cytopathic effect. Most of the cell population lifted off the flask by the third day post inoculation (*Figures 67 and 68*). Neurons infected with unpassaged Vero and C6/36 cell grown WNVS were found to show cytopathic effects earlier compared to passaged viruses which at the end of 4.5 days post infection still had some adherent neurons on the tissue culture dish surface. The remaining cells were small and appeared unhealthy. The passaged virus produced a higher and longer plateau of virus titre compared to the unpassaged viruses as seen by plaque assay in *Section 4.4.6*. This

corresponded to the photomicrographs of infected cells in which passaged virus infections did not kill all neural cells (*Figure 67 and 68*).

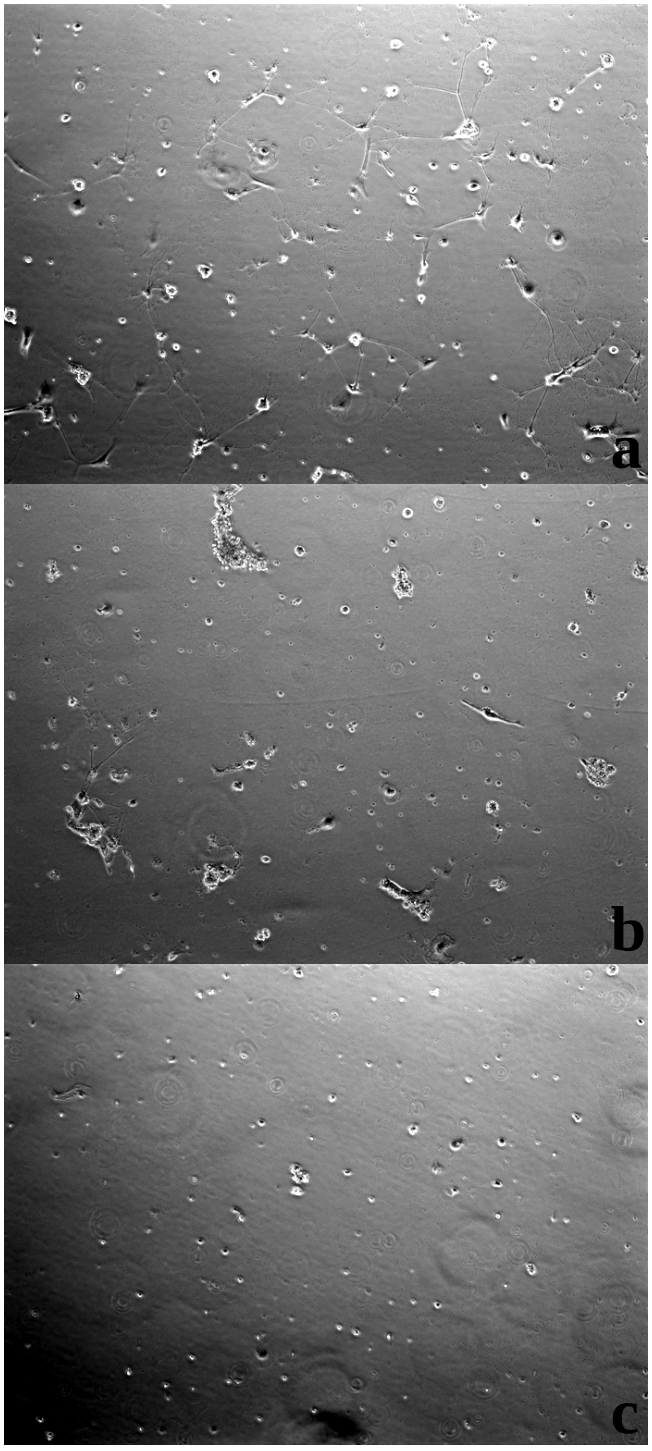

Figure 67: Micrographs from unpassaged C6/36 cell culture grown WNVS infection on primary neuronal cells at different hours post infection a (24 hours), b (48 hours), and c (72 hours). At 72 hours, only cell debris can be seen in the culture dish. Original magnification 10x.

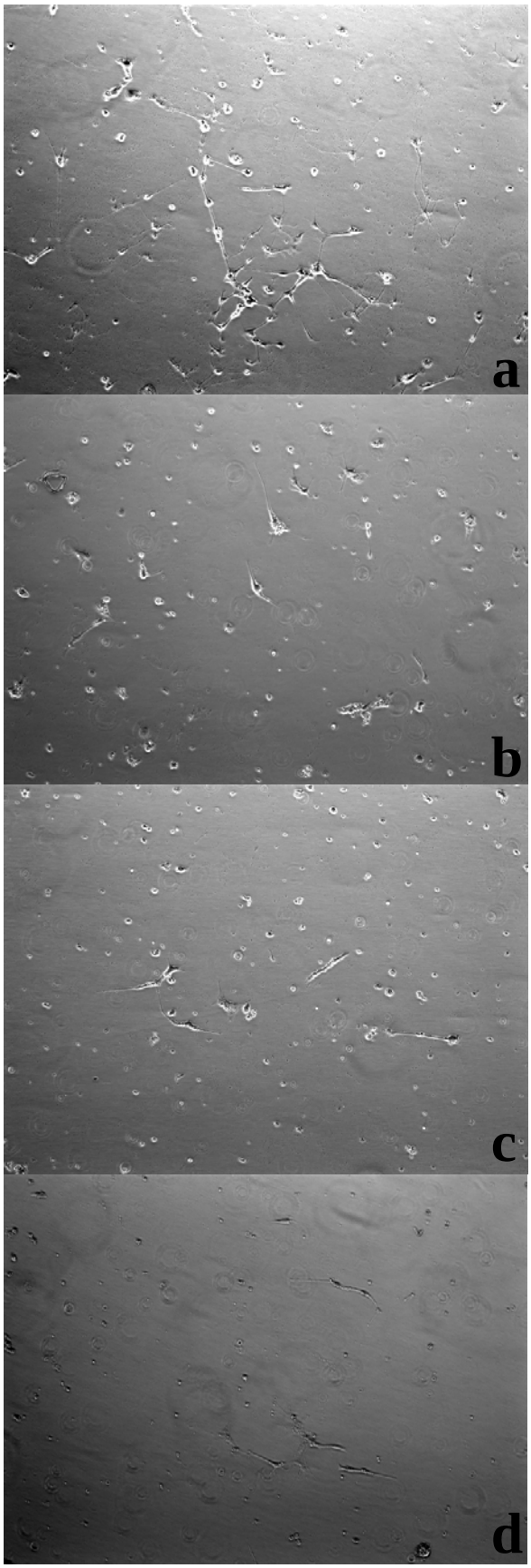

Figure 68: Micrographs of primary neuronal cells infected with passaged virus from the stock 10m2 virus at various time points of a (24 hours), b (48 hours), c (72 hours), and d (96 hours). At 96 hours post infection, there are some cells remaining.Original magnification 10x.

CHAPTER 5
RESULTS

5.0 RESULTS

5.1 DIRECT SEQUENCING OF UNPASSAGED VIRUS

The genome from stock WNVS grown on C6/36 cells (*Section 2.2*) used in this study was sequenced (*Section 2.4*). The resulting nucleotide as well as translated amino acid sequence were blasted against the complete WNVS genome sequence (AY688948) deposited in Genbank by Li and colleagues (2005) to detect any variation in unpassaged virus. Only one mutation was found in the NS2a protein at amino acid residue 2 where asparagine mutated to threonine. No other conserved or non – conserved mutations were observed throughout the entire RNA genome. This shows that the virus genome had not changed much despite approximately three years of passaging since the publication of Li and colleagues (2005).

5.2 DIRECT SEQUENCING OF PASSAGED VIRUSES

The five 'c' and five 'm' passage 10 viruses were sequenced directly as outlined in *Section 2.4*. Genetic domains encoding proteins C, E, NS2a, NS2b, NS4a, and NS4b were sequenced. Regions encoding C and E proteins were chosen to represent the structural proteins while NS2a, NS2b, NS4a, and NS4b represented the non – structural proteins. The prM, NS1, NS3, and NS5 genes were not selected as these genes code for vital proteins crucial for virus replication and growth. Mutations in this region will affect virus viability and growth significantly. As no drastic changes in virus titres were seen at the end of the 10 virus passaging rounds, it was assumed, although untested, that these regions had changed little. The virus genomes were not first cloned into an amplification vector as Pfu DNA polymerase was used which has 3' to 5' exonuclease proofreading

capabilities. Complete sets of target sequences were obtained from the ten passaged viruses.

5.2.1 Sequences of West Nile Virus (Sarafend) C Protein

The RNA isolates from the ten various passaged viruses was reverse transcribed, amplified, sequenced, and translated into protein sequences (*Section 2.4*). *Table 11* showed the various viruses' mutations in the C protein regions of the passaged virus genomes. All passaged viruses had mutations in the C protein regions. The passage 10c5 and 10m1 showed a mutation at the first amino acid that changed the start codon. As this mutation was found to be the consensus sequence through sequencing, it is a tolerable, non lethal mutation.

The other mutations were found at residues 24, 26, and 29 of C protein (*Table 11*). Residue 24 and 26 are at the start of the first α – helix while residue 29 is in the middle of it (*Figure 69*). It is known that these residues are part of the hydrophobic interior of the C protein 3 – helix core (Dokland *et al.*, 2004; Ma *et al.*, 2004). All three mutations from glycine to valine at residue 24, serine to alanine at residue 26 and glycine to valine at residue 29 caused an increase in nonpolarity and also increased the overall hydrophobicity as the hydropathy index increased significantly from -0.4 to 4.2 for G to V, and -0.8 to 1.8 for S to A mutations. The crystal structure also suggested that α – helix 1 is flexible and plays a functional role in assembly and RNA binding. The helix movement would expose the hydrophobic site to allow for interaction with host membrane during assembly (Kofler *et al.*, 2002). By maintaining the secondary structure stability, these residues played an important role in virus production.

Table 11: Mutations at the C protein region of passaged viruses. Hotspots are identified as amino acid residues 24 and 26 with 8 of the 10 passages having either one of these mutations. Both mutations increase the overall hydrophobicity of that area.

Passaged virus	Nucleotide Position	Nucleotide Change	Amino Acid residue	Amino Acid Change
10c1	76	T to G	26	S to A
10c2	71 to 72	GA to TG	24	G to V
	355 to 356	GC to TT	118	A to F
10c3	71 to 72	GA to TG	24	G to V
	369	T to A	123	A to V
10c4	71 to 72	GA to TG	24	G to V
10c5	2	T to G	1	M to R
	86	G to T	24	G to V
10m1	2	T to G	1	M to R
	86	G to T	29	G to V
10m2	71 to 72	GA to TG	24	G to V
10m3	76	T to G	26	S to A
10m4	76	T to G	26	S to A
10m5	71 to 72	GA to TG	24	G to V

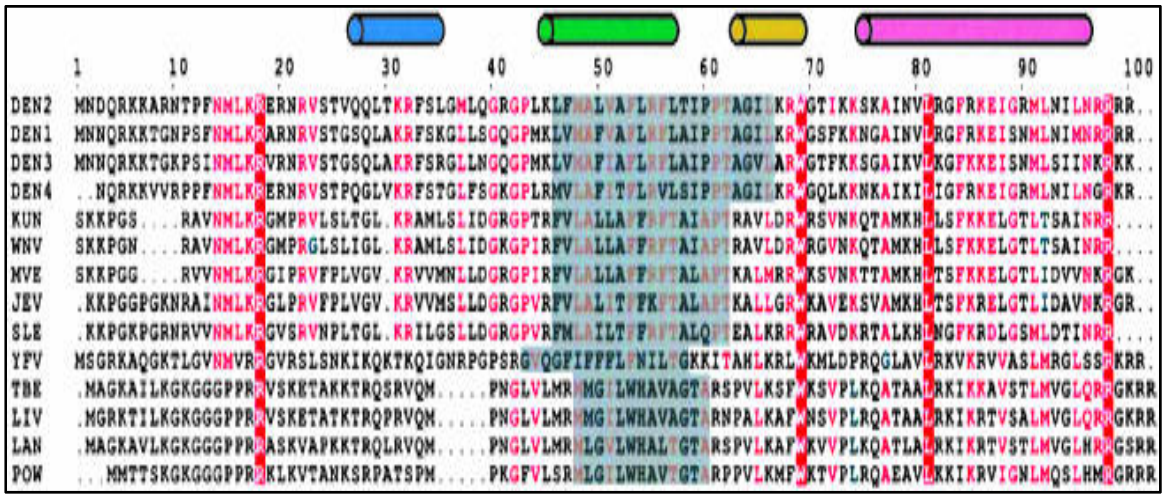

Figure 69: Multiple sequence alignment of flavivirus C proteins. Residues of high similarity are in red and conserved residues are highlighted. The four rods represent helices. Conserved hydrophobic regions are in grey. Hotspot mutation at residue 24 and 26 are at the start of helix 1. Den: dengue, Kun: Kunjin, WNV: West Nile, MVE: Murray Valley encephalitis, JEV: Japanese encephalitis, SLE: St. Louis encephalitis, YFV: yellow fever, TBE: tick borne encephalitis, LIV: louping ill, LAN: Langat, POW: Powassan (Ma et al., 2004).

Interestingly, when mutation points on *Table 11* were studied; either a mutation was seen at the residue 26 – 29 region or at the residue 24 position but never together. The significance of this is unknown but it may be a possible event of convergent evolution where each mutation increased virus pathogenicity and are just two different mechanisms. Also, the amino acid residues mutated to were similar indicating that non-conservative mutations to other amino acid residues may have deleterious or less beneficial effects. The plots by Protean software (DNASTAR Inc., USA) showed various changes in antigenicity, hydrophilicity, surface probability, and change in possible secondary structure, shown in *Figure 70*.

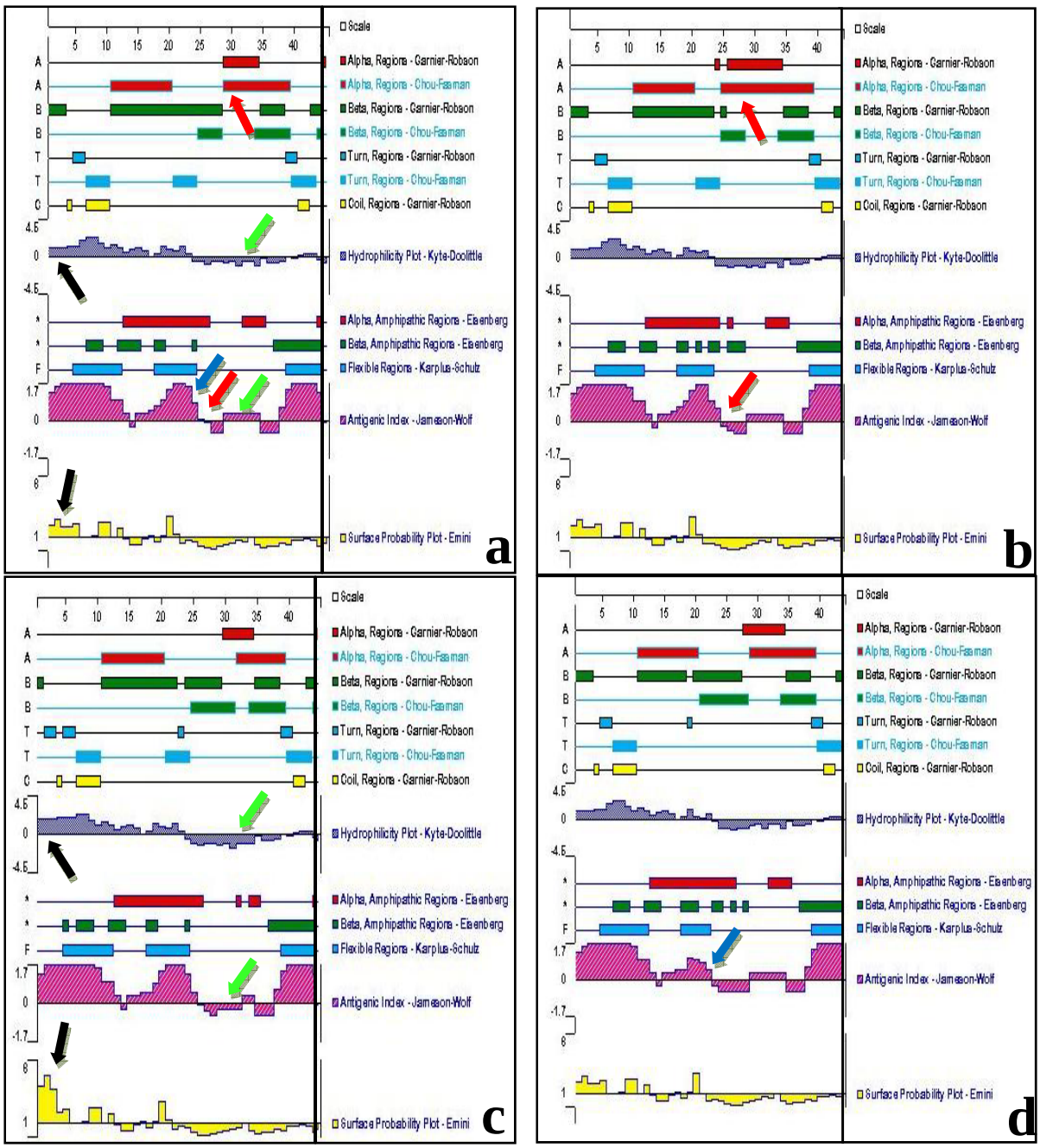

Figure 70: Protean automated predictions of C protein secondary structures from representative unpassaged (a) and passaged viruses 10c1 (b), 10c5 (c), and 10m2 (d). These passaged viruses contain mutations at amino acid residues 26 (b), 1 and 29 (c), and 24 (d). The mutation at amino acid residue 26 sees a change in alpha regions predicted as well as a drop in the antigenicity (red arrows) compared to the unpassaged virus plot, while changes in residue 29 causes a decrease in antigenic index and an increase in hydrophobicity (green arrows). Mutations at amino acid residue 1 shows an increase in surface probability and hydrophilicity (black arrows) while residue 24 causes a sharp decrease in antigenicity (blue arrows). All the other mutations do not display any significant change in predicted secondary structure or antigenicity.

5.2.2 Sequences of West Nile Virus (Sarafend) E Protein

A single mutation was found in the E protein region of 10c1 among all the passaged viruses (*Table 12*). The mutation at amino acid residue 150 was mapped to a conserved glycosylated loop in domain I (*Figure 71*) solved crystallographically by two groups (Kanai *et al.*, 2006; Rey *et al.*, 1995). This mutation caused a large increase in hydrophobicity but the relevance of this mutation was unknown as it is part of the position 145 – 162 loop exposed on the viral surface (Kanai *et al.*, 2006). Surface exposed residues would be in direct contact with the aqueous phase and could be negatively affected by such a mutation.

Table 12: The only amino acid mutation found in the E protein from all 10 various passages of passaged virus. The residue mutating from alanine to valine is found in domain I and retains the nonpolar charge but the mutation causes an increase in hydropathy index from 1.8 to 4.2.

Passaged virus	Nucleotide Position	Nucleotide Change	Amino Acid residue	Amino Acid Change
10c1	449	A to C	150	A to V

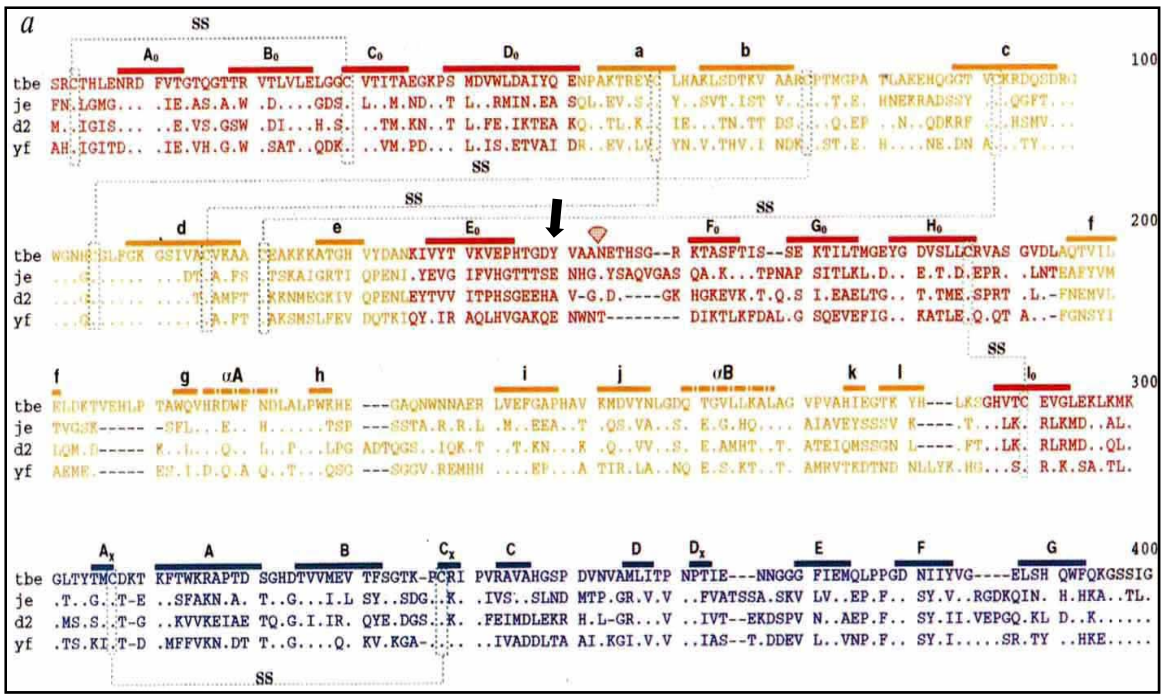

Figure 71: Multiple sequence alignment of 4 representative flavivirus E proteins. Bars above the sequences show areas of secondary structure. Residue 150 (black arrow) is in between beta sheets E_0 and F_0. TBE, JE, and YF has a polar, neutral, and hydrophilic residue in this position. Dengue however has a nonpolar hydrophobic residue, which is similar to the original Sarafend residue. The mutated amino acid (valine) is more hydrophobic compared to alanine. TBE: tick borne encephalitis, JE: Japanese encephalitis, YF: yellow fever virus (Rey et al., 2006).

5.2.3 Sequences of West Nile Virus (Sarafend) Non Structural 2a (NS2a) Protein

The passaged virus 10c2 showed 8 different nucleotide point mutations in the NS2a protein (*Table 13*). All the mutations were clustered to the first 6 amino acids indicating that this could be a potential multivariable site during the process of host adaptation.

Mutation at amino acid residue 2 of NS2a protein was found in 7 of the viruses sequenced. Of these, 4 viruses showed asparagine to isoleucine mutation while the remaining three mutated to threonine. This asparagine to threonine mutation was however also noted in the unpassaged virus implying that this mutation was the consequence of prolonged passaging in tissue culture and not mouse passaging.

Table 13: Amino acid changes in the NS2a coding region arising from mutations at the nucleotide level as compared to the WNVS virus sequence deposited in Genbank. Points of interest include a mutation from stock unpassaged virus at amino acid 2. All passaged viruses except 10c1 and 10c3 has mutations in this region. The 10c2 passaged virus shows the most difference with 8 nucleotide mutations resulting in 4 amino acid changes. All the mutations are mapped to the first 6 amino acids of NS2a signaling the importance of this hotspot during virus – host adaptation.

Passaged virus	Nucleotide Position	Nucleotide Change	Amino Acid residue	Amino Acid Change
Unpassaged	5	A to T	2	N to I
10c2	6	C to T	Conserved	
	7	G to T	3	A to S
	9	C to A	3	A to S
	11 to 12	AC to TT	4	D to V
	13 to 14	AT to GG	5	M to G
	16	A to C	6	I to L
10c4	5	A to T	2	N to I
10c5	5	A to T	2	N to I
10m1	5	A to C	2	N to T
10m2	5	A to C	2	N to T
	13	A to G	5	M to V
10m3	5	A to C	2	N to T
	330	A to G	Conserved	
10m4	5	A to T	2	N to I
	16	A to G	6	I to V
10m5	5	A to T	2	N to I

Evaluation of translated protein sequence of NS2a from passaged virus 10c2 and 10m2 as representative viruses against the unpassaged virus by Protean software (DNASTAR Inc., USA) revealed postulated changes in α – regions, β – regions, and antigenicity (*Figure 72*). The mutations observed completely abolished areas of predicted alpha helix secondary structures and increased antigenicity levels.

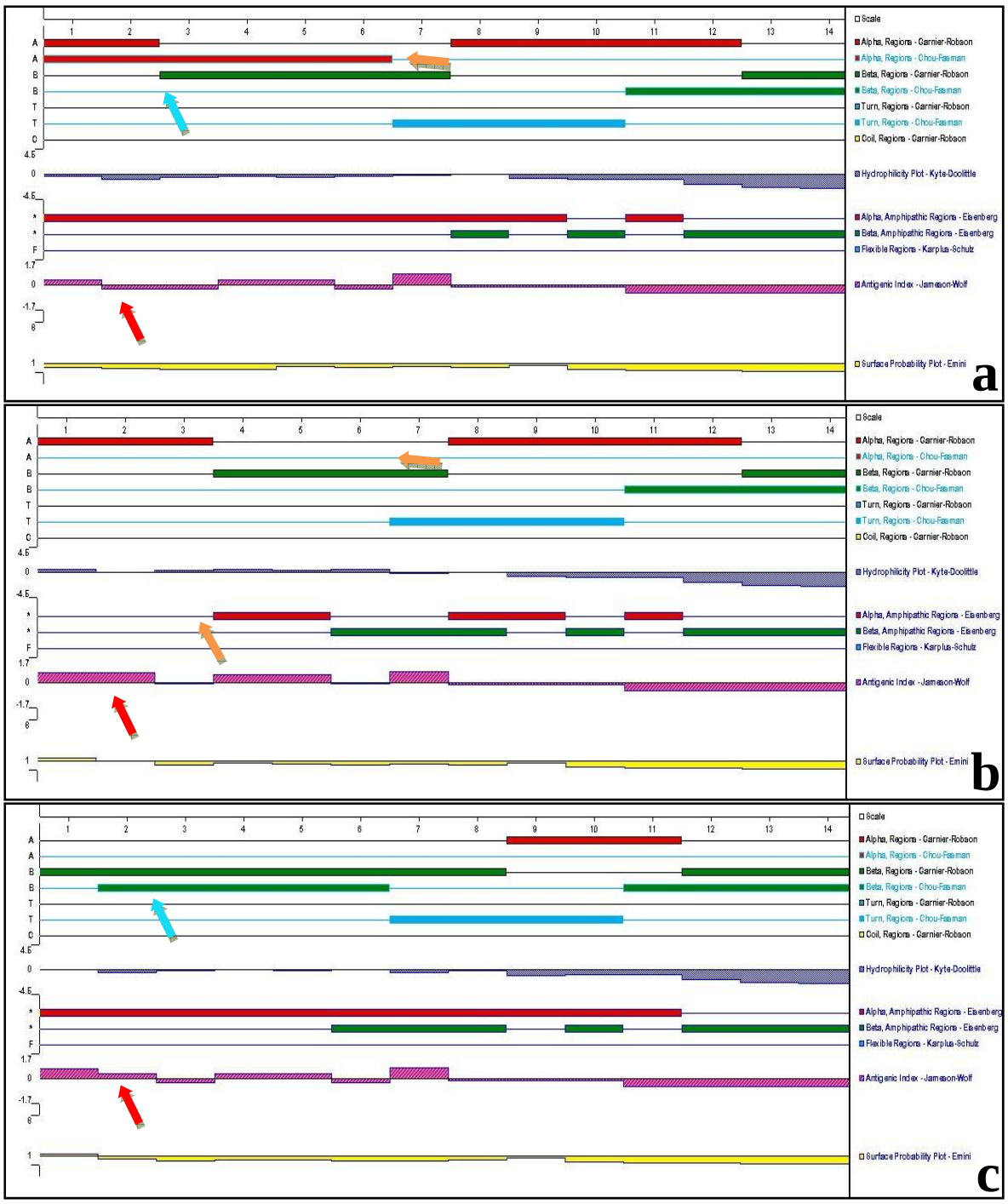

Figure 72: Protean outputs predicting various secondary structures at the first 14 amino acids of NS2a of unpassaged virus (a), passaged virus 10c2 (b), and 10m2 (c). Passaged virus 10c2 contains mutations at amino acid residues 3 to 6 while 10m2 has mutations at residues 2 and 5. Of notable difference in passaged virus secondary structure predictions for the first 5 amino acids are the disappearance of alpha regions (orange arrows), the prediction of beta regions (blue arrows) and increase in antigenicity (red arrows). Comparing the unpassaged virus with 10c2 virus, the whole putative region of alpha region by Chow-Fasman is deleted while antigenicity for the same area increased.

5.2.4 Sequences of West Nile Virus (Sarafend) Non Structural 2b, 4a, and 4b (NS2b, NS4a, and NS4b) Proteins

No mutation, silent or unconserved was found in any of the proteins abovementioned, compared to the original sequence from Genbank or unpassaged virus.

CHAPTER 6
DISCUSSION

6.0 DISCUSSION

The initial objective of this study was to employ BALB/c, an immunocompetent mouse as a model for flavivirus infection. However, early studies using DV2 NGC and WNVS virus on adult immunocompetent mice resulted in no detectable infections (*Sections 3.1.1 and 3.2.1*). Previous studies had shown that DV was able to only infect immunocompromised mouse models (Johnson and Roehrig, 1999; Lee *et al.*, 2006). West Nile virus (Sarafend) on the other hand was observed to infect B6 mice and caused 100 % mortality at high PFU levels (Wang *et al.*, 2003). This group however consistently passaged WNVS through suckling mice instead of cell culture. The disparity of results for WNVS infection between published literature and in this study could be due to the fact that the WNVS used here had been passaged repeatedly over the decades in cell culture causing it to be attenuated in terms of pathogenicity.

6.1 Tests with Dengue Virus

Tests on immunocompromised AG129 mice with DV2 NGC found the mice infectable with positive virus titres in serum, spleen, and liver (*Figures 6 to 8*). However, unlike previous publications (Chen *et al.*, 2004; Lin *et al.*, 1998; Shresta *et al.*, 2004a; Shresta *et al.*, 2004b), this virus did not cause any mortality or paralysis in AG129 mice. These studies also found that most mice developed severe paralysis. As dengue infection is not known to cause paralysis in humans, this reported observation may not a relevant phenotype for a dengue model.

In *Figures 13 to 14*, germinal centres were noted developing in both white and red pulp. This indicates that DV could stimulate the propagation of both B and T cells, respectively during early infection (*Figures 9 to 15*). T cell activation has only been observed after secondary DV infection in both human clinical samples and animal models but not at early time points after primary infection with DV (Yauch and Shresta, 2008). Even though dengue viruses used in this study were continually passaged in cell culture the virus remained antigenic. In spleens, virus antigens were found specifically in the cytoplasm of infiltrating cells (*Figure 10*) that gathered in the red pulp causing inflammation and splenomegaly (*Figure 9*). These would most likely be antigen presenting cells in the form of dendritic cells or macrophages gathered from circulating blood or lymph nodes as the same cell types were found susceptible to dengue virus infection in both mice and human (Blackley *et al.*, 2007; Clyde *et al.*, 2006; Kyle *et al.*, 2007). The work on dengue virus has been included to give a more complete overview of work done on different flaviviruses. It goes to show that the pathology and mechanisms are different as compared to West Nile virus and needs to be taken into account when comparing data from the two different viruses.

6.2 Passaging of West Nile Virus (Sarafend)

Passaging viruses can lead to either attenuation or increase in virulence. Studies have shown that passaging flavivirus through cell culture could lead to attenuation in various *in vivo* systems (Barrett *et al.*, 1990; Ciota *et al.*, 2007a; Dunster *et al.*, 1990; Goto *et al.*, 2003; Miller and Mitchell, 1986). A single mutation in DV genome could significantly

increase or reduce disease in mice (Bordignon *et al.*, 2007; Jia *et al.*, 2007; Lee *et al.*, 2006; Liu *et al.*, 2006). Similarly, in Japanese encephalitis, a single amino acid change in the envelope protein led to drastic change in virulence (Chiou and Chen, 2007). Even without any mutations after passaging, it was found that DV passaged through tissue culture was more rapidly cleared from the circulation or mice (Lee *et al.*, 2006). Because of the complexity surrounding four serotypes of DV and the different substrains available, in this study, it was more manageable to work with WNVS which the laboratory had been using and whose sequence was already determined. Additionally, WNVS can be grown to higher titres compared to DV. This would greatly ease subsequent experimentation.

Literature has shown that passaging WNV serially commonly causes cyclic movements of virus titre (Bordignon *et al.*, 2007; Jerzak *et al.*, 2007; Jerzak *et al.*, 2008). The cause of titre drop is uncertain as the authors could only state that virus adaptation to the host could be a reason why titres fluctuated between passages. The virus' ability to recover to normal titres after a drastic drop as in passage five (*Figure 37*) could be attributed to the reported existence of multiple genotypic variants or quasispecies found in all WNV populations (Ciota *et al.*, 2007b; Jerzak *et al.*, 2005) and has been proven in foot and mouth disease viruses (Martinez *et al.*, 1991).

This theory states that natural selection favours not simply the fastest growing replicator, but rather a virus with broad spectrum of mutants that are produced by erroneous copying

of the fittest sequence (Moya *et al.*, 2004). The fastest replicating RNA viral genomes could be out competed by those with lower replication rates if the latter is capable of generating mutations from closely related variations. These papers also noted sudden severe drops in virus titres during passaging at various rounds similar to the drop seen at passage 5 of the 'c' series (*Figure 37*). Arthropod – borne RNA viruses are known to alternate hosts in nature through a vertebrate and an invertebrate host. A virus population having genetically distinct subgroups could survive better when transmitted through different environments (Aaskov *et al.*, 2006). Additionally, even though the mutant spectrum may contain premature stop codons, it is still able to stimulate the host immune system that leads to clinical signs and the associated host response (Jerzak *et al.*, 2007). Complementation allows these seemingly unfit subgroups to persist in the virus population.

6.3 Plaque Size Change During Passaging

Virus plaque size change is postulated to be a reflection of variability in virus genome and virulence. Small plaque WNV (Kunjin) virus was reported to produce low titres and high levels of interferons while small plaque WNV (New York) virus was attenuated both *in vitro* and *in vivo* (Jia *et al.*, 2007; Liu *et al.*, 2006). Small plaque size thus seemed to correspond to lower virus replication efficiency. Plaque sizes of all passaged viruses were measured and plotted (*Figures 19 to 21*). The standard deviations of the plaque sizes from these graphs were also drawn (*Figures 22 to 24*).

Plaque size generally became larger in the 'm' passaged virus series and smaller in the 'c' series through passaging up to passage 5 (*Section 3.3*) but reverted to unpassaged virus size at passage 10 (*Figures 19 to 21*). Passaging the virus through different methods has adapted it differently and also caused a cyclic movement in plaque size. The passaged viruses were found to be more infective than unpassaged viruses and the smaller plaque size 'c' series were more pathogenic than the larger size 'm' series (*Section 4.3*). Ciota and colleagues (2008) passaged WNV virus through 20 rounds of mosquito cell culture. Average plaque sizes were measured at passage 10 and 20. Passage 20 viruses were larger in size while the average plaque sizes at passage 10 did not differ from unpassaged virus (Ciota *et al.*, 2008); this was mirrored in *Figures 19 to 21* where the fluctuation of virus particle sizes returned to baseline level for 'c' and 'm' at passage 10. This showed that plaque size change is cyclical during passaging.

Standard deviations of plaque sizes were calculated as a surrogate marker for diversity of virus population. It showed a cyclical pattern throughout the 10 passages for all the passaged viruses (*Figures 22 to 24*) suggesting that the virus genetic population was constantly adapting. The standard deviation of plaque sizes from C6/36 grown viruses became larger with passaging, indicated by the increasing standard deviation value with passaging (*Figure 24*). This is in line with the study of Ciota and colleagues (2007b) that suggested passaging WNV through a mosquito cell line caused a linear increase in genetic heterogenicity of the virus. Virus size diversity was found to fluctuate easily with passaging and could recover to baseline size in two to three passages (Jia *et al.*, 2007). It was also seen that pools of viruses with high size diversity or large mutant spectrum

caused lower mouse mortality (Jerzak *et al.*, 2007). From *Figures 22 to 24*, one notes the overall higher standard deviations for 'm' series passaged viruses correlating with its lower virus fitness seen throughout the results (*Sections 4.3 and 4.4.2*). There could have been some experimental errors in the results of *Figures 25 to 36* on various passages. However, the omission of particular passages from the figures would raise more questions and doubts, and hence the full dataset was shown.

6.4 Tests on Passaged Virus Virulence

Comparing unpassaged to passage 10 viruses, suckling mice inoculated with passage 10 viruses were found to die at earlier time points while inoculated adult mice showed virus positively in brains, livers, serum, and spleens up to day three post inoculation (*Sections 4.2 and 4.3*). Passaged viruses inoculated onto primary cells also gave higher and earlier peak virus titres compared to unpassaged viruses (*Section 4.2.6*). This effect of passaging was previously noted in DV passaged through AG129 mouse brains and C6/36 for ten rounds (Kyle *et al.*, 2007). The resultant virus caused peak virus titres in adult mice brains at day 2 instead of the unpassaged virus at day 4. The passaged DV could also kill single knockout A129 mice which has interferon α/β receptor knockout on which the unpassaged dengue could only cause paralysis. Comparing suckling mice inoculated with 'c' series and 'm' series viruses, the 'c' virus inoculated suckling mice died at an earlier time point as compared to the 'm' series highlighting that passaging using different passaging routines affected the level of virus adaptation (*Section 4.2*).

When comparing the survival times of suckling mice inoculated intracerebrally with various doses of passaged (*Figures 39 to 40*) or unpassaged (*Figure 18*) WNVS, no clear distinction of dose response over 2.5 logs difference in virus inoculum was noted. The mean survival times of suckling mice inoculated with WNVS were indistinguishable between various doses. This was also seen in published data for both Murray Valley encephalitis virus and WNVS virus where no clear dose response curve was seen in suckling mice inoculated with a virus range difference of 4 logs (Licon Luna *et al.*, 2002; Wang *et al.*, 2003). This was also observed in studies with WNV (New York) where a difference of 3 logs of virus resulted in the same mean survival time and viremia in adult mice (Arroyo *et al.*, 2001; Beasley *et al.*, 2005; Borisevich *et al.*, 2006; Shirato *et al.*, 2004). None of the authors suggested an explanation for this phenomenon.

Only two of the 20 inoculated BALB/c mice showed signs of neuroinvasiveness in the form of meningitis although multiple mice had positive virus titres in the brains. This mimics reported human cases where less than 1 % of infected individuals developed severe neuroinvasive disease (Kramer *et al.*, 2007; Mostashari *et al.*, 2001). The passaged virus was found to be both neuroinvasive and neurovirulent as shown when the virus was able to cross the blood brain barrier of adult mice (Monath *et al.*, 1983) and established viremia up to day three post inoculation (*Figure 42*). As the virus was found in the brains of adult mice at day one post inoculation, WNV was able to breach the blood brain barrier without the need for first infecting and replicating at a peripheral organ. This was shown to be possible in mice inoculated with WNV through the footpad (Hunsperger and Roehrig, 2006).

Comparing virus titres in adult mice brains inoculated with 10c4 and 10c5 passaged viruses at day 1 and 3 post inoculation, the titres increased dramatically from day 1 to day 3 indicating the virus' ability to replicate in the CNS. Moreover, in *Figure 42*, the virus titres from brain homogenates of mice inoculated with 10c4 and 10c5 passaged virus was positive although no virus was detected in the serum. The passaged virus was thus neurovirulent. This was again proven as passaged virus could productively infect neuronal cell cultures producing high virus titres for a week (*Section 4.4.7*). However, inflammation was noted in mice cerebella (*Figure 50*) which is typically not infected in human and nonhuman primate cases where neuroinvasion usually occurs in the substantia nigra, brainstem, basal ganglia, and cerebellum (Fratkin *et al.*, 2004; Maximova *et al.*, 2008; Sejvar *et al.*, 2003). The passaged virus was thus able to cross the blood brain barrier and infect mouse brain cells but in an atypical locale.

6.5 Infecting Primary Cells with Passaged Viruses

WNV is known to infect neurons and other CNS cells (Ceccaldi *et al.*, 2004; Shrestha *et al.*, 2003; Steele *et al.*, 2000) although different neural cell cultures differ in infectability according to its culture type (Ceccaldi *et al.*, 2004). This group found pure neuronal cell cultures very permissive to infection with up to 90 % of neurons infected at 48 hours post inoculation whereas primary mixed cultures of astrocytes/neuronal with a high percentage of astrocytes were resistant to WNV with only 10 % of astrocytes infected.

This study used two different primary cell cultures, a pure neuronal cell culture and a second mixed culture of astrocytes and oligodendrocytes. The results confirmed that neuronal cells were indeed more permissive to infection by WNVS as compared to the astrocyte/oligodendrocyte mixed culture (*Sections 4.4.2 and 4.4.6*). The neuronal cells showed a higher level of cytopathic effect at an earlier time point compared to the mixed culture. The time and peak titre virus production were also comparable to results obtained using WNV New York strain (Diniz *et al.*, 2006; Shrestha *et al.*, 2003). The photomicrographs from *Figure 67* shows only cell debris at 72 hours post inoculation with unpassaged virus. The same has been reported by Shrestha and colleagues (2003). In effect, WNVS has retained its neurovirulent trait in neuronal cells despite multiple cell passages. The 'c' and 'm' passaging regimes has caused the virus to increase in neurotropism, able to penetrate the blood brain barrier at an early time point and to produce higher titres for longer periods in neuronal primary cells.

Electron microscopy of remaining primary cells identified only oligodendroctyes but no astrocytes inferring that astrocytes were preferentially infected and killed by WNVS (*Section 4.4.5*). The inoculation of 10m2 on primary astrocyte/oligodendrocyte also proved that neural cells could be persistently infected for prolonged periods (*Figure 54*). West Nile virus has been isolated from the brains of monkeys, mice, and hamsters after 5.5 months, 35 days, and 53 days post inoculation respectively (Pogodina *et al.*, 1983; Shrestha and Diamond, 2004; Xiao *et al.*, 2001). Human primary astrocytes has also been found infectable by WNV but the level of infection was ~100 – fold lower than human primary neuronal cells (van Marle *et al.*, 2007). This suggested that astrocytes have a role

to play in the long term maintenance of WNV in the CNS and that WNV could persist in the CNS for prolonged periods without killing the host. Primary human oligodendrocyte cultures have also been shown to be less permissive for WNV replication compared to neurons and astrocytes (Cheeran *et al.*, 2005). This was in line with electron micrographs that showed oligodendrocytes remaining at the end of WNVS infection on an astrocyte/oligodendrocyte mixed culture (*Section 4.4.5*). Moreover, Jordan and group (2000) showed human primary oligodendrocytes to be uninfectable by WNV.

However, in terms of virus levels and sustainability, it was seen that the mixed cultures gave higher titres compared to the neuronal cells (*Figures 52, 53, and 66*). Peak virus levels lasted for longer periods in the mixed culture with the 10m2 virus – infected mixed culture showing positive virus titres up to week 16 post inoculation (*Figure 55*) but titres in inoculated neuronal cells persisted only up to day 7 (*Figure 66*). Similar observation was reported previously using WNV New York inoculated onto primary neural ICR mouse cells (Diniz *et al.*, 2006). That report showed virus titres lasting 5 days for neuronal cells and 16 weeks for astrocyte cultures. Levels of virus production on infected primary astrocytes and oligodendrocytes showed the 'c' series viruses having a notably higher starting virus titre compared to the 'm' series (*Figure 52*) confirming once again, that the 'c' passaged viruses were better adapted to infect various hosts and cells compared to the 'm' series.

Other articles have cited the CNS as a secondary site for WNV infection as virus was found only in the brain and spinal cord of inoculated B6 mice at day 9 post inoculation

(Garcia-Tapia *et al.*, 2007). At 4 days post inoculation, only skin, spleen, and kidneys were found as possible virus propagation sites. Different mice may show different primary organs of virus replication. The same report found inflammatory lesions in the cerebral cortex which corresponded to histopathology in *Figure 50*. Another report using WNVS found the virus in the CNS by 24 hours post inoculation at titres ranging from 10^3 to 10^8 PFU/g (Wang *et al.*, 2003). As such, it was obvious that different mouse species as well as viruses will show varying signs at different time points and cannot be generalised.

6.6 Changes in Virus Sequence

Attenuation or increased virulence can occur in viruses due to genetic modification at any part of the virus genome. The structural proteins are important for receptor binding, membrane fusion, and host immune system evasion. Any change in amino acid residue could lead to differences in virus receptor binding and tropism, conformational change, and protein stability. The non – structural proteins are important cofactors and contribute to enzymatic activities for the proper folding and maturation of the virus. Hotspots of mutation were noticed in the passaged virus sequences for C and NS2a proteins. There were more mutations in the 'c' series passaged viruses as compared to the 'm' series (*Tables 11 to 13*). This was also seen by Jerzak and group (2008) when viruses were passaged in both alternating and single host.

The mutations for C proteins were mostly concentrated at amino acid residue 24 (glycine to valine), 26 (serine to alanine), and 29 (glycine to valine). Either one of these mutations

(but not together) were found in 8 of the 10 passaged viruses. The amino acid changes at these sites of mutation were from and to the same amino acid species (*Table 11*) indicating that the selection stress was directed, resulting in similar amino acid mutations and the changes were not random.

The single mutation at amino acid residue 150 on E protein from alanine to valine (*Table 12*) represented a change on the surface of the protein. Surface exposed residues could influence receptor selectivity, vector preference and tissue tropism amongst other things. The residue does not have a known specific activity and was probably part of the linker protein between beta sheets (*Figure 70*). No previous publications on this residue could be found.

A mutation was seen in the unpassaged strain NS2a gene compared with the Genbank reference sequence, indicating that the virus was still mutating while being passaged through cell culture. In a Cuban dengue outbreak, the NS2a gene was found to bear the most mutations from retrospective analysis of DV4 strains from 20 years of sampling (Bennett *et al.*, 2003). This showed that NS2a gene was highly adaptive to change and its mutation could play a role in the evolution and survival of flaviviruses over prolonged periods. When comparing the mutations to pathology and viremia of adult and suckling mice inoculated with the passaged viruses, no obvious trend could be noted as there were relatively few mutations and almost all were concentrated at a few hotspots at the region of the first 6 amino acids of NS2a protein. However, no published work has indicated the

importance of this early region of NS2a protein as the cleavage site for NS1 – NS2a proteins was postulated to require the last 8 amino acids of NS1 and downstream sequences in the middle of NS2a (Chambers *et al.*, 1990; Falgout & Markoff, 1995). The mutations seen were very similar across the various repeats and no difference was noted between mutation rates or locus of the 'm' and 'c' series.

The other genes in the virus genome that were not sequenced are prM, NS1, NS3, and NS5. These genes carry important and very highly conserved, stable proteins or enzymes that are vital for proper virus infection and replication. Any mutation therein would affect the virus drastically in terms of viability.

The sequencing of C, E, NS2, and NS4 genes represents 4104 base pairs sequenced per virus genome out of the 10300 virus base pairs. From a total of 10 passaging rounds and 10 total repeats, 19 unique sites of nucleotide point mutation were detected from the sequencing results, conserved or unconserved. The rate of mutation per nucleotide passaged was thus 4.6×10^{-5} which is higher than virus mutation rates after passaging in a single host repeatedly which was reported to be approximately 1.7×10^{-5} (Jerzak *et al.*, 2008). This would suggest that theoretically, the passaging regime in this study exerted a high selective pressure on the virus causing increased rates of mutations.

The lack of mutations in the E, NS2b, NS4a, and NS4b sequences of passaged viruses could be due to two scenarios. Firstly there could be epigenetic changes that caused the increase in virulence seen. However, this phenomenon has not been described before in WNV and only once observed in DV (Lee *et al.*, 2006). The other possibility was that mutations in various passaged virus had taken place but the consensus sequence of the genes showed no mutations. As the consensus nucleotide sequence is a representative of the population average from the myriad of diverse viral genomes within a population (Aaskov *et al.*, 2006), signals from small subpopulations of mutated viruses would be masked by the more dominant unmutated population during sequencing. Only if individual plaque purified virus were isolated could these be sequenced (Ciota *et al.*, 2007b). This group passaged identical infectious clone – derived WNV through mosquito C6/36 and DF-1 cells for 40 and 20 rounds, respectively. The consensus sequence for both viruses came out similar to the unpassaged virus but when individual virus clones of the passaged virus were sequenced, the C6/36 cell culture passaged virus showed 18 nucleotide point mutations while the DF-1 cell culture passaged virus had 7 point mutations. Thus, the consensus sequence can be misleading as it does not represent the true repertoire of genetic diversity of a virus population (Aaskov *et al.*, 2006; Novella *et al.*, 2004). However, we do not have specialist equipment or resources to plaque purify the viruses and individually sequence them.

Still, multiple infections of the same cell are commonplace and with the high virus titre (10^8 PFU/ml) inoculated into mice, the long – term population size was large enough to complement defective or mutated viruses. It is also known that the transmission of

multiple lineages is advantageous as it ensures the presence of viruses differentially adapted to mouse or mosquito cells, decoying host immune responses, or allowing the production of more viral proteins (Aaskov *et al.*, 2006).

WNV has been shown to adapt differently to *in vivo* and *in vitro* hosts (Ciota *et al.*, 2007a). Passaging WNV in mosquito cell culture *in vitro* repeatedly was not sufficient to adapt the virus to infecting whole mosquitoes *in vivo*. This was attributed to the difference in complexity between whole organisms as compared to the simplistic monoclonal cell culture. Viral fitness within a whole mosquito would entail the virus' ability to infect and replicate in various mosquito cell types and to migrate from the midgut to the salivary glands (Kramer *et al.*, 1981). Extrapolating this, passaging WNV over time in a mammalian cell culture would lower the chance it could still productively infect the whole animal *in vivo*. This shows that the work herein was not perfect as mosquito cell culture was used instead of whole live mosquitoes but underscores the importance of passaging the virus *in vivo* in order to adapt WNVS to infect immunocompetent mice and to maintain its invasive properties in the long run.

6.7 Conclusions

The development of mouse models for flaviviruses remains a challenge today. The ideal model should be relevant in terms of route of infection and immunocompetence. The virus should induce similar signs of disease found in both humans and mice, manifesting a range of different symptoms from febrile disease, meningitis, encephalitis, to death.

West Nile Sarafend of lineage II is regarded to be less evolved as compared to lineage I flaviviruses, non – neuroinvasive, and highly attenuated in mice (Beasley *et al.*, 2005). This study has shown it possible to adapt a lineage II strain to become more infectious by alternate serial passaging through two different hosts mimicking a natural infectious cycle. This would allow for experiments to be carried out in BSL 2 facilities instead of the required BSL 3 facilities for WNV pathogenesis studies.

By this process of adaptation, plaque size and virus titres were observed to fluctuate in a cyclical pattern. The passaged viruses, when inoculated into immunocompetent mice were able to kill sucklings sooner and infect the brains, livers, and spleens of adults with positive virus titres up to day 3 post inoculation. Histological sections showed that the spleens were enlarged with massive leukocyte infiltration. The livers displayed pkynotic cells and large accumulations of inflammatory cells, while brains showed signs of meningoencephalitis. None of these signs were seen in mice inoculated with unpassaged viruses. The infection of passaged and unpassaged viruses onto primary neuronal and astrocyte/oligodendrocyte culture found astrocytes and neurons preferentially infected. Passaged viruses produced higher virus titres in neuronal cells compared to unpassaged viruses. Sequencing results indicated hot spots in the NS2a amino acid position 2 and structural protein C amino acid positions 24, 26, and 29.

Comparing the mouse only passage ‘m’ against the mouse – C6/36 passage ‘c’ viruses, the ‘c’ series passaged viruses killed suckling mice earlier, had more positive titres in

adult mice organs, and gave higher titres when inoculated onto primary astrocyte cultures. It is possible that should this passaging continue the virus may become even more adapted and cause more severe disease and pathophysiological changes in adult mice. On the other hand, continued passaging may also result in virus attenuation.

More experiments could be done to further the knowledge of this study. To determine if the virus passaging in C6/36 cells is vital for the mutations seen, a repeated passaging of round – 10 viruses in Vero or BHK should cause the reversion of seen residue mutations to its original residues at passage 0. The mutation analysis was not completed as it omitted the sequence of genes encoding prM, NS1, and NS3. Completing it would give a clearer picture of the total mutations and if the total mutation frequencies between C and M strains are comparable. It would also be good to test the passaged strain of virus on immunocompetent mice such as AG129 as such would display more signs and symptoms when infected with virus compared to Balb/C. This study was also limited in the number of mouse organs tested. The kidney, spleen, and lymph node have all been implicated in virus replication and spread. It would be advantageous to see the virus titre and pathological trend in these organs throughout the passaging routine. Another interesting aspect of the virus passaging that would be interesting to follow would be the immunological response in mice. This includes the upregulation of innate and adaptive immune response. Levels of cytokines, circulating lymphocytes, and number of infiltrating T and B cells in various organs could be studied by Elisa, flow cytometry, and histology to observe the immunological stimulatory effect of passaged versus unpassaged viruses.

Viruses are known to be easily adaptable with high mutation rates during replication. Knowledge on what changes happen when West Nile virus is passaged through different hosts is important in epidemiological studies as well as to understand the effects of long term routine passaging in the laboratory. This allows the manipulation of this virus to display specific traits, tropism, or virulence for modelling the disease progression.

REFERENCES

REFERENCES

Aaskov, J., Buzacott, K., Thu, H. M., Lowry, K., and Holmes, E. C. (2006). Long-term transmission of defective RNA viruses in humans and *Aedes* mosquitoes. *Science* **311(5758),** 236-238.

Agapov, E. V., Murray, C. L., Frolov, I., Qu, L., Myers, T. M., and Rice, C. M. (2004). Uncleaved NS2-3 is required for production of infectious bovine viral diarrhea virus. *J Virol* **78(5),** 2414-2425.

An, J., Kimura-Kuroda, J., Hirabayashi, Y., and Yasui, K. (1999). Development of a novel mouse model for dengue virus infection. *Virology* **263(1),** 70-77.

An, J., Zhou, D. S., Kawasaki, K., and Yasui, K. (2003). The pathogenesis of spinal cord involvement in dengue virus infection. *Virchows Arch* **442(5),** 472-481.

Arroyo, J., Guirakhoo, F., Fenner, S., Zhang, Z. X., Monath, T. P., and Chambers, T. J. (2001). Molecular basis for attenuation of neurovirulence of a yellow fever Virus/Japanese encephalitis virus chimera vaccine (ChimeriVax-JE). *J Virol* **75(2),** 934-942.

Arroyo, J., Miller, C., Catalan, J., Myers, G. A., Ratterree, M. S., Trent, D. W., and Monath, T. P. (2004). ChimeriVax-West Nile virus live-attenuated vaccine: preclinical evaluation of safety, immunogenicity, and efficacy. *J Virol* **78(22),** 12497-12507.

Bakonyi, T., Hubalek, Z., Rudolf, I., and Nowotny, N. (2005). Novel flavivirus or new lineage of West Nile virus, central Europe. *Emerg Infect Dis* **11(2),** 225-231.

Barrett, A. D., Monath, T. P., Cropp, C. B., Adkins, J. A., Ledger, T. N., Gould, E. A., Schlesinger, J. J., Kinney, R. M., and Trent, D. W. (1990). Attenuation of wild-type yellow fever virus by passage in HeLa cells. *J Gen Virol* **71(Pt 10),** 2301-2306.

Beasley, D. W., Li, L., Suderman, M. T., and Barrett, A. D. (2002). Mouse neuroinvasive phenotype of West Nile virus strains varies depending upon virus genotype. *Virology* **296(1),** 17-23.

Beasley, D. W., Whiteman, M. C., Zhang, S., Huang, C. Y., Schneider, B. S., Smith, D. R., Gromowski, G. D., Higgs, S., Kinney, R. M., and Barrett, A. D. (2005). Envelope protein glycosylation status influences mouse neuroinvasion phenotype of genetic lineage 1 West Nile virus strains. *J Virol* **79(13),** 8339-8347.

Ben-Nathan, D., Huitinga, I., Lustig, S., van Rooijen, N., and Kobiler, D. (1996). West Nile virus neuroinvasion and encephalitis induced by macrophage depletion in mice. *Arch Virol* **141(3-4),** 459-469.

Ben-Nathan, D., Lustig, S., Tam, G., Robinzon, S., Segal, S., and Rager-Zisman, B. (2003). Prophylactic and therapeutic efficacy of human intravenous immunoglobulin in treating West Nile virus infection in mice. *J Infect Dis* **188(1),** 5-12.

Bennett, S. N., Holmes, E. C., Chirivella, M., Rodriguez, D. M., Beltran, M., Vorndam, V., Gubler, D. J., and McMillan, W. O. (2003). Selection-driven evolution of emergent dengue virus. *Mol Biol Evol* **20(10),** 1650-1658.

Bernard, K. A., and Kramer, L. D. (2001). West Nile virus activity in the United States, 2001. *Viral Immunol* **14(4),** 319-338.

Berthet, F. X., Zeller, H. G., Drouet, M. T., Rauzier, J., Digoutte, J. P., and Deubel, V. (1997). Extensive nucleotide changes and deletions within the envelope glycoprotein gene of Euro-African West Nile viruses. *J Gen Virol* **78(9),** 2293-2297.

Betensley, A. D., Jaffery, S. H., Collins, H., Sripathi, N., and Alabi, F. (2004). Bilateral diaphragmatic paralysis and related respiratory complications in a patient with West Nile virus infection. *Thorax* **59(3),** 268-269.

Bethell, D. B., Flobbe, K., Cao, X. T., Day, N. P., Pham, T. P., Buurman, W. A., Cardosa, M. J., White, N. J., and Kwiatkowski, D. (1998). Pathophysiologic and prognostic role of cytokines in dengue hemorrhagic fever. *J Infect Dis* **177(3),** 778-782.

Blackley, S., Kou, Z., Chen, H., Quinn, M., Rose, R. C., Schlesinger, J. J., Coppage, M., and Jin, X. (2007). Primary human splenic macrophages, but not T or B cells, are the principal target cells for dengue virus infection in vitro. *J Virol* **81(24),** 13325-13334.

Bondre, V. P., Jadi, R. S., Mishra, A. C., Yergolkar, P. N., and Arankalle, V. A. (2007). West Nile virus isolates from India: evidence for a distinct genetic lineage. *J Gen Virol* **88(3),** 875-884.

Boonpucknavig, S., Vuttiviroj, O., and Boonpucknavig, V. (1981). Infection of young adult mice with dengue virus type 2. *Trans R Soc Trop Med Hyg* **75(5),** 647-653.

Bordignon, J., Strottmann, D. M., Mosimann, A. L., Probst, C. M., Stella, V., Noronha, L., Zanata, S. M., and Dos Santos, C. N. (2007). Dengue neurovirulence in mice: identification of molecular signatures in the E and NS3 helicase domains. *J Med Virol* **79(10),** 1506-1517.

Borisevich, V., Seregin, A., Nistler, R., Mutabazi, D., and Yamshchikov, V. (2006). Biological properties of chimeric West Nile viruses. *Virology* **349(2),** 371-381.

Brewer, G. J. (1997). Isolation and culture of adult rat hippocampal neurons. *J Neurosci Methods* **71(2),** 143-155.

Burt, F. J., Grobbelaar, A. A., Leman, P. A., Anthony, F. S., Gibson, G. V., and Swanepoel, R. (2002). Phylogenetic relationships of southern African West Nile virus isolates. *Emerg Infect Dis* **8(8),** 820-826.

CDC (2002a). Possible West Nile virus transmission to an infant through breast-feeding--Michigan, 2002. *MMWR Morb Mortal Wkly Rep* **51(39),** 877-878.

CDC (2002b). West Nile Virus activity--United States, 2001. *MMWR Morb Mortal Wkly Rep* **51(23),** 497-501.

CDC (2003). West Nile virus activity--United States, November 20-25, 2003. *MMWR Morb Mortal Wkly Rep* **52(47),** 1160.

CDC (2005). West Nile virus activity--United States, January 1-December 1, 2005. *MMWR Morb Mortal Wkly Rep* **54(49),** 1253-1256.

CDC (2007a). West Nile virus activity--United States, 2006. *MMWR Morb Mortal Wkly Rep* **56(22),** 556-559.

CDC (2007b). West Nile virus update--United States, January 1-September 11, 2007. *MMWR Morb Mortal Wkly Rep* **56(36),** 936-937.

CDC (2008). West Nile virus update--United States, January 1-July 22, 2008. *MMWR Morb Mortal Wkly Rep* **57(29),** 801.

Ceccaldi, P. E., Lucas, M., and Despres, P. (2004). New insights on the neuropathology of West Nile virus. *FEMS Microbiol Lett* **233(1),** 1-6.

Chambers, T. J., Hahn, C. S., Galler, R., and Rice, C. M. (1990). Flavivirus genome organization, expression, and replication. *Annu Rev Microbiol* **44**, 649-688.

Chambers, T. J., Halevy, M., Nestorowicz, A., Rice, C. M., and Lustig, S. (1998). West Nile virus envelope proteins: nucleotide sequence analysis of strains differing in mouse neuroinvasiveness. *J Gen Virol* **79(10),** 2375-2380.

Charlier, N., Leyssen, P., De Clercq, E., and Neyts, J. (2004). Rodent models for the study of therapy against flavivirus infections. *Antiviral Res* **63(2),** 67-77.

Cheeran, M. C., Hu, S., Sheng, W. S., Rashid, A., Peterson, P. K., and Lokensgard, J. R. (2005). Differential responses of human brain cells to West Nile virus infection. *J Neurovirol* **11(6),** 512-524.

Chen, H. C., Lai, S. Y., Sung, J. M., Lee, S. H., Lin, Y. C., Wang, W. K., Chen, Y. C., Kao, C. L., King, C. C., and Wu-Hsieh, B. A. (2004). Lymphocyte activation and hepatic cellular infiltration in immunocompetent mice infected by dengue virus. *J Med Virol* **73(3),** 419-431.

Chiou, S. S., and Chen, W. J. (2007). Phenotypic changes in the Japanese encephalitis virus after one passage in Neuro-2a cells: generation of attenuated strains of the virus. *Vaccine* **26(1),** 15-23.

Chowers, M. Y., Lang, R., Nassar, F., Ben-David, D., Giladi, M., Rubinshtein, E., Itzhaki, A., Mishal, J., Siegman-Igra, Y., Kitzes, R., Pick, N., Landau, Z., Wolf, D., Bin, H., Mendelson, E., Pitlik, S. D., and Weinberger, M. (2001). Clinical characteristics of the West Nile fever outbreak, Israel, 2000. *Emerg Infect Dis* **7(4),** 675-678.

Ciota, A. T., Lovelace, A. O., Jia, Y., Davis, L. J., Young, D. S., and Kramer, L. D. (2008). Characterization of mosquito-adapted West Nile virus. *J Gen Virol* **89(Pt 7),** 1633-1642.

Ciota, A. T., Lovelace, A. O., Jones, S. A., Payne, A., and Kramer, L. D. (2007a). Adaptation of two flaviviruses results in differences in genetic heterogeneity and virus adaptability. *J Gen Virol* **88(Pt 9),** 2398-2406.

Ciota, A. T., Lovelace, A. O., Ngo, K. A., Le, A. N., Maffei, J. G., Franke, M. A., Payne, A. F., Jones, S. A., Kauffman, E. B., and Kramer, L. D. (2007b). Cell-specific adaptation of two flaviviruses following serial passage in mosquito cell culture. *Virology* **357(2),** 165-174.

Ciota, A. T., Ngo, K. A., Lovelace, A. O., Payne, A. F., Zhou, Y., Shi, P. Y., and Kramer, L. D. (2007c). Role of the mutant spectrum in adaptation and replication of West Nile virus. *J Gen Virol* **88(Pt 3),** 865-874.

Clyde, K., Kyle, J. L., and Harris, E. (2006). Recent advances in deciphering viral and host determinants of dengue virus replication and pathogenesis. *J Virol* **80(23),** 11418-11431.

Cordoba, L., Escribano-Romero, E., Garmendia, A., and Saiz, J. C. (2007). Pregnancy increases the risk of mortality in West Nile virus-infected mice. *J Gen Virol* **88(2),** 476-480.

Cruz, L., Cardenas, V. M., Abarca, M., Rodriguez, T., Reyna, R. F., Serpas, M. V., Fontaine, R. E., Beasley, D. W., Da Rosa, A. P., Weaver, S. C., Tesh, R. B.,

Powers, A. M., and Suarez-Rangel, G. (2005). Short report: serological evidence of West Nile virus activity in El Salvador. *Am J Trop Med Hyg* **72(5),** 612-615.

Danscher, G., and Norgaard, J. O. (1983). Light microscopic visualization of colloidal gold on resin-embedded tissue. *J Histochem Cytochem* **31(12),** 1394-1398.

De Madrid, A. T., and Porterfield, J. S. (1974). The flaviviruses (group B arboviruses): a cross-neutralization study. *J Gen Virol* **23(1),** 91-96.

De Waele, M., De Mey, J., Renmans, W., Labeur, C., Jochmans, K., and van Camp, B. (1986). Potential of immunogold-silver staining for the study of leukocyte subpopulations as defined by monoclonal antibodies. *J Histochem Cytochem* **34(10),** 1257-1263.

DeSalvo, D., Roy-Chaudhury, P., Peddi, R., Merchen, T., Konijetti, K., Gupta, M., Boardman, R., Rogers, C., Buell, J., Hanaway, M., Broderick, J., Smith, R., and Woodle, E. S. (2004). West Nile virus encephalitis in organ transplant recipients: another high-risk group for meningoencephalitis and death. *Transplantation* **77(3),** 466-469.

Despres, P., Frenkiel, M. P., Ceccaldi, P. E., Duarte Dos Santos, C., and Deubel, V. (1998). Apoptosis in the mouse central nervous system in response to infection with mouse-neurovirulent dengue viruses. *J Virol* **72(1),** 823-829.

Ding, X., Wu, X., Duan, T., Siirin, M., Guzman, H., Yang, Z., Tesh, R. B., and Xiao, S. Y. (2005). Nucleotide and amino acid changes in West Nile virus strains exhibiting renal tropism in hamsters. *Am J Trop Med Hyg* **73(4),** 803-807.

Diniz, J. A., Da Rosa, A. P., Guzman, H., Xu, F., Xiao, S. Y., Popov, V. L., Vasconcelos, P. F., and Tesh, R. B. (2006). West Nile virus infection of primary mouse neuronal and neuroglial cells: the role of astrocytes in chronic infection. *Am J Trop Med Hyg* **75(4),** 691-696.

Dokland, T., Walsh, M., Mackenzie, J. M., Khromykh, A. A., Ee, K. H. & Wang, S. (2004). West Nile virus core protein; tetramer structure and ribbon formation. *Structure* **12**, 1157-1163.

Drake, J. W., and Holland, J. J. (1999). Mutation rates among RNA viruses. *Proc Natl Acad Sci U S A* **96(24),** 13910-13913.

Dunster, L. M., Gibson, C. A., Stephenson, J. R., Minor, P. D., and Barrett, A. D. (1990). Attenuation of virulence of flaviviruses following passage in HeLa cells. *J Gen Virol* **71(3),** 601-607.

Eckels, K. H., Dubois, D. R., Summers, P. L., Schlesinger, J. J., Shelly, M., Cohen, S., Zhang, Y. M., Lai, C. J., Kurane, I., Rothman, A., Hasty, S., and Howard, B. (1994). Immunization of monkeys with baculovirus-dengue type-4 recombinants containing envelope and nonstructural proteins: evidence of priming and partial protection. *Am J Trop Med Hyg* **50(4),** 472-478.

Elshuber, S., and Mandl, C. W. (2005). Resuscitating mutations in a furin cleavage-deficient mutant of the flavivirus tick-borne encephalitis virus. *J Virol* **79(18),** 11813-11823.

Estrada-Franco, J. G., Navarro-Lopez, R., Beasley, D. W., Coffey, L., Carrara, A. S., Travassos da Rosa, A., Clements, T., Wang, E., Ludwig, G. V., Cortes, A. C., Ramirez, P. P., Tesh, R. B., Barrett, A. D., and Weaver, S. C. (2003). West Nile virus in Mexico: evidence of widespread circulation since July 2002. *Emerg Infect Dis* **9(12),** 1604-1607.

Falgout, B., and Markoff, L. (1995). Evidence that flavivirus NS1-NS2A cleavage is mediated by a membrane-bound host protease in the endoplasmic reticulum. *J Virol* **69**, 7232-7243.

Farrar, J., and Newton, C. (2000). Neurological aspects of tropical disease. *J Neurol Neurosurg Psychiatry* **68(2),** 135-136.

Faulk, W. P., and Taylor, G. M. (1971). An immunocolloid method for the electron microscope. *Immunochemistry* **8(11),** 1081-1103.

Ferlenghi, I., Clarke, M., Ruttan, T., Allison, S. L., Schalich, J., Heinz, F. X., Harrison, S. C., Rey, F. A., and Fuller, S. D. (2001). Molecular organization of a recombinant subviral particle from tick-borne encephalitis virus. *Mol Cell* **7(3),** 593-602.

Filler, T. J., and Peuker, E. T. (2000). Reflection contrast microscopy (RCM): a forgotten technique? *J Pathol* **190(5),** 635-638.

Fratkin, J. D., Leis, A. A., Stokic, D. S., Slavinski, S. A., and Geiss, R. W. (2004). Spinal cord neuropathology in human West Nile virus infection. *Arch Pathol Lab Med* **128(5),** 533-537.

Gao, K., Morris, R. E., and Wei, C. (1995). Epipolarization microscopic immunogold assay: a combination of immunogold silver staining, enzyme-linked-immunosorbent assay and epipolarization microscopy. *Biotech Histochem* **70(4),** 211-216.

Garcia-Tapia, D., Hassett, D. E., Mitchell, W. J., Jr., Johnson, G. C., and Kleiboeker, S. B. (2007). West Nile virus encephalitis: sequential

histopathological and immunological events in a murine model of infection. *J Neurovirol* **13(2),** 130-138.

Garcia-Tapia, D., Loiacono, C. M., and Kleiboeker, S. B. (2006). Replication of West Nile virus in equine peripheral blood mononuclear cells. *Vet Immunol Immunopathol* **110(3-4),** 229-244.

George, S., Gourie-Devi, M., Rao, J. A., Prasad, S. R., and Pavri, K. M. (1984). Isolation of West Nile virus from the brains of children who had died of encephalitis. *Bull World Health Organ* **62(6),** 879-882.

Glass, W. G., Lim, J. K., Cholera, R., Pletnev, A. G., Gao, J. L., and Murphy, P. M. (2005). Chemokine receptor CCR5 promotes leukocyte trafficking to the brain and survival in West Nile virus infection. *J Exp Med* **202(8),** 1087-1098.

Golde, W. T., Gollobin, P., and Rodriguez, L. L. (2005). A rapid, simple, and humane method for submandibular bleeding of mice using a lancet. *Lab Anim (NY)* **34(9),** 39-43.

Goto, A., Hayasaka, D., Yoshii, K., Mizutani, T., Kariwa, H., and Takashima, I. (2003). A BHK-21 cell culture-adapted tick-borne encephalitis virus mutant is attenuated for neuroinvasiveness. *Vaccine* **21(25-26),** 4043-4051.

Gubler, D. J., and Kuno, G. (1997). "Dengue and dengue hemorrhagic fever." Eds. CAB International, Wallingford, Oxon, UK ; New York, pp. 115-132.

Hamilton, P. K., and Taylor, R. M. (1954). Report of clinical case of West Nile virus infection probably acquired in the laboratory. *Am J Trop Med Hyg* **3(1),** 51-53.

Hayes, E. B., and Gubler, D. J. (2006). West Nile virus: epidemiology and clinical features of an emerging epidemic in the United States. *Annu Rev Med* **57,** 181-194.

Holgate, C. S., Jackson, P., Cowen, P. N., and Bird, C. C. (1983). Immunogold-silver staining: new method of immunostaining with enhanced sensitivity. *J Histochem Cytochem* **31(7),** 938-944.

Hotta, H., Murakami, I., Miyasaki, K., Takeda, Y., Shirane, H., and Hotta, S. (1981). Inoculation of dengue virus into nude mice. *J Gen Virol* **52(1),** 71-76.

Huang, K. J., Li, S. Y., Chen, S. C., Liu, H. S., Lin, Y. S., Yeh, T. M., Liu, C. C., and Lei, H. Y. (2000). Manifestation of thrombocytopenia in dengue-2-virus-infected mice. *J Gen Virol* **81(9),** 2177-2182.

Hunsperger, E. A., and Roehrig, J. T. (2006). Temporal analyses of the neuropathogenesis of a West Nile virus infection in mice. *J Neurovirol* **12(2),** 129-139.

Iglesias, M. C., Frenkiel, M. P., Mollier, K., Souque, P., Despres, P., and Charneau, P. (2006). A single immunization with a minute dose of a lentiviral vector-based vaccine is highly effective at eliciting protective humoral immunity against West Nile virus. *J Gene Med* **8(3),** 265-274.

International Committee on Taxonomy of Viruses., Van Regenmortel, M. H. V., and International Union of Microbiological Societies. Virology Division. (2000). "Virus taxonomy : classification and nomenclature of viruses : seventh report of the International Committee on Taxonomy of Viruses." Academic Press, San Diego, pp. 859-866.

Jain, N., Fisk, D., Sotir, M., and Kehl, K. S. (2007). West Nile encephalitis, status epilepticus and West Nile pneumonia in a renal transplant patient. *Transpl Int* **20(9),** 800-803.

Jamieson, D. J., Ellis, J. E., Jernigan, D. B., and Treadwell, T. A. (2006). Emerging infectious disease outbreaks: old lessons and new challenges for obstetrician-gynecologists. *Am J Obstet Gynecol* **194(6),** 1546-1555.

Jerzak, G. V., Bernard, K. A., Kramer, L. D., and Ebel, G. D. (2005). Genetic variation in West Nile virus from naturally infected mosquitoes and birds suggests quasispecies structure and strong purifying selection. *J Gen Virol* **86(Pt 8),** 2175-2183.

Jerzak, G. V., Bernard, K. A., Kramer, L. D., Shi, P. Y., and Ebel, G. D. (2007). The West Nile virus mutant spectrum is host-dependant and a determinant of mortality in mice. *Virology* **360(2),** 469-476.

Jerzak, G. V., Brown, I., Shi, P. Y., Kramer, L. D., and Ebel, G. D. (2008). Genetic diversity and purifying selection in West Nile virus populations are maintained during host switching. *Virology* **374(2),** 256-260.

Jessie, K., Fong, M. Y., Devi, S., Lam, S. K., and Wong, K. T. (2004). Localization of dengue virus in naturally infected human tissues, by immunohistochemistry and in situ hybridization. *J Infect Dis* **189(8),** 1411-1418.

Jia, X. Y., Briese, T., Jordan, I., Rambaut, A., Chi, H. C., Mackenzie, J. S., Hall, R. A., Scherret, J., and Lipkin, W. I. (1999). Genetic analysis of West Nile New York 1999 encephalitis virus. *Lancet* **354(9194),** 1971-1972.

Jia, Y., Moudy, R. M., Dupuis, A. P., 2nd, Ngo, K. A., Maffei, J. G., Jerzak, G. V., Franke, M. A., Kauffman, E. B., and Kramer, L. D. (2007). Characterization

of a small plaque variant of West Nile virus isolated in New York in 2000. *Virology* **367(2),** 339-347.

Johnson, A. J., and Roehrig, J. T. (1999). New mouse model for dengue virus vaccine testing. *J Virol* **73(1),** 783-786.

Jordan, I., Briese, T., Fischer, N., Lau, J. Y., and Lipkin, W. I. (2000). Ribavirin inhibits West Nile virus replication and cytopathic effect in neural cells. *J Infect Dis* **182(4),** 1214-1217.

Julander, J. G., Winger, Q. A., Olsen, A. L., Day, C. W., Sidwell, R. W., and Morrey, J. D. (2005). Treatment of West Nile virus-infected mice with reactive immunoglobulin reduces fetal titers and increases dam survival. *Antiviral Res* **65(2),** 79-85.

Kanai, R., Kar, K., Anthony, K., Gould, L. H., Ledizet, M., Fikrig, E., Marasco, W. A., Koski, R. A. and Modis, Y. (2006). Crystal structure of West Nile virus envelope glycoprotein reveals viral surface epitopes. *J Virol* **80**, 11000-11008.

Khromykh, A. A., Varnavski, A. N., Sedlak, P. L., and Westaway, E. G. (2001). Coupling between replication and packaging of flavivirus RNA: evidence derived from the use of DNA-based full-length cDNA clones of Kunjin virus. *J Virol* **75(10),** 4633-4640.

Killen, H., and O'Sullivan, M. A. (1993). Detection of dengue virus by *in situ* hybridization. *J Virol Methods* **41(2),** 135-146.

Kofler, R. M., Heinz, F. X., and Mandl, C. W. (2002). Capsid protein C of tick-borne encephalitis virus tolerates large internal deletions and is a favorable target for attenuation of virulence. *J Virol* **76**, 3534-3543.

Komar, N., Langevin, S., Hinten, S., Nemeth, N., Edwards, E., Hettler, D., Davis, B., Bowen, R., and Bunning, M. (2003). Experimental infection of North American birds with the New York 1999 strain of West Nile virus. *Emerg Infect Dis* **9(3),** 311-322.

Kramer, L. D., Hardy, J. L., Presser, S. B., and Houk, E. J. (1981). Dissemination barriers for western equine encephalomyelitis virus in *Culex tarsalis* infected after ingestion of low viral doses. *Am J Trop Med Hyg* **30(1),** 190-197.

Kramer, L. D., Li, J., and Shi, P. Y. (2007). West Nile virus. *Lancet Neurol* **6(2),** 171-181.

Kummerer, B. M., and Rice, C. M. (2002). Mutations in the yellow fever virus nonstructural protein NS2A selectively block production of infectious particles. *J Virol* **76(10),** 4773-4784.

Kurane, I., Kontny, U., Janus, J., and Ennis, F. A. (1990). Dengue-2 virus infection of human mononuclear cell lines and establishment of persistent infections. *Arch Virol* **110(1-2),** 91-101.

Kyle, J. L., Beatty, P. R., and Harris, E. (2007). Dengue virus infects macrophages and dendritic cells in a mouse model of infection. *J Infect Dis* **195(12),** 1808-1817.

Lanciotti, R. S., Roehrig, J. T., Deubel, V., Smith, J., Parker, M., Steele, K., Crise, B., Volpe, K. E., Crabtree, M. B., Scherret, J. H., Hall, R. A., MacKenzie, J. S., Cropp, C. B., Panigrahy, B., Ostlund, E., Schmitt, B., Malkinson, M., Banet, C., Weissman, J., Komar, N., Savage, H. M., Stone, W., McNamara, T., and Gubler, D. J. (1999). Origin of the West Nile virus responsible for an outbreak of encephalitis in the northeastern United States. *Science* **286(5448),** 2333-2337.

Lee, E., Wright, P. J., Davidson, A., and Lobigs, M. (2006). Virulence attenuation of Dengue virus due to augmented glycosaminoglycan-binding affinity and restriction in extraneural dissemination. *J Gen Virol* **87(Pt 10),** 2791-2801.

Lei, H. Y., Yeh, T. M., Liu, H. S., Lin, Y. S., Chen, S. H., and Liu, C. C. (2001). Immunopathogenesis of dengue virus infection. *J Biomed Sci* **8(5),** 377-388.

Li, J., Bhuvanakantham, R., Howe, J. & Ng, M. L. (2005). Identifying the region influencing the cis-mode of maturation of West Nile (Sarafend) virus using chimeric infectious clones. *Biochem Biophys Res Commun* **334**, 714-720.

Licon Luna, R. M., Lee, E., Mullbacher, A., Blanden, R. V., Langman, R., and Lobigs, M. (2002). Lack of both Fas ligand and perforin protects from flavivirus-mediated encephalitis in mice. *J Virol* **76(7),** 3202-3211.

Lin, Y. L., Liao, C. L., Chen, L. K., Yeh, C. T., Liu, C. I., Ma, S. H., Huang, Y. Y., Huang, Y. L., Kao, C. L., and King, C. C. (1998). Study of Dengue virus infection in SCID mice engrafted with human K562 cells. *J Virol* **72(12),** 9729-9737.

Lindenbach, B. D., and Rice, C. M. (1999). Genetic interaction of flavivirus nonstructural proteins NS1 and NS4A as a determinant of replicase function. *J Virol* **73(6),** 4611-4621.

Linke, S., Ellerbrok, H., Niedrig, M., Nitsche, A., and Pauli, G. (2007). Detection of West Nile virus lineages 1 and 2 by real-time PCR. *J Virol Methods* **146(1-2),** 355-358.

Liu, W. J., Wang, X. J., Clark, D. C., Lobigs, M., Hall, R. A., and Khromykh, A. A. (2006). A single amino acid substitution in the West Nile virus nonstructural

protein NS2A disables its ability to inhibit alpha/beta interferon induction and attenuates virus virulence in mice. *J Virol* **80(5),** 2396-2404.

Loeb, M., Hanna, S., Nicolle, L., Eyles, J., Elliott, S., Rathbone, M., Drebot, M., Neupane, B., Fearon, M., and Mahony, J. (2008). Prognosis after West Nile virus infection. *Ann Intern Med* **149**, 232-241.

Lorenz, I. C., Allison, S. L., Heinz, F. X., and Helenius, A. (2002). Folding and dimerization of tick-borne encephalitis virus envelope proteins prM and E in the endoplasmic reticulum. *J Virol* **76(11),** 5480-5491.

Lucia, H. L., and Kangwanpong, D. (1994). Identification of dengue virus-infected cells in paraffin-embedded tissue using *in situ* polymerase chain reaction and DNA hybridization. *J Virol Methods* **48(1),** 1-8.

Lum, L. C., Lam, S. K., Choy, Y. S., George, R., and Harun, F. (1996). Dengue encephalitis: a true entity? *Am J Trop Med Hyg* **54(3),** 256-259.

Lvov, D. K., Butenko, A. M., Gromashevsky, V. L., Kovtunov, A. I., Prilipov, A. G., Kinney, R., Aristova, V. A., Dzharkenov, A. F., Samokhvalov, E. I., Savage, H. M., Shchelkanov, M. Y., Galkina, I. V., Deryabin, P. G., Gubler, D. J., Kulikova, L. N., Alkhovsky, S. K., Moskvina, T. M., Zlobina, L. V., Sadykova, G. K., Shatalov, A. G., Lvov, D. N., Usachev, V. E., and Voronina, A. G. (2004). West Nile virus and other zoonotic viruses in Russia: examples of emerging-reemerging situations. *Arch Virol. Suppl.* **18,** 85-96.

Ma, L., Jones, C. T., Groesch, T. D., Kuhn, R. J., and Post, C. B. (2004). Solution structure of dengue virus capsid protein reveals another fold. *Proc Natl Acad Sci U S A* **101(10),** 3414-3419.

Macedo de Oliveira, A., Beecham, B. D., Montgomery, S. P., Lanciotti, R. S., Linnen, J. M., Giachetti, C., Pietrelli, L. A., Stramer, S. L., and Safranek, T. J. (2004). West Nile virus blood transfusion-related infection despite nucleic acid testing. *Transfusion* **44(12),** 1695-1699.

Mackenzie, J. S., Gubler, D. J., and Petersen, L. R. (2004). Emerging flaviviruses: the spread and resurgence of Japanese encephalitis, West Nile and dengue viruses. *Nat Med* **10(12),** S98-S109.

Mandl, C. W., Guirakhoo, F., Holzmann, H., Heinz, F. X., and Kunz, C. (1989). Antigenic structure of the flavivirus envelope protein E at the molecular level, using tick-borne encephalitis virus as a model. *J Virol* **63(2),** 564-571.

Marciniak, C., Sorosky, S., and Hynes, C. (2004). Acute flaccid paralysis associated with West Nile virus: motor and functional improvement in 4 patients. *Arch Phys Med Rehabil* **85(12),** 1933-1938.

Marianneau, P., Megret, F., Olivier, R., Morens, D. M., and Deubel, V. (1996). Dengue 1 virus binding to human hepatoma HepG2 and simian Vero cell surfaces differs. *J Gen Virol* **77(10),** 2547-2554.

Marianneau, P., Steffan, A. M., Royer, C., Drouet, M. T., Jaeck, D., Kirn, A., and Deubel, V. (1999). Infection of primary cultures of human Kupffer cells by Dengue virus: no viral progeny synthesis, but cytokine production is evident. *J Virol* **73(6),** 5201-5206.

Martinez, M. A., Carrillo, C., Gonzalez-Candelas, F., Moya, A., Domingo, E., and Sobrino, F. (1991). Fitness alteration of foot-and-mouth disease virus mutants: measurement of adaptability of viral quasispecies. *J Virol* **65(7),** 3954-3957.

Mashimo, T., Lucas, M., Simon-Chazottes, D., Frenkiel, M. P., Montagutelli, X., Ceccaldi, P. E., Deubel, V., Guenet, J. L., and Despres, P. (2002). A nonsense mutation in the gene encoding 2'-5'-oligoadenylate synthetase/L1 isoform is associated with West Nile virus susceptibility in laboratory mice. *Proc Natl Acad Sci U S A* **99(17),** 11311-11316.

Mattar, S., Edwards, E., Laguado, J., Gonzalez, M., Alvarez, J., and Komar, N. (2005). West Nile virus antibodies in Colombian horses. *Emerg Infect Dis* **11(9),** 1497-1498.

Maximova, O. A., Ward, J. M., Asher, D. M., St Claire, M., Finneyfrock, B. W., Speicher, J. M., Murphy, B. R., and Pletnev, A. G. (2008). Comparative neuropathogenesis and neurovirulence of attenuated flaviviruses in nonhuman primates. *J Virol* **82(11),** 5255-5268.

Miller, B. R., and Mitchell, C. J. (1986). Passage of yellow fever virus: its effect on infection and transmission rates in *Aedes aegypti*. *Am J Trop Med Hyg* **35(6),** 1302-1309.

Monath, T. P., Cropp, C. B., and Harrison, A. K. (1983). Mode of entry of a neurotropic arbovirus into the central nervous system. Reinvestigation of an old controversy. *Lab Invest* **48(4),** 399-410.

Montgomery, S. P., Brown, J. A., Kuehnert, M., Smith, T. L., Crall, N., Lanciotti, R. S., Macedo de Oliveira, A., Boo, T., and Marfin, A. A. (2006). Transfusion-associated transmission of West Nile virus, United States 2003 through 2005. *Transfusion* **46(12),** 2038-2046.

Mostashari, F., Bunning, M. L., Kitsutani, P. T., Singer, D. A., Nash, D., Cooper, M. J., Katz, N., Liljebjelke, K. A., Biggerstaff, B. J., Fine, A. D., Layton, M. C., Mullin, S. M., Johnson, A. J., Martin, D. A., Hayes, E. B., and Campbell, G.

L. (2001). Epidemic West Nile encephalitis, New York, 1999: results of a household-based seroepidemiological survey. *Lancet* **358(9278),** 261-264.

Moya, A., Holmes, E. C., and Gonzalez-Candelas, F. (2004). The population genetics and evolutionary epidemiology of RNA viruses. *Nat Rev Microbiol* **2(4),** 279-288.

Mukhopadhyay, S., Kim, B. S., Chipman, P. R., Rossmann, M. G., and Kuhn, R. J. (2003). Structure of West Nile virus. *Science* **302(5643),** 248.

Mukhopadhyay, S., Kuhn, R. J., and Rossmann, M. G. (2005). A structural perspective of the flavivirus life cycle. *Nat Rev Microbiol* **3(1),** 13-22.

Murray, C. L., Jones, C. T., and Rice, C. M. (2008). Architects of assembly: roles of Flaviviridae non-structural proteins in virion morphogenesis. *Nat Rev Microbiol* **6(9),** 699-708.

Murtagh, B., Wadia, Y., Messner, G., Allison, P., Harati, Y., and Delgado, R. (2005). West Nile virus infection after cardiac transplantation. *J Heart Lung Transplant* **24(6),** 774-776.

Nash, D., Mostashari, F., Fine, A., Miller, J., O'Leary, D., Murray, K., Huang, A., Rosenberg, A., Greenberg, A., Sherman, M., Wong, S., and Layton, M. (2001). The outbreak of West Nile virus infection in the New York City area in 1999. *N Engl J Med* **344(24),** 1807-1814.

Neelissen, J. A., Schrijvers, A. H., Junginger, H. E., and Bodde, H. E. (1999). Reflection contrast microscopy for high resolution detection of (3)H-estradiol in ultrathin sections of human stratum corneum. *Microsc Res Tech* **47(4),** 286-290.

Novella, I. S., Ball, L. A., and Wertz, G. W. (2004). Fitness analyses of vesicular stomatitis strains with rearranged genomes reveal replicative disadvantages. *J Virol* **78(18),** 9837-9841.

O'Leary, D. R., Kuhn, S., Kniss, K. L., Hinckley, A. F., Rasmussen, S. A., Pape, W. J., Kightlinger, L. K., Beecham, B. D., Miller, T. K., Neitzel, D. F., Michaels, S. R., Campbell, G. L., Lanciotti, R. S., and Hayes, E. B. (2006). Birth outcomes following West Nile Virus infection of pregnant women in the United States: 2003-2004. *Pediatrics* **117(3),** e537-e545.

O'Leary, D. R., Marfin, A. A., Montgomery, S. P., Kipp, A. M., Lehman, J. A., Biggerstaff, B. J., Elko, V. L., Collins, P. D., Jones, J. E., and Campbell, G. L. (2004). The epidemic of West Nile virus in the United States, 2002. *Vector Borne Zoonotic Dis* **4(1),** 61-70.

Pealer, L. N., Marfin, A. A., Petersen, L. R., Lanciotti, R. S., Page, P. L., Stramer, S. L., Stobierski, M. G., Signs, K., Newman, B., Kapoor, H., Goodman, J. L.,

and Chamberland, M. E. (2003). Transmission of West Nile virus through blood transfusion in the United States in 2002. *N Engl J Med* **349(13),** 1236-1245.

Petersen, L. R., and Marfin, A. A. (2002). West Nile virus: a primer for the clinician. *Ann Intern Med* **137(3),** 173-179.

Petersen, L. R., and Roehrig, J. T. (2001). West Nile virus: a reemerging global pathogen. *Emerg Infect Dis* **7(4),** 611-614.

Peyrefitte, C. N., Pastorino, B., Bessaud, M., Tolou, H. J., and Couissinier-Paris, P. (2003). Evidence for *in vitro* falsely-primed cDNAs that prevent specific detection of virus negative strand RNAs in dengue-infected cells: improvement by tagged RT-PCR. *J Virol Methods* **113(1),** 19-28.

Platonov, A. E., Shipulin, G. A., Shipulina, O. Y., Tyutyunnik, E. N., Frolochkina, T. I., Lanciotti, R. S., Yazyshina, S., Platonova, O. V., Obukhov, I. L., Zhukov, A. N., Vengerov, Y. Y., and Pokrovskii, V. I. (2001). Outbreak of West Nile virus infection, Volgograd Region, Russia, 1999. *Emerg Infect Dis* **7(1),** 128-132.

Pletnev, A. G., Swayne, D. E., Speicher, J., Rumyantsev, A. A., and Murphy, B. R. (2006). Chimeric West Nile/dengue virus vaccine candidate: preclinical evaluation in mice, geese and monkeys for safety and immunogenicity. *Vaccine* **24(40-41),** 6392-6404.

Pogodina, V. V., Frolova, M. P., Malenko, G. V., Fokina, G. I., Koreshkova, G. V., Kiseleva, L. L., Bochkova, N. G., and Ralph, N. M. (1983). Study on West Nile virus persistence in monkeys. *Arch Virol* **75(1-2),** 71-86.

Prins, F. A., Velde, I. C., and de Heer, E. (2006). Reflection contrast microscopy: The bridge between light and electron microscopy. *Methods Mol Biol* **319,** 363-401.

Quirin, R., Salas, M., Zientara, S., Zeller, H., Labie, J., Murri, S., Lefrancois, T., Petitclerc, M., and Martinez, D. (2004). West Nile virus, Guadeloupe. *Emerg Infect Dis* **10(4),** 706-708.

Raut, C. G., Deolankar, R. P., Kolhapure, R. M., and Goverdhan, M. K. (1996). Susceptibility of laboratory-bred rodents to the experimental infection with dengue virus type 2. *Acta Virol* **40(3),** 143-146.

Reed, K. E., Gorbalenya, A. E., and Rice, C. M. (1998). The NS5A/NS5 proteins of viruses from three genera of the family flaviviridae are phosphorylated by associated serine/threonine kinases. *J Virol* **72(7),** 6199-6206.

Rey, F. A., Heinz, F. X., Mandl, C., Kunz, C., and Harrison, S. C. (1995). The envelope glycoprotein from tick-borne encephalitis virus at 2 A resolution. *Nature* **375(6529),** 291-298.

Roberts, A., Deming, D., Paddock, C. D., Cheng, A., Yount, B., Vogel, L., Herman, B. D., Sheahan, T., Heise, M., Genrich, G. L., Zaki, S. R., Baric, R., and Subbarao, K. (2007). A mouse-adapted SARS-coronavirus causes disease and mortality in BALB/c mice. *PLoS Pathog* **3(1),** 23-37.

Rosen, L., Khin, M. M., and U, T. (1989). Recovery of virus from the liver of children with fatal dengue: reflections on the pathogenesis of the disease and its possible analogy with that of yellow fever. *Res Virol* **140(4),** 351-360.

Rossi, S. L., Fayzulin, R., Dewsbury, N., Bourne, N., and Mason, P. W. (2007). Mutations in West Nile virus nonstructural proteins that facilitate replicon persistence *in vitro* attenuate virus replication *in vitro* and *in vivo*. *Virology* **364(1),** 184-195.

Russell, R. C., and Dwyer, D. E. (2000). Arboviruses associated with human disease in Australia. *Microbes Infect* **2(14),** 1693-1704.

Sabin, A. B. (1952). Research on dengue during World War II. *Am J Trop Med Hyg* **1**, 30-50.

Samuel, M. A., and Diamond, M. S. (2005). Alpha/beta interferon protects against lethal West Nile virus infection by restricting cellular tropism and enhancing neuronal survival. *J Virol* **79(21),** 13350-13361.

Scherbik, S. V., Paranjape, J. M., Stockman, B. M., Silverman, R. H., and Brinton, M. A. (2006). RNase L plays a role in the antiviral response to West Nile virus. *J Virol* **80(6),** 2987-2999.

Scherret, J. H., Mackenzie, J. S., Hall, R. A., Deubel, V., and Gould, E. A. (2002). Phylogeny and molecular epidemiology of West Nile and Kunjin viruses. *Curr Top Microbiol Immunol* **267,** 373-390.

Scherret, J. H., Poidinger, M., Mackenzie, J. S., Broom, A. K., Deubel, V., Lipkin, W. I., Briese, T., Gould, E. A., and Hall, R. A. (2001). The relationships between West Nile and Kunjin viruses. *Emerg Infect Dis* **7(4),** 697-705.

Schlesinger, R. W. (1980). "The Togaviruses : biology structure, replication." Academic Press, New York, pp. 107-174.

Sejvar, J. J., Bode, A. V., Marfin, A. A., Campbell, G. L., Ewing, D., Mazowiecki, M., Pavot, P. V., Schmitt, J., Pape, J., Biggerstaff, B. J., and Petersen, L. R. (2005). West Nile virus-associated flaccid paralysis. *Emerg Infect Dis* **11(7),** 1021-1027.

Sejvar, J. J., Haddad, M. B., Tierney, B. C., Campbell, G. L., Marfin, A. A., Van Gerpen, J. A., Fleischauer, A., Leis, A. A., Stokic, D. S., and Petersen, L. R. (2003). Neurologic manifestations and outcome of West Nile virus infection. *JAMA* **290(4),** 511-515.

Sen, G. C. (2001). Viruses and interferons. *Annu Rev Microbiol* **55,** 255-281.

Shirato, K., Miyoshi, H., Goto, A., Ako, Y., Ueki, T., Kariwa, H., and Takashima, I. (2004). Viral envelope protein glycosylation is a molecular determinant of the neuroinvasiveness of the New York strain of West Nile virus. *J Gen Virol* **85(Pt 12),** 3637-3645.

Shresta, S., Kyle, J. L., Robert Beatty, P., and Harris, E. (2004a). Early activation of natural killer and B cells in response to primary dengue virus infection in A/J mice. *Virology* **319(2),** 262-273.

Shresta, S., Kyle, J. L., Snider, H. M., Basavapatna, M., Beatty, P. R., and Harris, E. (2004b). Interferon-dependent immunity is essential for resistance to primary dengue virus infection in mice, whereas T- and B-cell-dependent immunity are less critical. *J Virol* **78(6),** 2701-2710.

Shrestha, B., and Diamond, M. S. (2004). Role of CD8+ T cells in control of West Nile virus infection. *J Virol* **78(15),** 8312-8321.

Shrestha, B., Gottlieb, D., and Diamond, M. S. (2003). Infection and injury of neurons by West Nile encephalitis virus. *J Virol* **77(24),** 13203-13213.

Shrestha, B., Samuel, M. A., and Diamond, M. S. (2006a). CD8+ T cells require perforin to clear West Nile virus from infected neurons. *J Virol* **80(1),** 119-129.

Shrestha, B., Wang, T., Samuel, M. A., Whitby, K., Craft, J., Fikrig, E., and Diamond, M. S. (2006b). Gamma interferon plays a crucial early antiviral role in protection against West Nile virus infection. *J Virol* **80(11),** 5338-5348.

Sitati, E. M., and Diamond, M. S. (2006). CD4+ T-cell responses are required for clearance of West Nile virus from the central nervous system. *J Virol* **80(24),** 12060-12069.

Skupski, D. W., Eglinton, G. S., Fine, A. D., Hayes, E. B., and O'Leary, D. R. (2006). West Nile virus during pregnancy: a case study of early second trimester maternal infection. *Fetal Diagn Ther* **21(3),** 293-295.

Smith, G. W., and Wright, P. J. (1985). Synthesis of proteins and glycoproteins in dengue type 2 virus-infected Vero and *Aedes albopictus* cells. *J Gen Virol* **66(Pt 3),** 559-571.

Smithburn, K. C. (1942). Differentiation of the West Nile virus from the viruses of St.Louis and Japanese B encephalitis. *J Immunol* **44(1),** 25–31.

Smithburn, K. C., Hughes, T. P., and Burke, A. W. (1940). A neurotropic virus isolated from the blood of a native of Uganda. *Am. J. Trop. Med. Hyg.* **20(4),** 471-472.

Steele, K. E., Linn, M. J., Schoepp, R. J., Komar, N., Geisbert, T. W., Manduca, R. M., Calle, P. P., Raphael, B. L., Clippinger, T. L., Larsen, T., Smith, J., Lanciotti, R. S., Panella, N. A., and McNamara, T. S. (2000). Pathology of fatal West Nile virus infections in native and exotic birds during the 1999 outbreak in New York City, New York. *Vet Pathol* **37(3),** 208-224.

Swayne, D. E., Beck, J. R., Smith, C. S., Shieh, W. J., and Zaki, S. R. (2001). Fatal encephalitis and myocarditis in young domestic geese (*Anser anser domesticus*) caused by West Nile virus. *Emerg Infect Dis* **7(4),** 751-753.

Tsai, T. F., Popovici, F., Cernescu, C., Campbell, G. L., and Nedelcu, N. I. (1998). West Nile encephalitis epidemic in southeastern Romania. *Lancet* **352(9130),** 767-771.

Tscherne, D. M., Jones, C. T., Evans, M. J., Lindenbach, B. D., McKeating, J. A., and Rice, C. M. (2006). Time- and temperature-dependent activation of hepatitis C virus for low-pH-triggered entry. *J Virol* **80(4),** 1734-1741.

Turell, M. J., Dohm, D. J., Sardelis, M. R., Oguinn, M. L., Andreadis, T. G., and Blow, J. A. (2005). An update on the potential of north American mosquitoes (Diptera: *Culicidae*) to transmit West Nile Virus. *J Med Entomol* **42(1),** 57-62.

Umrigar, M. D., and Pavri, K. M. (1977). Comparative serological studies on Indian strains of West Nile virus isolated from different sources. *Indian J Med Res* **65(5),** 603-612.

van den Broek, M. F., Muller, U., Huang, S., Zinkernagel, R. M., and Aguet, M. (1995). Immune defence in mice lacking type I and/or type II interferon receptors. *Immunol Rev* **148(1),** 5-18.

van Marle, G., Antony, J., Ostermann, H., Dunham, C., Hunt, T., Halliday, W., Maingat, F., Urbanowski, M. D., Hobman, T., Peeling, J., and Power, C. (2007). West Nile virus-induced neuroinflammation: glial infection and capsid protein-mediated neurovirulence. *J Virol* **81(20),** 10933-10949.

Wadei, H., Alangaden, G. J., Sillix, D. H., El-Amm, J. M., Gruber, S. A., West, M. S., Granger, D. K., Garnick, J., Chandrasekar, P., Migdal, S. D., and Haririan, A. (2004). West Nile virus encephalitis: an emerging disease in renal transplant recipients. *Clin Transplant* **18(6),** 753-758.

Walter Reed Biosystematics Unit (2008). Systematic Catalog of the Culicidae. Available from: www.mosquitocatalog.org. Accessed 31 January 2008.

Wang, T., Town, T., Alexopoulou, L., Anderson, J. F., Fikrig, E., and Flavell, R. A. (2004a). Toll-like receptor 3 mediates West Nile virus entry into the brain causing lethal encephalitis. *Nat Med* **10(12),** 1366-1373.

Wang, Y., Lobigs, M., Lee, E., and Mullbacher, A. (2003). CD8+ T cells mediate recovery and immunopathology in West Nile virus encephalitis. *J Virol* **77(24),** 13323-13334.

Wang, Y., Lobigs, M., Lee, E., and Mullbacher, A. (2004b). Exocytosis and *Fas* mediated cytolytic mechanisms exert protection from West Nile virus induced encephalitis in mice. *Immunol Cell Biol* **82(2),** 170-173.

Wang, Y., Lobigs, M., Lee, E., Koskinen, A., and Mullbacher, A. (2006). CD8(+) T cell-mediated immune responses in West Nile virus (Sarafend strain) encephalitis are independent of gamma interferon. *J Gen Virol* **87(12),** 3599-3609.

Watson, J. T., Pertel, P. E., Jones, R. C., Siston, A. M., Paul, W. S., Austin, C. C., and Gerber, S. I. (2004). Clinical characteristics and functional outcomes of West Nile Fever. *Ann Intern Med* **141(5),** 360-365.

Wicker, J. A., Whiteman, M. C., Beasley, D. W., Davis, C. T., Zhang, S., Schneider, B. S., Higgs, S., Kinney, R. M., and Barrett, A. D. (2006). A single amino acid substitution in the central portion of the West Nile virus NS4B protein confers a highly attenuated phenotype in mice. *Virology* **349(2),** 245-253.

Wu, S. J., Hayes, C. G., Dubois, D. R., Windheuser, M. G., Kang, Y. H., Watts, D. M., and Sieckmann, D. G. (1995). Evaluation of the severe combined immunodeficient (SCID) mouse as an animal model for dengue viral infection. *Am J Trop Med Hyg* **52(5),** 468-476.

Xiao, S. Y., Guzman, H., Zhang, H., Travassos da Rosa, A. P., and Tesh, R. B. (2001). West Nile virus infection in the golden hamster (*Mesocricetus auratus*): a model for West Nile encephalitis. *Emerg Infect Dis* **7(4),** 714-721.

Yang, K. D., Lee, C. S., Hwang, K. P., Chu, M. L., and Shaio, M. F. (1995). A model to study cytokine profiles in primary and heterologously secondary Dengue-2 virus infections. *Acta Virol* **39(1),** 19-21.

Yap, T. L., Xu, T., Chen, Y. L., Malet, H., Egloff, M. P., Canard, B., Vasudevan, S. G., and Lescar, J. (2007). Crystal structure of the dengue virus RNA-dependent RNA polymerase catalytic domain at 1.85-angstrom resolution. *J Virol* **81(9),** 4753-4765.

Yauch, L. E., and Shresta, S. (2008). Mouse models of dengue virus infection and disease. *Antiviral Res* **80(2)**, 87-93.

Young, B., and Heath, J. W. (2006). *Wheater's functional histology : a text and colour atlas*. Edinburgh: Churchill Livingstone/Elsevier. pp. 123-137.

Zhang, Y. M., Hayes, E. P., McCarty, T. C., Dubois, D. R., Summers, P. L., Eckels, K. H., Chanock, R. M., and Lai, C. J. (1988). Immunization of mice with dengue structural proteins and nonstructural protein NS1 - expressed by baculovirus recombinant induces resistance to dengue virus encephalitis. *J Virol* **62(8),** 3027-3031.

APPENDICES

APPENDIX 1

Solutions for Cell Culture

The following are formulations for the preparation of media used in the growing of various cell lines used throughout the project. All contents except foetal bovine serum and antibiotic - antimycotic were warmed to 25 ˚C and added to a glass beaker already containing 90 % of the final required volume of water. A magnetic stirrer was used to agitate the contents until all solids were fully dissolved.

a) Growth Medium, M199 for Vero Cells (~pH 7.3).

Items	Amount	Source
Medium M199	1 bottle (commercial)	Sigma-Aldrich, St. Louis, USA
$NaHCO_3$	2.2 g	Merck KGaA, Germany
Foetal bovine serum	100 ml	PAA Laboratories GmbH, Austria
Deionised water	900 ml	Barnstead, New Hampshire, USA

b) Growth Medium, RPMI for BHK Cell (~pH 7.3).

Items	Amount	Source
RPMI-1640	10.63g	M0393, Sigma-Aldrich, St. Louis, USA
$NaHCO_3$	2.0 g	Merck KGaA, Germany
Foetal bovine serum	100 ml	PAA Laboratories GmbH, Austria
Deionised water	900 ml	Barnstead, New Hampshire, USA

c) Growth Medium, L15 for C6/36 Cells (~pH 7.3).

Items	Amount	Source
L15	1 bottle (commercial)	L4386, Sigma-Aldrich, St. Louis, USA
Foetal bovine serum	100 ml	PAA Laboratories GmbH, Austria
Deionised water	900 ml	Barnstead, New Hampshire, USA

d) Growth Medium, Dulbecco's Modified Eagle's Medium (DME), for primary astrocytes and glial cells (~pH 7.3).

Items	Amount	Source
DME Medium	1 bottle (commercial)	D1152, Sigma-Aldrich, St. Louis, USA
Foetal bovine serum	100 ml	PAA Laboratories GmbH, Austria
$NaHCO_3$	3.7 g	Merck KGaA, Germany
Deionised water	890 ml	Barnstead, New Hampshire, USA
Antibiotic - Antimycotic	10 ml	Gibco, Invitrogen Corp., Carlsbad, USA

The pH of the media were then adjusted to approximately pH 7.3 with a handheld pH meter (Beckman Coulter Inc., Fullerton, USA). The solution was then sterilised by filtration in a sterile environment through a 0.2 µm PES membrane bottle top filter unit (Nalge Nunc International, Roskilde, Denmark). From each bottle, a 20 ml aliquot of filtered media was used for screening of microbial contamination by incubation at 37 ˚C for three days before the addition of serum and antibiotic - antimycotic. Foetal bovine serum for the L15 and DME growth media was heat inactivated at 56 ˚C for 30 minutes in a pre – warmed water bath before being added into the sterile media. The serum supplemented media were kept at 4 °C. The cell culture media were warmed up in water bath to 37 ˚C before use.

e) 1 M Hydrochloric Acid

Hydrochloric acid (37 % - Merck KGaA, Germany) was diluted by 1 : 10 in deionised water (Barnstead, New Hampshire, USA) to create a 1 M solution of hydrochloric acid, for use in adjusting the pH of media. Storage was at 25 ˚C.

f) 1 M Sodium Hydroxide

Sodium hydroxide pellets (BDH Ltd., Poole, England) was weighed out to 50 g and mixed into 1 litre of deionised water (Barnstead, New Hampshire, USA) to create a 1 M solution of sodium hydroxide, for use in adjusting the pH of media. Storage was at 25 ˚C.

g) Phosphate Buffered Saline (PBS)

Items	Amount	Source
NaCl	8.0 g	Lab Scan Limited, Ireland
KCl	0.2 g	Merck KGaA, Germany
Na_2HPO_4	1.15 g	Merck KGaA, Germany
KH_2PO_4	0.2 g	Merck KGaA, Germany
Deionised water	900 ml	Barnstead, New Hampshire, USA

The above materials were dissolved in 1 litre of deionised water. The pH was adjusted to 7.2 using either 1 M HCl or 1 M NaOH. The solution was aliquoted and sterilised for 15 minutes at 121° C, 15 lbs. pressure (Hirayama Corp., Saitama, Japan). Storage was at 25 ˚C.

h) Trypsin

Trypsin solution for the dissociation of cells from culture flask was made by diluting 10 ml of sterile porcine pancreas derived trypsin 10 x solution (Sigma-Aldrich Corp., St. Louis, USA) in 90 ml PBS (*Appendix 1e*). This 1 x stock of trypsin was stored at 4 °C and warmed to 37 °C before use.

i) Papain Solution

Items	Amount	Source
DNAse	0.5 mg	Worthington Biochemical Corp., USA
EBSS	0.5 ml	E2888, Sigma-Aldrich, St. Louis, USA
Papain	200 units	Worthington Biochemical Corp., USA

The above reagents were mixed together and kept at room temperature.

j) Poly – L – lysine for coating flasks

Poly – L – lysine was prepared from powder (P6282, Sigma-Aldrich, St. Louis, USA) into a stock solution of 10 mg in 5 ml of distilled water (Barnstead, New Hampshire, USA). The stock was then diluted 1 : 100 in distilled water to obtain a working concentration and sterilized by a 0.2 µm syringe filter (Sartorius – Stedim AG, Germany). This solution was used to plate the flask or coverslips overnight at room temperature. The next day, the solution was removed and the surface washed twice with distilled water. The flasks and coverslips were then left in a laminar flow to dry before plating of cells.

APPENDIX 2

Materials for Virus Infection, Growth of Virus and Plaque Assay

a) Virus Diluent, Hanks' Balanced Salts (pH 7.2 - 7.4)

Items	Amount	Source
Hanks' Balanced Salts	1 bottle (commercial)	H6163, Sigma-Aldrich, St. Louis, USA
Deionised water	1000 ml	Barnstead, New Hampshire, USA

The powdered Hanks' Balanced Salt was added to a glass beaker containing 90 % of the final required volume of water. A magnetic stirrer was used to agitate the contents until all solids were fully dissolved. The solution was made up to 1000 ml and then tittered using a pH meter (Beckman Coulter Inc., Fullerton, USA) to approximately pH 7.3. The solution was then sterilised by filtration through 0.2 µm PES membrane bottle top filter unit (Nalge Nunc International, Rochester, USA). Storage was at 4 °C. Virus diluent was warmed to 37 ˚C before use.

b) Maintenance Media, L15, for C6/36 Cell Culture

Items	Amount	Source
L15	1 bottle (commercial)	L4386, Sigma-Aldrich, St. Louis, USA
Foetal bovine serum	20 ml	PAA Laboratories GmbH, Austria
Deionised water	980 ml	Barnstead, New Hampshire, USA

Maintenance media for C6/36 cells were prepared in the same way as the growth media for the same cell line in *Appendix 1c*, except for the volume difference of foetal bovine serum and deionised water.

c) Maintenance Media, M199, for Vero Cell Culture

Items	Amount	Source
Medium M199	1 bottle (commercial)	Sigma-Aldrich, St. Louis, USA
$NaHCO_3$	2.2 g	Merck KGaA, Germany
Foetal bovine serum	20 ml	PAA Laboratories GmbH, Austria
Deionised water	980 ml	Barnstead, New Hampshire, USA

Maintenance media for Vero cells were prepared in the same way as the growth media for the same cell line in *Appendix 1a*, except for the volume difference of foetal bovine serum and deionised water.

d) Maintenance Media, DME Medium, for primary Neural Cells

Items	Amount	Source
DME Medium	1 bottle (commercial)	D1152, Sigma-Aldrich, St. Louis, USA
Foetal bovine serum	20 ml	PAA Laboratories GmbH, Austria
$NaHCO_3$	3.7 g	Merck KGaA, Germany
Deionised water	970 ml	Barnstead, New Hampshire, USA
Antibiotic - Antimycotic	10 ml	Gibco, Invitrogen Corp., Carlsbad, USA

Maintenance media for primary neuronal cells were prepared in the same way as the growth media for the same cell line in *Appendix 1d*, except for the volume difference of foetal bovine serum and deionised water.

e) Overlay Medium (pH 7.2 - 7.4)

Items	Amount	Source
RPMI-1640	10.63 g	M0393, Sigma-Aldrich, St. Louis, USA
$NaHCO_3$	2.0 g	Merck KGaA, Germany
Foetal bovine serum	20 ml	PAA Laboratories GmbH, Austria
Deionised water	680 ml	Barnstead, New Hampshire, USA
Carboxymethylcellulose (CMC)	4.0 g	Merck KGaA, Germany

Four grams of CMC was mixed well into 200 ml of deionised water. The mixture was then sterilised by autoclaving at 15 minutes, 121 °C, 15 lbs. pressure, and then left to cool. Double strength RPMI was made by adding the RPMI – 1640 powder to 480 ml of deionised water. Sodium bicarbonate was added and the media was adjusted to pH 7.3. It was then filtered through a 0.2 µm PES membrane bottle top filter unit (Nalge Nunc International, Rochester, USA). Two hundred µl of the double strength media was added to cooled CMC solution and mixed well. Storage was at 4 °C. Overlay medium was warmed to 37 ˚C before use.

f) 0.5 % Crystal Violet / 25 % Formaldehyde Solution

Items	Amount	Source
Crystal violet powder	5.0 g	Sigma-Aldrich, St. Louis, USA
37 % Formaldehyde solution	300 ml	Merck KGaA, Germany
PBS	200 ml	See *Appendix 1g*

The above materials were mixed together and stored at room temperature.

APPENDIX 3

Materials for Reverse Transcription and Polymerase Chain Reaction

a) DEPC – Treated Water

One litre of 0.1 % DEPC treated water was prepared by adding 1 ml of DEPC (Sigma-Aldrich, St. Louis, USA) to 100 ml of deionised water (Barnstead, New Hampshire, USA) and mixed well to bring the DEPC into solution. It was left to stir on a magnetic stirrer / hotplate overnight at 37 °C (Bibby Sterilin, Barloworld Scientific Ltd., London, UK). The solution was then autoclaved to remove any trace of DEPC for fifteen minutes at 121 °C, 15 lbs. pressure (Hirayama Corp., Saitama, Japan).

b) Transcription Mix

Items	**Volume in µl**
Nuclease – Free Water	5.5
ImProm – II 5X Buffer	4.0
Magnesium Chloride	2.0
dNTP Mix	1.0
Recombinant RNasein Ribonuclease Inhibitor	0.5
ImProm – II Reverse Transcriptase	1.0
Total	**14.0**

c) PCR Amplification Mix

Items	Volume in µl
10 x Pfx Amplification Buffer	5.0
10 mM dNTP mixture	1.5
50 mM $MgSO_4$	1.0
Primer Mix (10 µM each)	1.5
Platinum Pfx DNA Polymerase	0.8
Autoclaved Distilled Water	20.2
Total	**30.0**

APPENDIX 4

Materials for Agarose Gel Electrophoresis

a) 1.0 % Agarose Gel

Items	Amount	Source
Ultra – Pure Agarose	1.0 g	Invitrogen Corp., Carlsbad, USA
1 x TBE	100 ml	Bio Rad Labs, California, USA
Ethidium Bromide (10 mg/ml)	6 µl	Bio Rad Labs, California, USA

The above mixture was topped up to 250 ml (excluding ethidium bromide) with deionised water and the mixture was boiled for three minutes in a microwave oven. The solution was allowed to cool to 45 °C before the addition of ethidium bromide. The solution was mixed well before pouring into the agarose gel apparatus in the fume cupboard.

b) Tris – Borate – EDTA Buffer (TBE)

The stock solution of 10 x TBE buffer (Bio Rad Labs, California, USA) was diluted by adding 10 ml of the 10 x TBE buffer to 90 ml of deionized water to obtain the 1 x TBE buffer.

c) Three Molar Potassium Acetate

Potassium Acetate (Sigma-Aldrich, St. Louis, USA) was weighed out and 2.95 g were added to 10 ml of deionised water (Barnstead, New Hampshire, USA). The solution was stirred and when all solids were dissolved, it was adjusted to pH 5.6 with glacial acetic acid (Merck KGaA, Germany). The solution was stored at 25 ˚C.

APPENDIX 5

Materials for Bio - Imaging

a) 4 % Paraformaldehyde in PBS

Items	Amount	Source
Paraformaldehyde	4.0 g	Merck KGaA, Germany
PBS	100 ml	*Appendix 1g*

Paraformaldehyde powder was first dissolved in 800 ml of PBS by heating to 60 ºC on a hotplate (Bibby Sterilin, Barloworld Scientific Ltd., London, UK). A few drops of 1 M NaOH solution (*Appendix 1f*) were added to clear the solution. The solution was cooled and topped up to 100 ml with PBS (*Appendix 1g*).

b) Overnight Automated Embedding Program

No.	Medium	Duration	Temperature	Source
1	70 % ethanol	30 minutes	25 ˚C	Merck KGaA, Germany
2	80 % ethanol	30 minutes	25 ˚C	Merck KGaA, Germany
3	95 % ethanol	45 minutes	25 ˚C	Merck KGaA, Germany
4	95 % ethanol	45 minutes	25 ˚C	Merck KGaA, Germany
5	Absolute ethanol	90 minutes	25 ˚C	Merck KGaA, Germany
6	Absolute ethanol	90 minutes	25 ˚C	Merck KGaA, Germany
7	Xylene	30 minutes	25 ˚C	Merck KGaA, Germany
8	Xylene	30 minutes	25 ˚C	Merck KGaA, Germany
9	Xylene	30 minutes	25 ˚C	Merck KGaA, Germany
10	Paraffin wax	120 minutes	60 ˚C	Fisher Sci., USA
11	Paraffin wax	120 minutes	60 ˚C	Fisher Sci., USA
12	Paraffin wax	120 minutes	60 ˚C	Fisher Sci., USA

c) Ethanol Concentration Preparation for Dewaxing

Absolute ethanol was purchased from Merck KGaA, Germany while deionised water was filtered through a Barnstead E-pure system (Barnstead, New Hampshire, USA).

Item	Pure Ethanol volume (ml)	Deionised Water volume (ml)
95 % Ethanol	95	5
70 % Ethanol	70	30
50 % Ethanol	50	50
25 % Ethanol	25	75

d) Dewaxing Protocol

No.	Solution
1	Absolute alcohol
2	Absolute alcohol
3	95 % alcohol
4	95 % alcohol
5	70 % alcohol
6	Tap water

e) Acid Alcohol (1 %)

The two liquids were mixed together and stored at 4˚C.

Item	Amount (ml)	Source
Ethanol (70 %)	99	*Appendix 5c*
Glacial Hydrochloric acid	1	Sigma-Aldrich, St. Louis, USA

f) Alkaline Solution

The two liquids were mixed thoroughly and stored at room temperature.

Item	Amount (ml)	Source
Ammonia hydroxide	1	Fisher Scientific, USA
Deionised Water	250	Barnstead, New Hampshire, USA

g) Eosin

Item	Amount	Source
Eosin powder (82 %)	5.0 g	Sigma-Aldrich, St. Louis, USA
Deionised Water	1000 ml	Barnstead, New Hampshire, USA

Eosin was mixed in 990 ml of water. Using 1 M hydrochloric acid or 1 M sodium hydroxide (*Appendices 1e and 1f*), the pH was adjusted to 7.4. The solution was topped up to 1 litre and kept at room temperature.

h) Hematoxylin and Eosin Staining Protocol

No.	Reagent	Time	Source
1	Harris' hematoxylin	10 minutes	Sigma-Aldrich, St. Louis, USA
2	Running tap water	2 minutes	-
3	Acid alcohol (1 %)	2 dips	*Appendix 5e*
4	Running tap water	1 minute	-
5	Alkaline solution	3 dips	*Appendix 5f*
6	Running tap waster	3 minutes	-
7	Alcohol (70 %)	5 dips	*Appendix 5c*
8	Eosin	5 minutes	*Appendix 5g*
9	Running tap water	30 seconds	-

APPENDIX 6

Materials for Immunohistochemistry

a) Sodium Citrate Buffer for Antigen Retrieval

Item	Amount	Source
Tri – Sodium Citrate dihydrate	2.94 g	Sigma-Aldrich, St. Louis, USA
Deionised Water	1000 ml	Barnstead, New Hampshire, USA
Tween – 20	0.5 ml	ICN Biomedicals, USA

The sodium powder was mixed into 1 litre of water and titred to approximately pH 6.0. Then, 0.5 ml of Tween – 20 was added and mixed. The solution was stored at 4 ˚C until used.

b) 0.6 % H_2O_2 in Methanol

The two liquids were mixed thoroughly and stored at 4 ˚C.

Item	Amount (ml)	Source
H_2O_2 30 %	2	Merck KGaA, Germany
Methanol	98	Merck KGaA, Germany

c) Tris-Buffered Saline (TBS)

Item	Amount	Source
Sodium Chloride	8.0 g	Lab Scan Limited, Ireland
Tris	0.61 g	USB Corp., Ohio, USA
Hydrochloric Acid	3.8 ml	*Appendix 1e*
Deionised Water	1000 ml	Barnstead, New Hampshire, USA

The chemicals were dissolved in 990 ml of water. Using 1 M hydrochloric acid (*Appendix 1e*), the pH was adjusted to 7.6. Deionised water was then used to top up the solution to 1 litre and kept at 4˚C.

APPENDIX 7

Materials for Immunogold – Silver Staining (IGSS)

a) Bovine Serum Albumin (BSA) Blocking Solution

Item	Amount	Source
Bovine Serum Albumin	5.0 g	Gibco, Invitrogen Corp., Carlsbad, USA
Phosphate Buffered Saline	100 ml	*Appendix 1g*

BSA was dissolved in 95 ml PBS. Using 1 M hydrochloric acid or 1 M sodium hydroxide (*Appendices 1e and 1f*), the pH was adjusted to 7.4. The solution was then topped up to 100 ml and kept at - 20 ˚C.

b) Aldehyde Blocking Solution

Item	Amount	Source
Glycine	0.94 g	Merck KGaA, Germany
Phosphate Buffered Saline	250 ml	*Appendix 1g*

Glycine was dissolved in 245 ml PBS. Using 1 M hydrochloric acid or 1 M sodium hydroxide (*Appendices 1e and 1f*), the pH was adjusted to 7.4. The solution was then topped up to 250 ml and kept at - 20 ˚C.

c) Aurion BSA – C Wash Solution

Item	Amount	Source
BSA – C	1 ml	Aurion immunoGold, Netherlands
Phosphate Buffered Saline	100 ml	*Appendix 1g*

BSA – C was mixed with 95 ml of PBS. Using 1 M hydrochloric acid or 1 M sodium hydroxide (*Appendices 1e and 1f*), the pH was adjusted to 7.4. The solution was then topped up to 100 ml and kept at - 20 ˚C.

d) 2 % Gultaraldehyde Fixative Solution

Item	Amount	Source
Glutaraldehyde	2.0 g	Sigma-Aldrich, St. Louis, USA
Phosphate Buffered Saline	100 ml	*Appendix 1g*

Reagents were mixed and stored at 4 ˚C.

APPENDIX 8

Materials for Electron Microscopy (EM)

a) 4 % Glutaraldehyde and 4 % Paraformaldehyde

Item	Amount	Source
25 % Glutaraldehyde	16 ml	Agar Scientific, USA
25 % Paraformaldehyde	16 ml	Agar Scientific, USA
Phosphate Buffered Saline	68 ml	*Appendix 1g*

Items were mixed in a glass bottle in the fume hood before storage at 4 ^{o}C.

b) 1 % Osmium Tetroxide in 1 x PBS

Item	Amount	Source
Osmium tetroxide	1.0 g	TAAB Lab. Equipment Ltd., England
Phosphate Buffered Saline	100 ml	*Appendix 1g*

The ampoule was opened in a brown glass bottle with the buffer inside. Mixture was swirled to ensure that the osmium tetroxide was dissolved totally. The solution was stored at -20 °C.

c) LR White

Item	Amount	Source
LR White	500 ml	Ted Pella Inc., California, USA
Benzyol peroxide	28.7 g	Ted Pella Inc., California, USA

The 2 items were mixed well in a fume hood before storage at 4 ^{o}C.

d) Saturated Aqueous Uranyl Acetate

Item	Amount	Source
Ryter kellenburger buffer	5 ml	*Appendix 11f*
0.1 M $CaCl_2$	5 ml	Merck KGaA, Germany
0.1 M HCl	6.5 ml	Merck KGaA, Germany
Uranyl acetate	1.3 g	Merck KGaA, Germany

The above items were added to 13 ml of deionised water and stored at room temperature in a bottle covered with aluminum foil. The saturated solution was centrifuged at 2000 x *g* before use.

e) Reynold's Lead Citrate solution

Item	Amount	Source
Lead citrate	1.3 g	BDH Ltd., Poole, England
Sodium citrate	1.8 g	Merck KGaA, Germany

The items were added to 30 ml of deionised water and stirred continuously for about 45 minutes to ensure the complete conversion of lead nitrate (impurity) to lead citrate. Subsequently, 8 ml of 1 M NaOH (*Appendix 1f*) was added and the solution topped up to 50 ml with deionised water. The solution was stored at 4 ^{o}C.